8-2009

UNDERSTANDING THE ANTIOXIDANT MECHANISM OF INORGANIC SELENIUM, OXO- SULFUR, AND POLYPHENOL COMPOUNDS, AND THE BIOLOGICAL IMPLICATIONS OF FUNCTIONALIZED NANOPARTICLES

Ria Ramoutar
Clemson University, rramout@clemson.edu

UNDERSTANDING THE ANTIOXIDANT MECHANISM OF INORGANIC SELENIUM, OXO- SULFUR, AND POLYPHENOL COMPOUNDS, AND THE BIOLOGICAL IMPLICATIONS OF FUNCTIONALIZED NANOPARTICLES

A Dissertation
Presented to
The Graduate School of
Clemson University

In Partial Fulfillment
of the Requirements for the Degree
Doctor of Philosophy
Chemistry

---

by
Ria R. Ramoutar
August 2009

Accepted by:
Dr. Julia Brumaghim, Committee Chair
Dr. Kenneth A. Christensen
Dr. William T. Pennington
Dr. Jason McNeill

ABSTRACT

Inorganic selenium, oxo-sulfur, and polyphenol compounds are found in foods and dietary supplements, and are recognized for their nutritional benefits and their potential to treat or prevent diseases caused by oxidative stress. In our experiments to determine the effects of inorganic selenium compounds on iron-mediated DNA damage, Na_2SeO_3 and SeO_2 exhibit antioxidant and pro-oxidant activities depending on concentrations of both the compound and hydrogen peroxide. Additional experiments demonstrate that iron coordination is a novel mechanism responsible for the observed activities. In similar experiments, oxo-sulfur compounds prevent Cu^+/H_2O_2-mediated DNA damage significantly more than DNA damage from Fe^{2+}/H_2O_2. UV-vis and gel electrophoresis experiments also confirm that copper coordination is primarily responsible for the DNA damage inhibition, a novel mechanism that extends to all tested sulfur and selenium antioxidants. Electrospray ionization mass spectroscopy indicates that these sulfur and selenium compounds generally bind Cu^+ in a 1:1 ratio.

Combinations of bioactive components in foods can affect activity of antioxidants. For example, adding one equivalent of caffeine to polyphenols has no effect on DNA damage prevention by epigallocatechin gallate, but significantly decreases the antioxidant ability of quercetin. In addition, DNA damage prevention studies on peach extracts indicate that genetically-modified peach cultivars prevent more DNA damage than unmodified cultivars. In contrast, tetraphenyl-porphyrin-doped conjugated polymer dot nanoparticles cause DNA backbone and base damage upon irradiation, suggesting that these nanoparticles may be efficient photosensitizers for photodynamic therapy

(PDT). Our studies also show H_2O_2 formation by and iron association with polyethylene glycol (PEG) and PEG-functionalized beads at biologically-relevant concentrations. Since Fe^{2+} and H_2O_2 react to form damaging hydroxyl radical, use of PEG-functionalized nanoparticles in medical applications may cause oxidative stress. Overall, this work has elucidated of antioxidant and pro-oxidant mechanisms of inorganic selenium, oxo-sulfur, and polyphenol compounds, as well as the potential toxicity of functionalized nanomaterials used for PDT and other medical applications.

DEDICATIONS

I dedicate this dissertation to my parents, Phagoo and Gowra Ramoutar, and sisters Reshma and Asha for their encouragement, love and support that allowed me to achieve this measure of academic success. The strength and support of my family made me believe that all things are possible through hard work and dedication.

ACKNOWLEDGEMENTS

Firstly, I would like to thank my advisor, Dr. Julia L. Brumaghim, for allowing me to participate in research projects in the very interesting and exciting field of bioinorganic chemistry. I would like to thank Dr. Brumaghim for her continuous mentoring, guidance, and support throughout my graduate academic career. I am especially grateful for the invaluable knowledge and experience gained from her.

I would also like to thank Mrs. Barbara Lewis for making my experience as a teaching assistant very interesting and enjoyable. It was truly a pleasure working under her supervision. Special thanks to both Joy Castro and Carolyn Quarles for training and assisting me in both ICP and ESI mass spectroscopies. I would like to acknowledge my collaborators, including Dr. Jason McNeill, Dr. Albert Abbott, and Dr. Pamela Riggs-Gelasco.

I would especially like to thank my family and friends in Trinidad and Tobago and Canada for their continuous love, support, and guidance, which has been invaluable to me throughout my academic career while in the United States. I would also like to acknowledge Rajashree Sathyamurthy, Mark Bradshaw, Erin Battin, and Jared Knutt, for their ongoing support and friendship. Special thanks to the Brumaghim group members, including Andrea Verdan, for their witty comments, humor, support and friendship, which made research an enjoyable experience.

TABLE OF CONTENTS

LIST OF TABLES

Table **Page**

LIST OF FIGURES

Figure **Page**

CHAPTER ONE

A REVIEW OF THE ANTIOXIDANT AND ANTICANCER PROPERTIES AND MECHANISMS OF INORGANIC SELENIUM, OXO-SULFUR, AND OXO-SELENIUM COMPOUNDS

Introduction

The generation of reactive oxygen species (ROS) has dual functionality in biological systems, with both beneficial and detrimental effects in cells.[1,2] ROS generation at low or moderate concentrations aids in the defense against infectious agents and functions in several cell signaling pathways.[1,2] The damaging effects of ROS such as the superoxide anion radical ($O_2^{\bullet-}$), hydrogen peroxide (H_2O_2), and hydroxyl radical ($^{\bullet}OH$) caused by the overproduction of these species results in oxidative stress, an unavoidable consequence of aerobic cellular respiration.[1-6] ROS damage to lipids, proteins, and DNA[1,2,6,7] is a result of this oxidative stress and leads to several health conditions including aging,[1] cancer,[1,8] neurodegenerative diseases such as Parkinson's and Alzheimer's,[9-12] and cardiovascular diseases such as arteriosclerosis.[13-16]

Reactive oxygen species are generated during the reduction of molecular oxygen (O_2) to produce water (H_2O) via metabolic processes catalyzed by cytochrome oxidase in biological systems.[5,17] The primary ROS formed as a byproduct of this respiratory process is the superoxide anion radical ($O_2^{\bullet-}$), generated when molecular oxygen gains an electron from either the mitochondrial electron transport chain (Reaction 1) or as a result of UV-irradiation (Reaction 2).[1,4,5,17] Further reduction of $O_2^{\bullet-}$, either directly or through

enzyme- or metal-catalyzed reactions, results in the formation of secondary ROS such as hydrogen peroxide (H_2O_2; Reaction 3) and the hydroxyl radical ($^{\bullet}OH$; Reaction 4).[1,4,5,17] Hydrogen peroxide is also produced directly by protonation of the superoxide radical anion in solution (Reaction 3), and indirectly upon oxidation of iron-sulfur clusters (Reaction 5).[18,19]

$$O_2 + e^- \rightarrow 2\ O_2^{\bullet-} \quad (1)$$

$$O_2 + h\nu \rightarrow 2\ O_2^{\bullet-} \quad (2)$$

$$2\ O_2^{\bullet-} + 2H^+ \rightarrow H_2O_2 + O_2 \quad (3)$$

$$O_2^{\bullet-} + H_2O_2 + H^+ \rightarrow {}^{\bullet}OH + O_2 + H_2O \quad (4)$$

$$O_2^{\bullet-} + [2Fe^{2+}2Fe^{3+}4S] + 2H^+ \rightarrow [Fe^{2+}3Fe^{3+}4S] + H_2O_2 \quad (5)$$

Compared to other ROS, hydrogen peroxide is a non-radical species with relatively low reactivity.[20] It is one of the more commonly studied ROS, and is produced endogenously by various physiological processes including respiratory burst and oxidative phosphorylation.[21] Calculations to determine the steady-state intracellular concentrations of hydrogen peroxide in unstressed *E. coli* cells determined a value of ~20 nM, with a high rate of H_2O_2 production ranging from 9-22 μM/s.[22] Thus, any imbalance between the rate of H_2O_2 generation and decomposition may result in significantly increased H_2O_2 concentrations and resultant oxidative stress.[22,23 24]

Linn and colleagues reported bimodal cell killing when *E. coli* is exposed to H_2O_2. Mode I cell killing occurs at low concentrations of H_2O_2 (1-5 mM) and is faster than Mode II, which occurs at H_2O_2 concentrations greater than 10 mM.[24,25] Mammalian cells also show the same bimodal killing as *E. coli* upon hydrogen peroxide challenge,[26]

and these bimodal kinetics are also observed for iron-mediated oxidative DNA damage *in vitro*, where maximal damage under Mode I conditions occurred at 50 μM H_2O_2 and for Mode II conditions, at H_2O_2 concentrations >10 mM.[24,25,27] Significantly, H_2O_2 reacts with redox-active metal ions to generate hydroxyl radical.[5,17,18,20,28] *In vivo*, hydroxyl radical has an extremely short half-life (~10^{-9} s)[29,30] and reacts quickly with biomolecules in proximity to its site of generation, resulting in DNA damage, lipid peroxidation, thiol depletion, and changes in calcium homeostatsis.[1,21,31]

Iron and copper are the most commonly studied redox-active metal ions found in biological systems and are essential in many proteins and enzymes, including ferritin, transferrin, ceruplasmin, and superoxide dismutase.[32] In *E. coli*, normal intracellular non-protein-bound (labile) iron concentrations are ~20 μM. However, this concentration increases significantly to 80-320 μM upon disruption of iron homeostasis and oxidative stress.[20,31,33,34] Although the intracellular concentration of non-protein- bound copper was calculated to be approximately 10^{-18} M in yeast, significant amounts of labile copper are observed in mouse Golgi and mitochondria.[35-37] Studies have also reported extracellular copper concentrations in blood serum and cerebrospinal fluid between 10-25 μM and 0.5-2.5 μM, respectively, whereas copper concentrations in the synaptic cleft are approximately 30 μM.[38,39] Neural copper concentrations are significantly higher in the locus ceruleus (stress and panic response center) and substantia nigra (dopamine production region) with concentrations of 1.3 mM and 0.4 mM, respectively.[38,40]

In the reduced state, Fe^{2+} and Cu^{+} are oxidized by H_2O_2 to Fe^{3+} and Cu^{2+}, generating hydroxyl radical in the Fenton or Fenton-like reaction (Reaction 6).[1,21,28,41-43]

$$Fe^{2+} \text{ or } Cu^{+} + H_2O_2 \rightarrow Fe^{3+} \text{ or } Cu^{2+} + {}^{\bullet}OH + OH^{-} \qquad (6)$$

This production of $^{\bullet}OH$ becomes catalytic *in vivo* due to the presence of cellular reductants such as NADH, which reduce Fe^{3+} and Cu^{2+} back to their reduced forms. In fact, iron-mediated generation of $^{\bullet}OH$ is the main cause of oxidative DNA damage and cell death in prokaryotes[26] and eukaryotes, including human cells, under oxidative stress conditions,[25,26,43] and is a root cause of several health conditions such as cancer, aging, and cardiovascular and neurodegenerative diseases.[9,14,43,44]

Cellular defenses against the harmful effects of oxidative stress involve both enzymatic and nonenzymatic antioxidant activities.[1,4] Enzymatic defense requires enzymes such as glutathione peroxidases (GPx), catalases, and superoxide dismutases (SOD) that act by directly scavenging ROS or by producing nonenzymatic antioxidants such as glutathione (GSH), thioredoxin, ubiquinone, and menaquinone.[1,4] Nonenzymatic defenses involve antioxidants such as carotenoids, lipoic acid, and vitamins C and E to prevent against the damaging effects of oxidative stress.[1,45] Both vitamins C and E reduce oxidative stress and malformations in the offspring of rats with diabetes.[46-48] Studies have also focused on various selenium, sulfur, and polyphenol compounds to act as antioxidants by preventing ROS-mediated DNA damage.[23,49-54]

Selenium has been extensively studied for its antioxidant and cancer preventative properties and is an essential trace element in human and animal metabolism.[55-58] It is found in many dietary supplements and multivitamins in forms such as selenite (Na_2SeO_3), selenate (Na_2SeO_4), or selenomethionine (SeMet).[56,59] Selenite and selenate are also found in fertilizers, animal feed, infant formulas, and protein shakes.[56,60]

Selenium is incorporated as selenocysteine (SeCys) in selenoproteins P, W, and R, as well as in the active sites of enzymes such as glutathione peroxidases (GPx) and thioredoxin reductases.[23,52,57,61-63] In cells, these selenoproteins have important antioxidant activities and protect the mitochondria, plasma membrane, and DNA from oxidative damage by ROS.[60,64] For example, GPx is found in the cytosol of cells and exerts its antioxidant activity by reducing intracellular hydrogen peroxide to water, preventing the generation of ROS.[62,63,65-68] Although selenoproteins are a significant part of the antioxidant properties of selenium, they have been extensively discussed[62,69,70] and are not the focus of this review.

Studies to determine the antioxidant activity of small-molecule selenium- and sulfur-containing compounds have focused mainly on the organoselenium and organosulfur compounds since they are more bioavailable and are more readily incorporated into amino acids and proteins compared to the inorganic forms.[62,71] Consumption of food products high in selenomethionine (SeMet) results in incorporation of this amino acid into proteins by replacing its sulfur analog, methionine (Met).[72] SeMet is also more efficiently absorbed and retained than the inorganic sodium selenite and selenate.[73] While the organoselenium compounds have received a significant amount of attention for their role as antioxidants,[49,74-76] several studies indicate that inorganic selenium compounds such as selenite, selenate, selenium dioxide (SeO_2) and sodium selenide (Na_2Se; Figure 1.1) also exhibit similar antioxidative properties.[23,51,55,57,58,77-79]

Fruits, vegetables, and dietary supplements also contain oxo-sulfur compounds (Figure 1.2) such as allicin, methylcysteine sulfoxide (MeCysSO), methyl methane

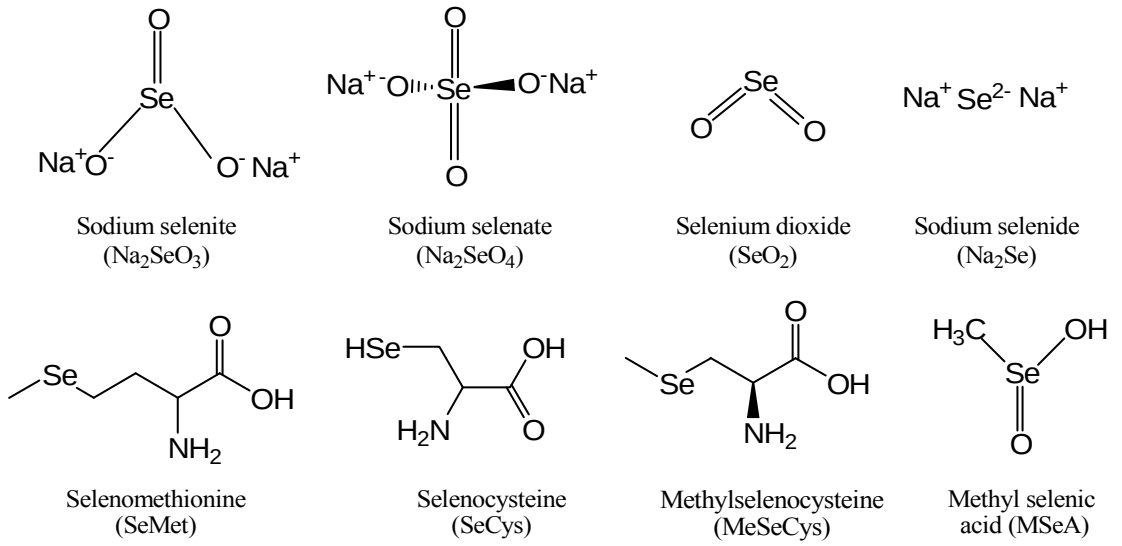

Figure 1.1. Structures of inorganic and other selenium compounds discussed in this chapter.

thiosulfonate (MMTS), and dimethyl sulfone or methylsulfonyl methane (Me_2SO_2), which are also effective in preventing oxidative damage to cellular components.[53,54,80-86] Understanding the effects of oxidation on the antioxidant properties of organosulfur compounds is also important because compounds such as methionine are susceptible to oxidation by ROS.[87-89] To prevent the disruption of protein function upon methionine oxidation to methionine sulfoxide (MetSO), cells have dedicated methionine reductase enzymes (Msr) to reduce MetSO back to Met.[88,90-93]

Research has focused primarily on the ability of organoselenium and organosulfur compounds in their reduced forms to prevent oxidative DNA damage and to treat or prevent diseases caused by oxidative stress. However, it is important to acknowledge the fact that inorganic selenium and oxo-sulfur compounds are abundant in many food products such as dietary supplements, protein shakes, infant formulas, fruits, and vegetables. This review will therefore discuss the role and biochemical mechanisms of

inorganic selenium, oxo-selenium, and oxo-sulfur compounds to act as antioxidants and pro-oxidants, both in vivo and in vitro, for the treatment or prevention of ROS-mediated diseases.

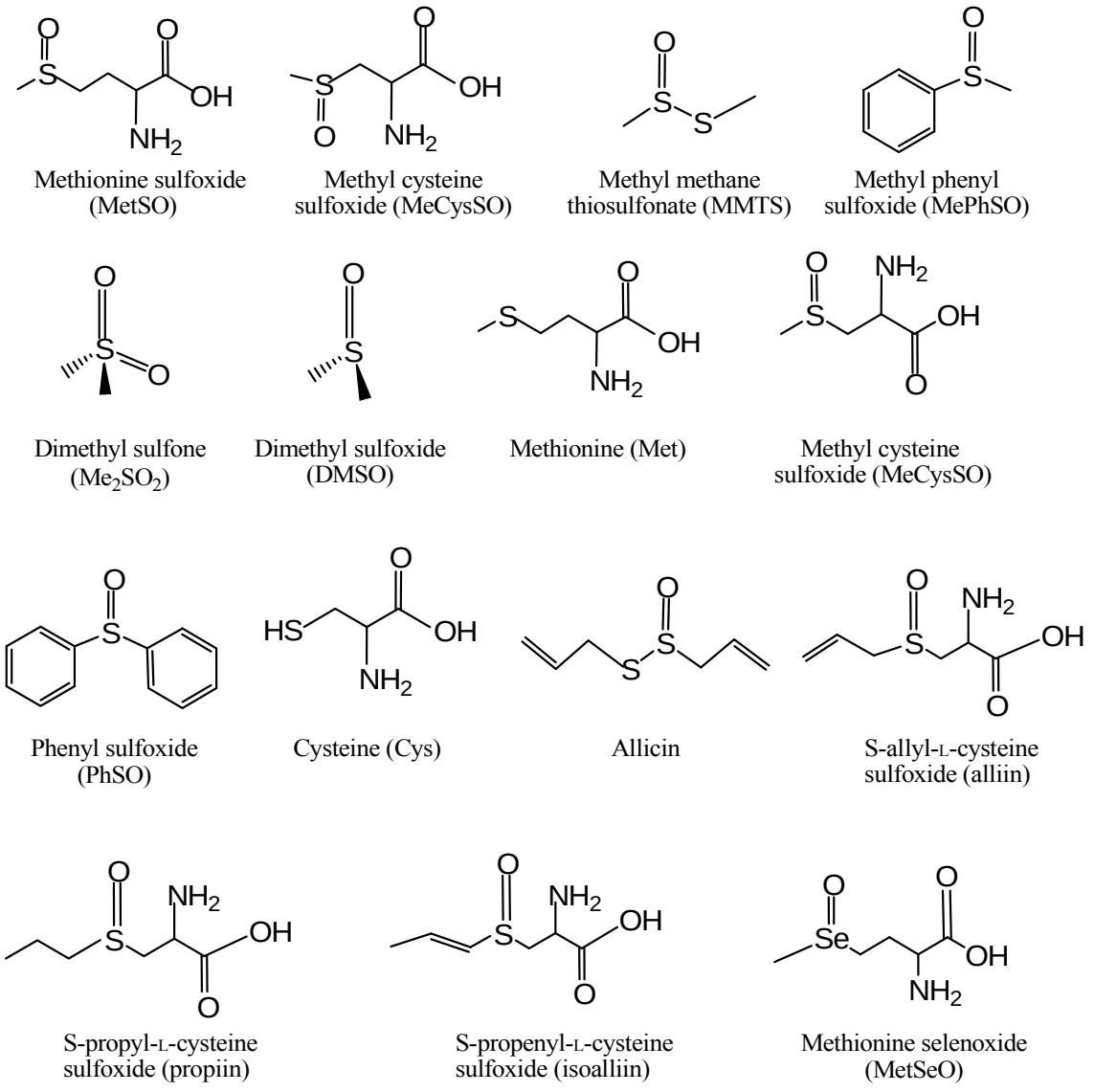

Figure 1.2. Structures of oxo-sulfur and oxo-selenium compounds discussed in this chapter.

Selenium bioavailability, related pathologies, and biological effects

Selenium is an important micronutrient for both humans and animals and is obtained through the diet from several sources including cereals, grains, nuts, vegetables, meat, and seafood.[62,94,95] The recommended daily allowance (RDA) for selenium ranges from 55 to an upper limit of 350-400 μg/day, and daily intake comes from dietary supplementation and foods rich in this mineral.[56,96] Although selenium toxicity has been observed for supplementation greater than 400 μg/d,[60,97] it is important to note that some studies conducted with a selenium intake ranging from 750 to 850 μg/d (~0.01 mg/kg) reported no signs of selenium toxicity in humans.[98,99] Animal studies reported selenium toxicity within 12 h upon supplementation of 2 mg/kg selenium.[100,101] These seemingly contradictory results of selenium toxicity in humans highlight the need for additional studies to establish accurate upper level RDA values for selenium supplementation.

The selenium content of plant and animal products in the diet is important to maintain adequate selenium status and is highly dependent on regionally-variable selenium concentrations in soil.[48,56,62,63,66,68,99] In the United States, for example, soil in northern Nebraska and the Dakotas has high selenium levels, but areas such as the Keshan province of China and some parts of Finland, New Zealand, Australia, and North America (northeast, northwest, Midwest, and southeast regions) have low soil selenium levels.[66,68,99,102-105] To increase the selenium content in soils, and therefore increase animal and human consumption of selenium, these countries have implemented the use of fertilizers enriched with selenite or selenate for agricultural crops.[106-110] In the United States, selenite supplementation in animal feed has been shown to improve animal

performance and increase the selenium dietary intake for Americans consuming meat products.[60]

Pathologies associated with selenium deficiency and toxicity

Selenium deficiency occurs in regions where the selenium content in soil is low and can result in diseases such as hypothyroidism, weakened immune defenses, and cardiovascular diseases.[63,111,112] Keshan disease is a cardiomyopathy endemic to the Keshan province of China. This disease affects young children and women of child-bearing age as a result of low iodine and selenium content in food products, leading to low blood plasma selenium levels.[113-117] The average intake of selenium for the development of symptoms due to deficiency was 10 μg/d with symptoms such as congestive heart failure, stroke or sudden death.[62,117]

Also resulting from low selenium and iodine intake is the endemic osteoarthropathy known as Kashin-Beck disease found in several areas of China.[115,116] Bone and joint deformations in growing children are characteristic of this disease.[118] The average serum selenium levels of patients with Kashin-Beck disease is significantly lower (11 ng/mL) than those without these mineral deficiencies (60-105 ng/mL).[119] Serum thyroxine levels are also much lower in patients with Kashin-Beck disease, resulting in higher incidences of goiter than those unaffected by the disease.[120] In farm animals, selenium deficiency causes a muscular dystrophy known as white muscle disease.[68] This disease usually affects growing animals such as lambs and calves between 1 and 3 months old with symptoms including stiffness, inability to move, weakness,

tiredness, accelerated breathing, elevated temperatures, difficulty in feeding, and death.[68,121]

Intake of selenium higher than the upper limit range 350-400 μg/d[56,96] of the RDA is also of major concern to humans and animals since it can result in selenium toxicity or selenosis.[60,97] Acute selenosis is caused by consumption of high levels of selenium in a short period of time. Upon ingestion of 17.2 μg/mL selenium due to incorrect dosage in animal feed, pigs showed signs of acute selenium toxicity, including paralysis, hyperesthesia, anorexia, and tremors.[97,122] Signs of acute selenosis in buffalo include anorexia, alopecia, mild convulsions, and lowered body temperature.[97,123,124] Symptoms of chronic selenosis include hair loss, deformation or cracks on the skin, horns, and hooves of animals, resulting in the sloughing of hooves and staggering.[60,97,125] In humans, signs of selenosis include garlic breath, hair and nail loss, thickened and brittle nails, teeth deformation, skin lesions, and lowered hemoglobin levels upon dietary selenium intake of 5 mg/d.[98]

Although countries have implemented the use of fertilizers containing selenite and selenate to supplement foods grown in selenium-deficient soil, the effects of selenium supplementation vary for each of these inorganic selenium compounds. In an attempt to prevent or reduce the prevalence of selenium deficiency diseases in China, both selenite and selenate were introduced into the soils of rice crops.[117] In unsupplemented soil, selenium content is extremely low, less than 0.06 μg/g. Rice crops grown in selenite- or selenate-enriched soils had significantly increased selenium levels of 0.471 μg/g and 0.64 μg/g, respectively, with no adverse effects on the plants.[117] In Chile, ryegrass

supplemented with 0.1 μg/g selenite or selenate increases selenium content from 0.07 μg/g for grass grown in untreated soil to 0.28 μg/g and 5.72 μg/g, respectively.[66] Soil enrichment at higher levels of selenate (4-10 μg/g), resulted in stunted growth of ryegrass, with selenium content ranging from 150 to 247 μg/g.[66] Surprisingly, selenite-enriched soils (6-10 μg/g) decreased lipid peroxidation in the plants, whereas selenate supplementation of soil at the same levels had the opposite effect. Higher lipid peroxidation levels for plants grown in selenate supplemented soil may account for the observed stunting of plant growth.[66]

Because inorganic forms of selenium effectively increase selenium levels in plant crops and prevent selenium deficiency diseases in people that consume them, it is important to understand the effect of selenite and selenate supplementation in crops. Plants more efficiently absorb selenate, as indicated by the higher concentrations of selenium in plants supplemented with selenate as compared to selenite supplementation, but selenite may be safer to use in fertilizers, since there are fewer adverse effects with supplementation at high concentrations.[66]

To better treat selenium deficiency and to prevent selenium toxicity, an accurate evaluation of the effects of inorganic selenium compounds in fertilizers is required. Selenite- and selenate-enriched pastures and salt licks are also used to increase selenium concentrations in livestock.[68] It is therefore also important to understand the effects of this supplementation on animals, and further studies are necessary to determine the appropriate levels and forms of inorganic selenium supplementation that are most effective.

In humans, selenium deficiency causes poor immune response by reducing T-cell counts and impairing lymphocyte proliferation and response.[63,126] Studies have shown that human supplementation of 200 μg/d of sodium selenite over an eight-week period resulted in enhanced T-lymphocyte response.[127] In HIV and AIDS patients, selenium deficiency is associated with decreased immune cell count, higher rates of disease progression, and increased risk of death.[128,129] Additionally, selenium was found to protect cells from oxidative stress, resulting in slower progression of this disease.[130]

A study performed over a period of 5 years on HIV-positive children found that those with low selenium levels died at a younger age than patients with higher selenium status.[131] These experiments were corroborated by another study involving HIV-positive men and women that linked increased death rates with selenium deficiency.[132,133] Clinical studies performed on male patients with AIDS and AIDS-related complex (ARC) showed that blood selenium levels increased upon supplementation of 400 μg/d Se-enriched yeast from 0.142 μg/mL to 0.240 μg/mL over a period of 70 days.[134,135] Similar results were also observed in AIDS patients supplemented with sodium selenite (80 μg/d).[134,136] These investigations indicate that both organic and inorganic selenium supplementation is effective for the treatment of patients with immune deficiencies.[133]

Numerous studies indicate that selenium also plays an important role in cancer prevention and treatment.[48,137,138] In a random, double-blind cancer prevention trial, the incidence of prostate cancer was reduced by 63% compared to the placebo group upon selenium supplementation of 200 μg/d as selenium-enriched yeast. Similar studies also showed a significant decrease in lung and colorectal cancers, as well as in total cancer

mortality rates.[139,140] In a separate trial, patients with uterine cervical carcinoma were found to have low glutathione peroxidases and selenium levels.[141]

Antioxidant and anticancer activities of inorganic selenium compounds

ROS generation is directly linked to cellular and DNA damage and is the primary cause of many diseases.[9,14,18,44,142] Antioxidants have been used to prevent or reduce the effects of ROS-mediated DNA and other cellular damage, and selenium has been extensively studied for its antioxidant properties.[55,57,58] Inorganic selenium compounds can also act as pro-oxidants to produce DNA damage and cell death, an activity that plays an important role in the treatment of cancer.[23,51,143-146] Although sometimes confused in the literature, this distinction between antioxidant (cancer prevention) and pro-oxidant (cancer treatment) behavior is important to make, since the chemical and cellular mechanisms behind each type of activity are distinct. The behavior of these inorganic selenium compounds is complex, and in several studies, both antioxidant and pro-oxidant behavior have been observed for the same selenium compound depending on experimental conditions.

The main inorganic selenium compound used in most cancer treatment studies is sodium selenite; however, a few studies use other forms, such as sodium selenate and selenium dioxide.[57,62,143-145,147,148] Selenate and selenite (0.1 μg/mL) are effective dietary supplements for the inhibition of tumor cell growth in rodents.[145,147] These two inorganic selenium compounds also strongly inhibit the growth of mammalian tumor cells at cell cycle phases specific for each compound.[144] Selenite-treatment (10 μM) of human

lymphocyte cells resulted in accumulation in the S-phase with irreversible growth inhibition, whereas selenate-treated (250 μM) cells accumulated in the G_2 phase with reversible inhibitory effects.[144] In a separate study, selenium dioxide (1.5 μM) was found to be effective in the enhancement of lymphocyte progression into the S phase of the cell cycle in patients with stage IV cancer, resulting in restoration of immune function and control of cancer progression.[143] Takahashi *et al*. showed that both selenite (10 μM) and selenium dioxide (100 μM) induced ~ 80% apoptosis in human oral squamous carcinoma (HSC-3) cells after treatment for 72 h, whereas selenate had no effect on cell survival.[57]

Brumaghim *et al*. have shown that inorganic selenium compounds exert both antioxidant and pro-oxidant activities against iron-mediated oxidative DNA damage.[23] Selenite progressively inhibited DNA damage at all concentrations tested (0-5000 μM), with 91% inhibition at the highest concentration under Mode I conditions (50 μM H_2O_2).[23] Selenate and selenide had no effect on damage under similar conditions, whereas SeO_2 was found to be both a pro-oxidant and antioxidant, increasing DNA damage by 20% at 50 μM, but inhibiting 100% DNA damage at 5000 μM.[23] Similar studies performed with organoselenium compounds, SeMet (1-1000 μM) showed no antioxidant activity, whereas methyl selenocysteine prevented ~ 76% iron-mediated DNA damage at very high concentrations (20,000 μM).[149]

In contrast, under Mode II conditions (50 mM H_2O_2), Na_2SeO_3 showed pro-oxidant activity at all concentrations tested (0.5-5000 μM), damaging 90 % DNA at the highest concentration in the absence of iron. However, SeO_2 was an efficient antioxidant under similar conditions, preventing 81% iron-mediated DNA damage, whereas Na_2SeO_4

and Na_2Se had no effect on such damage.[23] The antioxidant behavior of these inorganic selenium compounds has been attributed to the oxidation state of the selenium atom, rather than the overall charge of the selenium compound.[23] Inorganic selenium compounds in the +4 oxidation state (Na_2SeO_3 and SeO_2) were more effective antioxidants than Na_2SeO_4 and Na_2Se, with selenium oxidation states of +6 and -2, respectively.[23] In a separate study Hamilton *et al.* found that Na_2SeO_4 (6.2 mM) was effective at inhibiting DNA damage caused by alkylating agents.[77]

High levels of selenite (1 μg/mL) were also shown to increase thioredoxin reductase activity twofold in rat kidney, liver, and lung tissues as compared to rats with normal selenite intake (0.1 μg/mL).[150] In human colon cancer cells supplemented with various dosages of selenite (0.1, 1, and 10 μM), thioredoxin reductase activity increased with increasing selenium concentration, resulting in a 65-fold increase at the highest concentration tested.[151]

Although these studies make a strong case for selenium supplementation for the prevention or treatment of cancer, additional studies are required to better compare and elucidate the structural and chemical properties of inorganic selenium compounds that contribute to antioxidant or pro-oxidant behavior. For example, while selenite has been shown to be a more effective antioxidant compared to selenate in many studies, selenite can also oxidatively damage DNA under conditions of oxidative stress. This pro-oxidant effect is not observed with selenate, suggesting that selenate may be safer for use in human or animal supplementation.

Selenium speciation and anticancer activity

Selenium bioavailability differs for organic and inorganic compounds, and studies have shown that the formulation of the selenium compound, and not the presence of the element itself, is essential for chemopreventative activity.[152-154] It is therefore critical to elucidate the specific selenium compounds that are required for such activity. For example, sodium selenite (5-10 μM) introduced into cell culture media induced DNA single strand breaks and cell death via necrosis.[152,153,155,156] Organoselenium compounds (10-50 μM), however, caused cell death by apoptosis with no DNA single strand breaks.[152,153] Similar results were obtained in a separate study by Thompson *et al*. to determine the effect of selenium form on mouse mammary carcinoma cells.[157] Although all selenium compounds tested inhibited cell proliferation and induced cell death, selenite and selenide induced both DNA single- (51-59%) and double-strand breaks (4.8-14.6 %) in a concentration-dependent manner (1-5 μM); no DNA damage was observed for the organic forms, methyselenocyanate (2-7 μM) and methylselenocysteine (20-100 μM).[157]

In another study, selenite was found to be more potent than either selenocystamine or selenomethionine in inducing apoptosis in mouse keratinocyte (BALB/cMK2) cells.[142] In this experiment, selenite (10 μg/mL) produced 100% apoptosis, whereas selenocystamine produced 2.8% apoptosis at the same concentration.[142] Selenocystamine (250 μg/mL) was capable of inducing 100% apoptosis, whereas selenomethionine (5-250 μg/mL) showed no effect with BALB/cMK2 cells.[142] A study to determine whether sodium selenite and methylselenic acid (MSeA) repressed interleukin-6-mediated (IL-6) androgen receptor action in prostate cancer progression

indicated that selenite significantly inhibited IL-6 activity in human prostate cancer (LNCaP) cells, but MSeA did not.[158]

Although these investigations indicate that the inorganic forms of selenium may be more effective for the prevention or treatment of diseases compared to the organic forms, further studies are necessary to evaluate the effects of selenium speciation for such purposes. While most studies have focused solely on selenite, the examination of other inorganic selenium compounds such as selenate, selenide, and selenium dioxide, in addition to organoselenium compounds, in antioxidant and anticancer experiments would aid in understanding the effects of selenium speciation within these inorganic and organo-selenium compounds on ROS-induced DNA damage and cell death.

Mechanisms of antioxidant and anticancer activity for inorganic selenium compounds

While the precise mechanisms of cancer prevention or treatment has not been elucidated for inorganic selenium compounds, several reports indicate that the protection against oxidative damage may involve selenoproteins, such as GPx and thioredoxin reductase, and may require supranutritional levels of selenium.[55,150,151,159-168] One proposed mechanism for the effects of cancer treatment by selenium compounds is the direct action of pro-oxidant selenometabolites to generate ROS, resulting in cellular toxicity.[57,148,169]

This ROS-generation mechanism involves the metabolism of selenite and selenate to generate hydrogen selenide (H_2Se), a by-product of selenium metabolic pathway.[148,170-172] High levels of selenide can then react with oxygen to produce ROS resulting in

oxidative damage to cells.[148,170,171] It has been suggested that the cytotoxicity of inorganic selenium compounds such as selenite and selenium dioxide is due to the formation of selenotrisulfides (RSSeSR), such as selenoglutathione, upon reaction with disulfide peptides or proteins (Reaction 7).[148,170,171] In more recent studies, this mechanism has also been attributed to the pro-oxidant effect of inorganic selenium compounds in different cell lines.[57,142,173-175]

This proposed mechanism for selenite cytotoxicity has been further supported by generation of superoxide upon reduction of selenotrisulfide (GSSeSG) to selenopersulfide anion ($GSSe^-$).[148] The selenopersulfide anion, in turn, is reduced by thiols to generate H_2Se (Reactions 7-9).[148] Selenide then reacts with oxygen to form elemental selenium (Se^0) and $O_2^{\bullet-}$ (Reaction 10).[148,170,171] Studies showing that selenite and selenium dioxide, but not selenate, are cytotoxic via this mechanism have been previously reviewed by Spallholz.[148]

$$SeO_3^{2-} + 4GSH + 2H^+ \rightarrow GSSG + GSSeSG + 3H_2O \quad (7)$$

$$GSSeSG + GSH \rightarrow GSSG + GSSe^- + H^+ \quad (8)$$

$$2GSSe^- + 4NADPH \rightarrow 2H_2Se + GSSG + 4NADP^+ \quad (9)$$

$$H_2Se + O_2 \rightarrow Se^0 + O_2^{\bullet-} + 2H^+ \quad (10)$$

In contrast, the mechanism for the antioxidant ability of both inorganic and organoselenium compounds in preventing iron-mediated oxidative DNA damage is through metal coordination between the iron and the selenium compounds.[23,149] Since Na_2SeO_3 and SeO_2 (0.5-5000 μM) showed no effect on DNA damage produced by completely coordinated $[Fe(EDTA)]^{2-}$ (400 μM), coordination of Fe^{2+} to inorganic

selenium compounds is a primary mechanism for both their antioxidant and pro-oxidant activities.[23] These results were also observed for organoselenium compounds under similar conditions.[49] For inorganic selenium compounds, oxidation state of the selenium atom may play a role in their ability to prevent iron-mediated DNA damage.[23] Although metal coordination to inorganic selenium compounds has not been directly observed in biological systems, iron, copper, mercury, and aluminum react with selenite, selenate or selenium dioxide to form complexes such as $Fe_2(H_2O)_4(SeO_3)_2$, $FeH(SeO_3)_2$, $Fe(HSeO_3)_3$ and $Al_2(SeO_3)_3 \cdot 3H_2O$,[176,177] where iron is coordinated through oxygen atoms of inorganic selenium compounds such as selenite (Figure 1.3).

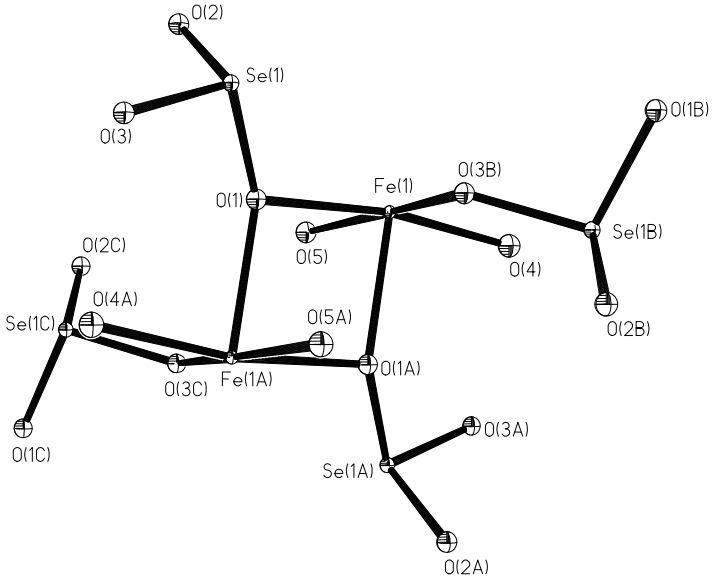

Figure 1.3. Coordination of iron to selenite in $Fe_2(H_2O)_4(SeO_3)_2$ reported by Xiao *et al.*[177]

Bioavailability and activity of oxo-sulfur and oxo-selenium compounds

Fruits, vegetables, cereal, nuts, and teas have been widely studied for their ability to ameliorate oxidative stress and their potential to prevent or treat cancer, aging, and

cardiovascular diseases.[54,62,94,95,178-180] The antioxidant capabilities of many foods are attributed to their vitamin, polyphenolic, selenium, and sulfur content.[53,54,62] Although there are many members of the *Allium* genus, including onions, leeks, scallions, and chives, garlic has been widely studied for its antioxidant activity.[53,54,81] For many centuries, garlic (*Allium sativum* Liliaceae) has been cultivated and used in food preparation for its distinct flavor and aroma, as well as for its medicinal properties.[53,54,81] Throughout the years, this bulb has been used to treat the plague, animal bites, leprosy, and cancer, as well as bacterial, immune, and cardiovascular diseases.[53,54,81,181-188]

The characteristic flavor and aroma of garlic are attributed to the volatile organosulfur compounds produced upon tissue damage and enzymatic hydrolysis from non-volatile precursors.[81,189] The vegetative parts of garlic are odorless and comprised of non-volatile sulfur storage compounds known as *S*-alk(en)yl-L-cysteine sulfoxides.[81,189] These compounds (Figure 1.2) are stored in the cytosol of undamaged *Allium* tissues protected from the enzyme alliinase, which is found in the vacuoles.[81,189] Upon tissue damage, alliinase and *S*-alk(en)yl-L-cysteine sulfoxides react to generate sulfenic acid that then undergoes condensation to form the volatile thiosulfonate compounds.[81,189] The *S*-alk(en)yl-L-cysteine sulfoxides detected in garlic and several other varieties of the *Allium* genus are S-allyl-L-cysteine sulfoxide (alliin, ACSO), *S*-methyl-L-cysteine sulfoxide (methiin, MeCysSO, MCSO), *S*-propyl-L-cysteine sulfoxide (propiin, PCSO) and *S*-trans-1-propenyl-L-cysteine sulfoxide (isoalliin, TPCSO).[81,189-192]

The medicinal properties of garlic are primarily attributed to the thiosulfonate compound, allicin produced from allin by alliinase when garlic is crushed (Figure

1.4).[193,194] While alliin is the main *S*-alk(en)yl-L-cysteine sulfoxide found in garlic, and is responsible for the volatile odor of cut or crushed garlic, MeCysSO is the most ubiquitous found in onions, chives, leeks and scallions in various quantities.[81]

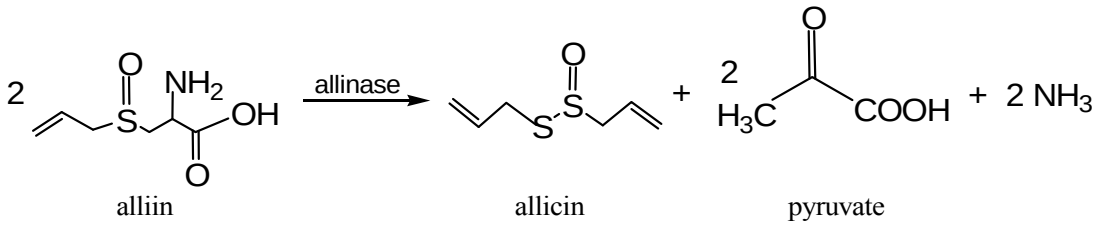

alliin allicin pyruvate

Figure 1.4. Production of allicin from alliin by alliinase.

In folk medicine, cauliflower (*Brassica oleracea* Liliaceae var. *botrytis*) is also used for its medicinal purposes.[80] The juice extracts from raw cauliflower leaves are expectorants and are used in the treatment of gastric and duodenum ulcers, whereas the stewed leaves have been used as antipyretics or antirheumatics.[80] These medicinal properties have been attributed to *S*-methyl methane thiosulfonate (MMTS), an oxo-sulfur compound found in cauliflower, broccoli, and cabbage, as well as in the *Allium* vegetables.[80,195-197]

Dimethyl sulfone or methylsulfonylmethane (Me_2SO_2) is another oxo-sulfur compound found in vegetables including broccoli, peppers, asparagus, and cabbage.[82,83] It can also be found in trace amounts in fish, meat, unpasteurized milk, beverages, and eggs and has more recently been used as a dietary supplement.[84-86] Currently, Me_2SO_2 is sold in over 30 products in combination with other dietary supplements such as chondroitin sulfate and glucosamine, and in more than 50 different products as a single agent in tablets, capsules, creams, and lotions.[198] Although some physicians suggest a daily dose of only 300 mg, the recommended daily dose of Me_2SO_2 is reported to be between 1000-

6000 mg when taken as a dietary supplement.[82] Me_2SO_2 is a metabolite of dimethyl sulfoxide (DMSO), a by-product of algae and phytoplankton decay, and is commercially synthesized by reacting hydrogen peroxide with DMSO to produce Me_2SO_2 and water (Reaction 11).[198,199] Studies have shown that ~15% of orally ingested DMSO is recovered as Me_2SO_2 in urine.[198-200]

$$Me_2SO + H_2O_2 \rightarrow Me_2SO_2 + H_2O \qquad (11)$$

Amino acids are major targets for oxidation by reactive oxygen species, and this oxidation can disrupt protein structure and function.[87] Methionine can be oxidized to methionine sulfoxide (MetSO) by ROS and reactive nitrogen species (RNS) such as hydrogen peroxide, hydroxyl radical, and peroxynitrite anion.[88,89,201] ROS-mediated oxidation of Met results in mixtures of *R*- and *S*-isomers of MetSO.[202] Metal-catalyzed oxidation of methionine occurs through Fenton or Fenton-like reactions when peptides reduce metals such as iron and copper subsequently producing hydroxyl radical upon reaction with hydrogen peroxide.[88,203-205]

MetSO can also be formed from methionine oxidized by H_2O_2 alone in the absence of metal ions (Figure 1.5),[206,207] and both peroxynitrous acid (ONOOH) and peroxynitrite also react with methionine to produce MetSO.[89,201] Methionine oxidation can result in changes in protein hydrophobicity, alterations in protein conformation, and disruption of biological function.[92,203,208-213] However, cells contain two enzymes that reduce MetSO to Met, repairing the oxidative damage.[88,90-92] Methionine sulfoxide reducatse A (MsrA) specifically reduces the *S*-isomer of MetSO, and methionine

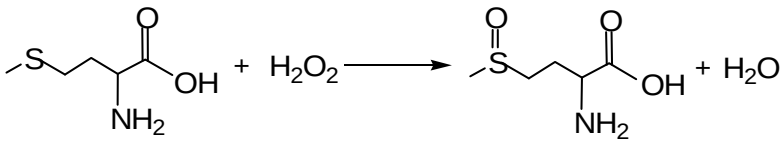

Figure 1.5. Oxidation of methionine to methionine sulfoxide by hydrogen peroxide.

sulfoxide reductase B (MsrB) is specific for reduction of the *R*-isomer.[88,90,92] Based on the reversibility of MetSO generation, MetSO formation is proposed to be important in regulating cell functions.[88,92,203,212,214-216] Interestingly, there have been reports on one biologically relevant oxo-seleno compound formed from the oxidation of selenomethionine (SeMet) by peroxynitrite to methionine selenoxide (MetSeO).[69,217,218] This oxidation is analogous to the peroxynitrite oxidation of methionine.[217]

Antioxidant and pro-oxidant effects of oxo-sulfur compounds in disease prevention

Many studies have reported on the antioxidant effects and amelioration of diseases using aged garlic extracts (AGE) and garlic essential oils.[219-221] Although these products are generally considered to be safe and may be effective in preventing diseases such as cancer, it is difficult to determine the bioactive sulfur component or mixture of components that is responsible for the observed biological effects.[219,220] Therefore, this review will focus on the ROS damage prevention (antioxidant) or ROS generation (pro-oxidant) abilities of individual oxo-sulfur compounds.

Several studies have shown that oxo-sulfur compounds play a significant role in preventing ROS-mediated cellular damage. For example, allicin, a major component in garlic, acts as a vasodilator, inhibits cholesterol biosynthesis, ameliorates serum lipid in

hyperlipidemic rabbits, and lowers intraocular pressure in normal rabbits.[193,222-225] In a separate study, both allicin and alliin had no effect in reducing lipid peroxidation induced by ferrous sulfate/ascorbic acid in microsomal membranes.[226] Another study to determine the effect of thiosulfonates on platelet aggregation showed that allicin inhibited 74% of such aggregation with an IC_{50} of 0.27 mM.[189] Hirsh *et al.* found that allicin (10-40 μM) inhibited cell proliferation in mammary, colon, and endometrial cancer cells with 50% inhibition at 10-25 μM.[193] Alliin, the precursor to allicin, showed no inhibitory effect at all concentrations tested (0-64 μM).[193]

Another oxo-sulfur compound found in *Allium* vegetables is MeCysSO; however, only a few studies have been performed on this possible antioxidant sulfur derivative, despite the fact that it is a major oxo-sulfur compound in garlic. MeCysSO is effective for the treatment of hyperglycemia and hyperlipidemia in diabetic rats.[227-230] In addition, daily oral administration of MeCysSO (200 mg/kg) for 45 days significantly controlled blood glucose and lipids in tissues and serum of diabetic rats.[227] The activities of HMG CoA reductases, liver hexokinase, and glucose-6-phosphate in these animals were close to normal upon MeCysSO treatment, effects similar to the anti-diabetic drugs glibenclamide and insulin.[227] Augustini *et al*. also observed that that MeCysSO was effective in lowering total cholesterol levels in rats.[229]

Similar to allicin, MMTS also has chemopreventative properties.[195] Nakamura *et al*. found that MMTS isolated from cauliflower homogenate showed strong antimutagenic activity against UV-induced mutation in wildtype *E. coli* (B/r WP2), but not in mutant cell strains lacking excision-repair activities.[195-197] A separate study by the

same group showed that MMTS (10 mg/kg) suppressed the frequency of aflotoxin B_1-induced chromosome aberrations after 2 h.[195] Additionally, Kawamori *et al*. reported that MMTS (20 and 100 ppm) inhibited 42 % and 21% of intestinal neoplasm incidences induced by azoxymethane in rats, respectively.[231]

MMTS also decreased the incidence of phenobarbital-promoted or diethylnitrosamine-initiated hepatocarcinogenesis in rats.[232] In *Drosophilia melanogaster* and mice micronuclei, MMTS was found to reduce mitomycin C-induced somatic mutation and recombination via oral administration.[232] Experiments performed with various antioxidants, including Kefir grain extracts, showed that both Kefir extracts (900-21,000 μg/mL) and MMTS (10 μg/mL) stimulated more than 50% thymine dimer repair in UVC-irradiated HMV-1 cells, whereas other antioxidants tested (epigallocatechin and vitamins A, C, E, and K) showed little repair enhancement (≤ 10-30 %).[233]

While the use of Me_2SO_2 in commercially available products is generally considered safe, little data is available to assess the safety and toxicity of this oxo-sulfur compound. Unconfirmed side effects of Me_2SO_2 consumption include headaches, hypertension, gastrointestinal symptoms, insomnia (if taken before bedtime), and increased hepatic enzyme levels.[198] The Me_2SO_2 oxo-sulfur compound has been used in the treatment of inflammation, parasitic infections, allergies, asthma, cancer, arthritis, and rheumatic pain.[198,199] Due to its sulfur content, it has also been used in the nourishment of hair, fingernails, and skin, and in the maintenance of normal connective tissues.[198,234] In one study to determine the acute (2000 mg/kg/day) and chronic (1500 mg/kg/day) effects

on rats, oral administration of Me_2SO_2 for 90 days did not affect body weight, histopathological lesions in tissues and organs, hematological parameters, or mortality.[82]

Early pharmacokinetic studies showed that ~64% of [^{35}S]Me_2SO_2 (21 mg/kg) was excreted within 24 h upon intraperitoneal administration to rats.[235] In a more recent study, the distribution of Me_2SO_2 administered orally for 7 days using a ^{35}S radioisotope tracer found that [^{35}S] Me_2SO_2 (470 mg/kg/day) was excreted in urine (~70%) and feces (~10%).[236] The highest levels of radioactivity were found in hair, blood, and spleen.[236] Further investigations of Me_2SO_2 pharmacokinetics in rats was performed by Magnuson *et al*.[84] They also used radiolabled [^{35}S]Me_2SO_2 to determine that Me_2SO_2 is rapidly absorbed, well distributed, and efficiently eliminated.[84] Oral administration of 500 mg/kg in rats showed that the majority of Me_2SO_2 was excreted in urine (~57%), with only 1.6% excreted in feces.[84] After 48 h, Me_2SO_2 was distributed evenly in several tissues, corresponding to blood concentrations of this compound.[84]

Two separate studies performed by Cottler-Fox *et al*. and Wever *et al*. found that Me_2SO_2 was present in human plasma and cerebrospinal fluid ranging from 0-25 μM,[237,238] and Lawrence *et al*. reported that this oxo-sulfur compound occurs naturally in blood with a concentration of 3 μM.[83] Me_2SO_2 was also detected by magnetic resonance spectroscopy in the brains of patients with memory loss and in normal patients given doses of 1-3 g/day.[239] In this investigation, Me_2SO_2 was found to be distributed equally between white and grey matter of the brain in all patients, ranging from 0.42-3.40 mmol/kg, with no adverse neurochemical or clinical effects.[239] Me_2SO_2 was also

detected in the brain at a concentration of 2.36 mM in a normal patient after taking Me_2SO_2 at a dosage of 181 mg/kg/day.[240]

While the suggested use of Me_2SO_2 is as a dietary supplement for the treatment of arthritis and allergies, only a few studies have reported such activities.[199,241,242] A 12-week randomized and controlled study on individuals with knee osteoarthritis was conducted, with each of the 118 patients given Me_2SO_2 (1.5 g/d). One-third reported decrease in pain; joint mobility and improved walking time was also observed.[242] In a second study, 21 patients with osteoarthritis given Me_2SO_2 (3 g) twice daily for a 12-week period showed decreases in pain (25%), stiffness (20%), physical function (31%), and total symptoms (25%).[198] Interestingly, in this study, patients in the placebo group also showed decreases in pain, stiffness, physical function, and total symptoms (~13%, 12%, 17%, and 14%, respectively).[198] Although Me_2SO_2 may ameliorate the effects of osteoarthritis, its full effects were not observed in such a short period of time, indicating the need for longer trials.[198] A study to evaluate the efficacy of Me_2SO_2 for reduction of seasonal allergy rhinitis (SAR) symptoms such as headaches, sinus infections, breathing difficulties, and nasal congestion was performed by Barrager *et al*.[199] The results of this study indicate that Me_2SO_2 supplementation of 2600 mg/d over a period of 30 days was effective in reducing the symptoms of SAR.[199] Me_2SO_2 was also found to have minimal side effects suggesting that this oxo-sulfur compound may be therapeutic and has pharmaceutical significance for the amelioration of SAR-associated symptoms.[199]

Antioxidant and pro-oxidant mechanisms of oxo-sulfur compounds

Although numerous studies show that oxo-sulfur compounds can be used in the treatment or prevention of several diseases including cancer and osteoarthritis, the mechanisms of such action has not been elucidated.[193-195,198,211,219,228,232] Studies by Weiner *et al*. indicate two possible mechanisms for the biological activity of allicin: radical scavenging or its ability to react with thiols.[194] Spin trapping techniques and EPR measurements were used to show that allicin efficiently scavenged $^{\bullet}OH$ produced by the Fenton reaction.[194] The ability of allicin to inhibit the functions of thiol-containing proteins such as papain and alcohol dehydrogenase was also suggested as a possible mechanism.[194]

The susceptibility of Met to oxidation results in antioxidant activities due to the radical scavenging capability of Met, and the ability of Msr to reduce MetSO back to Met.[211] Evidence of such antioxidant activity is observed in studies performed in yeast and *Drosophilia*, which showed that over-expression of the MsrA gene prevents oxidative stress induced by toxic levels of hydrogen peroxide and paraquat.[243,244] Studies performed on various bacterial strains and yeast lacking the MsrA gene found that these strains were more susceptible to paraquat- or H_2O_2-induced oxidative stress.[243,245,246] Under normal growth conditions, studies performed on MsrA knockout mice resulted in a 40% decrease of maximal life-span upon exposure to 100% oxygen.[247] In other studies, Met residues on the lipoprotein surface reduced low-density (LDL) and high-density (HDL) lipoprotein-generated peroxides and cholesterolester peroxide to their respective hydroxyl derivatives.[92,248]

The oxidation of methionine to methionine sulfoxide has been implicated in aging, Alzheimer's respiratory distress syndrome, and emphysema.[212,214] A study by Costabel *et al*. showed that methionine oxidation by neutrophil-generated ROS results in acute and chronic bronchitis, dependent on the Met/MetSO ratio in lavage fluid in the bronchialveolar.[249] An investigation by Stadtman *et al*. indicated that surface hydrophobicity of rat liver proteins increased with age over a period of 24 months.[210] This study also indicated that increases in both hydrophobicity and MetSO levels were caused by protein oxidation from ROS.[210]

Gradual decreases in the levels of MsrA activity in the brain and kidney tissues of rats was found to be age-related, whereas in liver tissues, no age-related loss of enzyme activity was observed.[250] MsrA activity in rat kidney and brain tissues decreased from ~5 pmol/μg/h and ~0.55 pmol/μg/h, respectively, at 5 months of age to ~3.5 pmol/μg/h and ~4 pmol/μg/h, respectively, at 25 months.[250] In addition, the proposed Met/MetSO antioxidant cycle may aid in the prevention of Alzheimer's disease.[88,251] A study performed by Marksbery *et al*. showed that in various brain regions of Alzheimer's patients, the level of MetSO and protein carbonyls, another measure of oxidative damage, was significantly greater than in the brains of patients without this disease.[251]

In an animal study, 67% of Met residues in rat brain calmodulin were oxidized to MetSO in aged rats.[252] Experiments by Wells-Knecht and co-workers showed that in humans, the methionine sulfoxide content of skin collagen increases from approximately 4% while young to approximately 12% at 80 years of age.[253] Collectively, these studies indicate the oxidation and reduction processes of methionine, as well as the expression of

MsrA, play an important role in the prevention of ROS-mediated diseases. Interestingly, methionine oxidation increases protein hydrophobicity, despite the fact that Met is more hydrophobic than MetSO.[210,254] Further investigations are therefore needed to better understand effects of the Met/MetSO oxidation cycle at the molecular level, since local changes in protein folding may play a role in hydrophobicity alterations.[214]

Similar to DNA inhibition experiments performed with inorganic selenium compounds, the ability of oxo-sulfur compounds to prevent metal-mediated DNA damage has also been investigated. MetSO, MeCysSO, MMTS, Me_2SO_2, and methyl phenyl sulfoxide (MePhSO; Figure 1.2) showed little inhibition of iron-mediated oxidative DNA damage. While MeCysSO and MMTS inhibited 17% and 20% DNA damage at 1000 μM, respectively, the other oxo-sulfur compounds showed no effect on DNA damage.[51] Likewise, Me_2SO_2 and MePhSO have no effect on copper-mediated DNA damage, whereas MMTS (1000 μM) is a pro-oxidant, producing 35% damaged DNA, and both MetSO and MeCysSO are efficient antioxidants with IC_{50} values of 18 ± 3 μM and 8.1 ± 1 μM, respectively.[51] Interestingly, the reduced forms of MeCysSO and MetSO, MeCys and Met, were also effective antioxidants with IC_{50} values of 8.9 ± 0.02 μM and 11.2 ± 0.02 μM, respectively.[49] Thus, the ability of these sulfur-containing amino acids to prevent copper-mediated DNA damage does not significantly change upon oxidation.[51]

Similar to the results obtained with the inorganic selenium compounds, metal coordination is also a mechanism for antioxidant activity of oxo-sulfur compounds.[23,49,51,74,149] Brumaghim *et al.* showed that sulfur compounds with the ability

to prevent copper-mediated DNA damage have a Cu-S charge transfer band at ~240 nm when combined with Cu^+, indicative of copper-sulfur coordination. Both MetSO and MeCysSO show similar UV bands with Cu^+, also indicating copper binding to these compounds.[49,51,74] Interestingly, in gel electrophoresis experiments using 2,2'-bipyridine (bipy) to completely coordinate Cu^+, MetSO and MeCysSO at 1000 μM, inhibited 43% and 88% of $[Cu(bipy)_2]^+$-mediated DNA damage, respectively, significantly less than the inhibition observed for uncoordinated Cu^+.[51] These studies also demonstrate that metal coordination is a primary mechanism for the antioxidant activity of MetSO and MeCysSO, but a second mechanism, such as radical scavenging, may also be responsible for their DNA damage prevention at high concentrations.[51] Under similar conditions, MMTS (5000 μM) is a pro-oxidant, damaging 44% DNA in the presence of $[Cu(bipy)_2]^+/H_2O_2$, indicating that copper coordination is not required for its pro-oxidant activities.[51] These experiments indicate that the antioxidant or pro-oxidant activities of sulfur compounds are quite complex, and highlight the importance of understanding the conditions and mechanisms for such behavior.

Recently, aryl sulfoxides such as phenyl sulfoxide (PhSO) and MePhSO (Figure 1.2) have been found to generate ROS upon irradiation, with implicated use in cancer therapy.[255-257] Interestingly, little has been reported on the effects of this ROS generation on DNA damage. Predecki *et al*. showed that photoactivation at 240 nm of PhSO and MePhSO results in 83% DNA damage at 180 μM and 360 μM, respectively.[256] In this experiment, 2,2,6,6-tetramethylpiperdine-1-oxyl (TEMPO) scavenged carbon-based radicals, indicating that the possible mechanism for photoinduced-DNA damage by aryl

sulfoxides is caused by hydrogen abstraction from the DNA backbone to produce a DNA radical.[256] It is assumed that the reaction between the DNA radical and oxygen is responsible for DNA damage generated by PhSO and MePhSO.[256,257] Oxygen, in its ground state ($^3O_2$), may also be necessary for the pro-oxidant effects of PhSO, since photo-induced DNA damage was inhibited in the absence of oxygen.[256] These studies clearly indicate that the mechanistic action of oxo-sulfur compounds either as antioxidants or pro-oxidants is quite complex, and further studies under biologically relevant conditions are essential to better understand the activity of these compounds in biological systems.

Oxo-selenium compounds

The naturally occurring amino acid, selenomethionine (SeMet) is found in many proteins in place of its sulfur analog, methionine.[258,259] Similar to methionine oxidation to its corresponding sulfoxide, SeMet is also oxidized by peroxynitrite and enzymes such as flavin-containing monooxygenases (FMOs) to methionine selenoxide (MetSeO).[69,217,218,258] A significant amount of research has investigated Met/MetSO interconversion, but little work has investigated the properties of MetSeO. Oxidation kinetics of SeMet are 10-1000 times faster than oxidation of methionine to produce MetSeO.[218] While the effects of MetSeO in biological systems have not been reported, it is possible that this compound may lead to similar changes in hydrophobicity, conformation, and disruption of biological functions associated with its sulfur analog, MetSO.[92,203,208-213] In light of this, Sies and colleagues investigated the reduction of

MetSeO to SeMet using glutathione (GSH) as a reductant.[217] This study showed that addition of MetSeO (0.4 mM) to increasing concentrations of GSH resulted in a loss of MetSeO with an increase in SeMet (Reaction 12), suggesting that GSH in low concentrations is effective in the protection against oxidants and that GSH may be responsible for redox cycling of selenoxides.[217]

$$\text{MetSeO} + 2\ \text{GSH} \rightarrow \text{SeMet} + \text{GSSG} + \text{H}_2\text{O} \qquad (12)$$

Apart from its role in protein function, SeMet metabolism by the methionine transsulfuration pathway produces selenocysteine, an essential amino acid for the function of several antioxidant enzymes including glutathione peroxidase and thioredoxin reductase.[258,260] Interestingly, FMOs also have been shown to oxidize other selenium compounds, including the selenium containing drug ebselen, to their corresponding selenoxides.[261] Thus, further investigations are necessary to determine the effects of oxidation on protein function and activity and the conditions required for antioxidant and pro-oxidant activity of oxidized sulfur and selenium compounds, including selenium-containing drugs.

Conclusions

Investigating the antioxidant and anticancer properties of inorganic selenium and oxo-sulfur compounds in the treatment of diseases such as cancer, aging, and neurodegenerative diseases generated from reactive oxygen species is an active and promising area of research. In the case of inorganic selenium compounds, sodium selenite is the compound of choice for both antioxidant and anticancer studies. While the

mechanism for its antioxidant activity is unclear, it has been proposed that the ability of selenocysteine containing enzymes such as GPx and thioredoxin reductases to prevent radical formation as a possible mechanism.[57] The generation of hydrogen selenide from selenometabolites such as selenite to produce toxic ROS is suggested as a possible mechanism for the pro-oxidant and anticancer properties of inorganic selenium compounds.[55,57]

The antioxidant activity of oxo-sulfur compounds is much less understood than that of the inorganic selenium compounds. Most studies have focused on allicin, an oxo-sulfur compound produced from crushed garlic; however, disparities concerning the antioxidant activity of allicin are attributed to other endogenous components remaining from the extraction process of crude garlic extracts.[53,54] While MMTS and other oxo-sulfur compounds may be effective in the treatment or prevention of cancer, their mode of action has not been investigated. Similarly, little is known about the antioxidant activity of MeCysSO, MetSeO and MePhSO; however, the ability of MetSO to prevent ROS-mediated diseases such as aging, emphysema, and Alzheimer's has been attributed to the cyclic interconversion of MetSO by methionine sulfoxide reductases.[212,214] Although MeCysSO and MetSeO are analogous to MetSO, little has been done to determine the effects of these compounds in biological systems. Since MeCysSO and MetSeO are formed from the oxidation of amino acids essential for protein function, investigating the ability of these compounds to act as antioxidants, as well as their role in disease prevention is of great interest. Therefore, further experiments including both *in vitro*, and cellular and animal studies are required to investigate such behaviors. In

addition, studies are also needed to determine the effects of the sulfur compounds' structural and chemical properties on their antioxidant activity.

Investigations of the ability of inorganic selenium and oxo-sulfur compounds to inhibit metal-mediated oxidative DNA damage determined that coordination between iron or copper and the antioxidant compound is required for prevention of DNA damage.[23,51] Additionally, the ability of oxo-sulfur compounds to scavenge radicals was also suggested as a possible mechanism for this activity, particularly at high concentrations.[51] Further investigations to determine the role of metal coordination and radical scavenging mechanisms of antioxidant behavior as well as the conditions required to observe pro-oxidant properties of oxo-sulfur compounds are necessary to fully understand the biological activities of these compounds.

In addition, the role of less studied compounds such as selenate, selenium dioxide, methylcysteine sulfoxide, and methionine selenoxide in the prevention of ROS-mediated disease is necessary to better understand and elucidate a mechanism for the antioxidant and pro-oxidant activities of both inorganic and oxo-sulfur compounds. Although the speciation of selenium compounds is an important factor in the biological activities of these compounds,[152-154] more studies using a larger number of selenium compounds including selenide, selenate, and selenoxides are required to fully understand this effect. Most of the inorganic selenium and oxo-compounds discussed in this review are obtained from food products such as vegetables, fruits, nuts, and dietary supplements. However, these foods and supplements may also contain other antioxidant or bioactive ingredients.[1,46,47] It is therefore equally important to determine the effects of other

bioactive compounds on the biological activity of inorganic and oxo-sulfur compounds. Additional studies exploring the antioxidant, pro-oxidant, and mechanistic actions of inorganic selenium, oxo-sulfur, and oxo-selenium compounds are essential to fully understand the biological implications of food products and supplements for both humans and animals.

References

(1) Valko, M.; Leibfritz, D.; Moncol, J.; Cronin, M. T.; Mazur, M.; Telser, J. *Int. J. Biochem. Cell Biol.* **2007**, *39*, 44-84.

(2) Valko, M.; Rhodes, C. J.; Moncol, J.; Izakovic, M.; Mazur, M. *Chem. Biol. Interact.* **2006**, *160*, 1-40.

(3) Storz, G.; Imlay, J. A. *Curr. Opin. Microbiol.* **1999**, *2*, 188-194.

(4) Farr, S. B.; Kogoma, T. *Microbiol. Rev.* **1991**, *55*, 561-585.

(5) Cadenas, E.; Davies, K. J. *Free Radic. Biol. Med.* **2000**, *29*, 222-230.

(6) Orrenius, S.; Gogvadze, V.; Zhivotovsky, B. *Annu. Rev. Pharmacol. Toxicol.* **2007**, *47*, 143-183.

(7) Marnett, L. J. *Carcinogenesis* **2000**, *21*, 361-370.

(8) Huang, X. *Mutat. Res.* **2003**, *533*, 153-171.

(9) Halliwell, B. *Drugs Aging* **2001**, *18*, 685-716.

(10) Markesbery, W. R. *Free Radic. Biol. Med.* **1997**, *23*, 134-147.

(11) Markesbery, W. R.; Carney, J. M. *Brain Pathol.* **1999**, *9*, 133-146.

(12) Markesbery, W. R.; Lovell, M. A. *Antioxid. Redox Signal.* **2006**, *8*, 2039-4205.

(13) Ide, T.; Tsutsui, H.; Hayashidani, S.; Kang, D.; Suematsu, N.; Nakamura, K.; Utsumi, H.; Hamasaki, N.; Takeshita, A. *Circ. Res.* **2001**, *88*, 529-535.

(14) Steinberg, D. *J. Biol. Chem.* **1997**, *272*, 20963-20966.

(15) Dhalla, N. S.; Temsah, R. M.; Nettican, T. *J. Hypertens.* **2000**, *18*, 655-673.

(16) Kastan, M. B. *Mol. Cancer Res.* **2008**, *6*, 517-524.

(17) McCormick, M. L.; Buettner, G. R.; Britigan, B. E. *J. Bacteriol.* **1998**, *180*, 622-625.

(18) Henle, E. S.; Linn, S. *J. Biol. Chem.* **1997**, *272*, 19095-19098.

(19) Flint, D. H.; Tuminello, J. F.; Emptage, M. H. *J. Biol. Chem.* **1993**, *268*, 22369-22376.

(20) Park, S.; Imlay, J. A. *J. Bacteriol.* **2003**, *185*, 1942-1950.

(21) Rodriguez, H.; Holmquist, G. P.; D'Agostino, R., Jr.; Keller, J.; Akman, S. A. *Cancer Res.* **1997**, *57*, 2394-2403.

(22) Seaver, L. C.; Imlay, J. A. *J. Biol. Chem.* **2004**, *279*, 48742-48750.

(23) Ramoutar, R. R.; Brumaghim, J. L. *J. Inorg. Biochem.* **2007**, *101*, 101028-35.

(24) Imlay, J. A.; Chin, S. M.; Linn, S. *Science* **1988**, *240*, 640-642.

(25) Imlay, J. A.; Linn, S. *Science* **1988**, *240*, 1302-1309.

(26) Hoffmann, M. E.; Mello-Filho, A. C.; Meneghini, R. *Biochim. Biophys. Acta* **1984**, *781*, 234-238.

(27) Henle, E. S.; Han, Z.; Tang, N.; Rai, P.; Luo, Y.; Linn, S. *J. Biol. Chem.* **1999**, *274*, 962-971.

(28) Nunoshiba, T.; Obata, F.; Boss, A. C.; Oikawa, S.; Mori, T.; Kawanishi, S.; Yamamoto, K. *J. Biol. Chem.* **1999**, *274*, 34832-34837.

(29) Pastor, N.; Weinstein, H.; Jamison, E.; Brenowitz, M. *J. Mol. Biol.* **2000**, *304*, 55-68.

(30) Emerit, J.; Beaumont, C.; Trivin, F. *Biomed. Pharmacother.* **2001**, *55*, 333-339.

(31) Stohs, S. J.; Bagchi, D. *Free Radic. Biol. Med.* **1995**, *18*, 321-336.

(32) Lippard, S. J.; Berg, J. M.; University Science Books: Mills Valley, 1994.

(33) Keyer, K.; Imlay, J. A. *Proc. Natl. Acad. Sci. USA* **1996**, *93*, 13635-13640.

(34) Woodmansee, A. N.; Imlay, J. A. *Methods Enzymol.* **2002**, *349*, 3-9.

(35) Lippard, S. J. *Science* **1999**, *284*, 748-749.

(36) Rae, T. D.; Schmidt, P. J.; Pufahl, R. A.; Culotta, V. C.; O'Halloran, T. V. *Science* **1999**, *284*, 805-808.

(37) Yang, L.; McRae, R.; Henary, M. M.; Patel, R.; Lai, B.; Vogt, S.; Fahrni, C. J. *Proc. Natl. Acad. Sci. USA* **2005**, *102*, 11179-11184.

(38) Que, E. L.; Domaille, D. W.; Chang, C. J. *Chem. Rev.* **2008**, *106*, 1517-1549.

(39) Brown, D. R.; Qin, K. F.; erms, J. W.; Madlung, A.; Manson, J.; Strome, R.; Fraser, P. E.; Kruck, T.; vonBohlen, A.; Schulz-Schaeffer, W.; Giese, A.; Weataway, D.; Krestzschmar, H. *Nature* **1997**, *390*, 684-687.

(40) Stockel, J.; Safar, J.; Wallace, A. C.; Cohen, F. E.; Prusiner, S. B. *Biochemistry* **1998**, *37*, 7185-7193.

(41) Imlay, J. A.; Linn, S. *J. Bacteriol.* **1986**, *166*, 519-527.

(42) Imlay, J. A.; Linn, S. *J. Bacteriol.* **1987**, *169*, 2967-2976.

(43) Mello-Filho, A. C.; Meneghini, R. *Mutat. Res.* **1991**, *251*, 109-113.

(44) Singal, P. K.; Khaper, N.; Palace, V.; Kumar, D. *Cardiovasc. Res.* **1998**, *40*, 426-432.

(45) Collins, A. R. *BioEssays* **1999**, *21*, 238-246.

(46) Siman, C. M.; Eriksson, U. J. *Diabetes* **1997**, *46*, 1054-1061.

(47) Siman, C. M.; Eriksson, U. J. *Diabetologia* **1997**, *40*, 1416-1424.

(48) Ames, B. N. *Mutat. Res.* **2001**, *475*, 7-20.

(49) Battin, E. E.; Brumaghim, J. L. *J. Inorg. Biochem.* **2008**, *102*, 2036-2042.

(50) Perron, N. R.; Hodges, J. N.; Jenkins, M.; Brumaghim, J. L. *Inorg. Chem.* **2008**, *47*, 6153-6161.

(51) Ramoutar, R. R.; L., B. J. *Main Group Chem.* **2007**, *6*, 143-153.

(52) Combs, G. F.; Gray, W. P. *Pharmacol. Ther.* **1998**, *79*, 179-192.

(53) Xiao, H.; Parkin, K. L. *J. Agric. Food Chem.* **2002**, *50*, 2488-2493.

(54) Yin, M.-C.; Cheng, W.-S. *J. Agric. Food Chem.* **1998**, *46*, 4097-4101.

(55) Holmgren, A. *Free Radic. Biol. Med.* **2006**, *41*, 862-865.

(56) Schrauzer, G. N. *J. Am. Coll. Nutr.* **2001**, *20*, 1-4.

(57) Takahashi, M.; Sato, T.; Shinohara, F.; Echigo, S.; Rikiishi, H. *Int. J. Oncol.* **2005**, *27*, 489-495.

(58) Zhong, W.; Oberley, T. D. *Cancer Res.* **2001**, *61*, 7071-7078.

(59) Finley, J. W.; Ip, C.; Lisk, D. J.; Davis, C. D.; Hintze, K. J.; Whanger, P. D. *J. Agric. Food Chem.* **2001**, *49*, 2679-2683.

(60) Spallholz, J. E.; Mallory Boylan, L.; Rhaman, M. M. *Sci. Total Environ.* **2004**, *323*, 21-32.

(61) Gladyshev, V. N.; Kryukov, G. V. *BioFactors* **2001**, *14*, 87-92.

(62) Tapiero, H.; Townsend, D. M.; Tew, K. D. *Biomed. Pharmacother.* **2003**, *57*, 134-144.

(63) Brown, K. M.; Arthur, J. R. *Public Health Nutr.* **2001**, *4*, 593-599.

(64) Stadtman, T. C. *Annu. Rev. Biochem.* **2002**, *71*, 1-16.

(65) Brigelius-Flohe, R. *Free Radic. Biol. Med.* **1999**, *27*, 951-965.

(66) Cartes, P.; Gianfreda, L.; Mora, M. L. *Plant Soil* **2005**, *276*, 359-367.

(67) Rotruck, J. T.; Pope, A. L.; Ganther, H. E.; Swanson, A. B.; Hafeman, D. G.; Hoekstra, W. G. *Science* **1973**, *179*, 588-590.

(68) Tinggi, U. *Toxicol. Lett.* **2003**, *137*, 103-110.

(69) Beilstein, M. A.; Whanger, P. D. *J. Nutr.* **1986**, *116*, 1711-1719.

(70) Abdulah, R.; Miyazaki, K.; Nakazawa, M.; Koyoma, H. *J. Trace Elem. Med. Biol.* **2005**, *19*, 141-150.

(71) Atmaca, G. *Yonsei Med. J.* **2004**, *45*, 776-788.

(72) Waschulewski, I. H.; Sunde, R. A. *Br. J. Nutr.* **1988**, *60*, 57-68.

(73) Fairweather-Tait, S. J. *Eur. J. Clin. Nutr.* **1997**, *51* S20-S23.

(74) Battin, E. E.; Perron, N. R.; Brumaghim, J. L. *Inorg. Chem.* **2006**, *45*, 499-501.

(75) Davis, C. D.; Feng, Y.; Hein, D. W.; Finley, J. W. *J. Nutr.* **1999**, *129*, 63-69.

(76) Ip, C.; Hayes, C. *Carcinogenesis* **1989**, *10*, 921-925.

(77) Hamilton, E. E.; Wilker, J. J. *J. Biol. Inorg. Chem.* **2004**, *9*, 894-902.

(78) Nilsonne, G.; Sun, X.; Nystrom, C.; Rundlof, A. K.; Potamitou Fernandes, A.; Bjornstedt, M.; Dobra, K. *Free Radic. Biol. Med.* **2006**, *41*, 874-885.

(79) Zhou, N.; Xiao, H.; Li, T. K.; Nur, E. K. A.; Liu, L. F. *J. Biol. Chem.* **2003**, *278*, 29532-29537.

(80) Lima, E. A. C.; Dire, G.; Mattos, D. M. M.; Freitas, R. S.; Gomes, M. L.; de Oliveira, M. B. N.; Faria, M. V. C.; Jales, R. L.; Bernardo-Filho, M. *Food Chem. Toxicol.* **2002**, *40*, 919-923.

(81) Rose, P.; Whiteman, M.; Moore, P. K.; Zhu, Y. Z. *Nat. Prod. Rep.* **2005**, *22*, 351-368.

(82) Horvath, K.; Noker, P. E.; Somfai-Relle, S.; Glavits, R.; Financsek, I.; Schauss, A. G. *Food Chem. Toxicol.* **2002**, *40*, 1459-1462.

(83) Lawrence, R. M. *Int. J. Anti-Aging Med.* **1998**, *1*, 50-57.

(84) Magnuson, B. A.; Appleton, J.; Ryan, B.; Matulka, R. A. *Food Chem. Toxicol.* **2007**, *45*, 977-984.

(85) Pearson, T. W.; Dawson, H. J.; Lackey, H. B. *J. Agric. Food Chem.* **1981**, *29*, 1089-1091.

(86) Silva Ferreira, A. C.; Rodrigues, P.; Hogg, T.; Guedes, D. P. *J. Agric. Food Chem.* **2003**, *51*, 727-732.

(87) Berlett, B. S.; Stadtman, E. R. *J. Biol. Chem.* **1997**, *272*, 20313-20316.

(88) Hoshi, T.; Heinemann, S. *J. Physiol.* **2001**, *531*, 1-11.

(89) Perrin, D.; Koppenol, W. H. *Arch. Biochem. Biophys.* **2000**, *377*, 266-272.

(90) Levine, R. L.; Berlett, B. S.; Moskovitz, J.; Mosoni, L.; Stadtman, E. R. *Mech. Ageing Dev.* **1999**, *107*, 323-332.

(91) Schoneich, C. *Arch. Biochem. Biophys.* **2002**, *397*, 370-376.

(92) Stadtman, E. R.; Moskovitz, J.; Levine, R. L. *Antioxid. Redox. Signal.* **2003**, *5*, 577-582.

(93) Kim, H. Y.; Gladyshev, V. N. *Biochem. J.* **2007**, *407*, 321-329.

(94) Pennington, J. A.; Schoen, S. A. *Int. J. Vitam. Nutr. Res.* **1996**, *66*, 350-362.

(95) Pennington, J. A.; Schoen, S. A. *Int. J. Vitam. Nutr. Res.* **1996**, *66*, 342-349.

(96) Burk, R. F. *Nutr. Clin. Care* **2002**, *5*, 75-79.

(97) Deore, M. D.; Srivastava, A. K.; Sharma, S. K. *Toxicology* **2005**, *213*, 169-174.

(98) Yang, G.; Wang, S.; Zhou, R.; Sun, S. *Am. J. Clin. Nutr.* **1983**, *37*, 872-881.

(99) Longnecker, M. P.; Taylor, P. R.; Levander, O. A.; Howe, M.; Veillon, C.; McAdam, P. A.; Patterson, K. Y.; Holden, J. M.; Stampfer, M. J.; Morris, J. S.; et al. *Am. J. Clin. Nutr.* **1991**, *53*, 1288-1294.

(100) Koller, L. D.; Exon, J. H. *Can. J. Vet. Res.* **1986**, *50*, 297-306.

(101) MacDonald, D. W.; Christian, R. G.; Strausz, K. I.; Roff, J. *Can. Vet. J.* **1981**, *22*, 279-281.

(102) Gissel-Nielsen, G.; Gupta, U. C.; Lamand, M.; Westermarck, T. *Adv. Agron.* **1984**, *37*, 397-460.

(103) Gupta, U. C.; Gupta, S. C. *Commun. Soil Sci. Plant Anal.* **2000**, *31*, 1791-1807.

(104) Gupta, U. C.; Watkinson, J. H. *Outlook Agric.* **1985**, *14*, 183-189.

(105) Kubota, J.; Allaway, W. H.; Carter, D. L.; Cary, E. E.; Lazar, V. A. *J. Agric. Food Chem.* **1967**, *15*, 448-453.

(106) Aro, A.; Alfthan, G.; Varo, P. *Analyst* **1995**, *120*, 841-843.

(107) Thomson, C. D.; Robinson, M. F. *Eur. J. Clin. Nutr.* **1996**, *50*, 107-114.

(108) Whelan, B. R.; Barrow, N. J. *Fert. Res.* **1994**, *38*, 183-188.

(109) Whelan, B. R.; Peter, D. W.; Barrow, N. J. *Aust. J. Agric. Res.* **1994**, *45*, 863-875.

(110) Whelan, B. R.; Peter, D. W.; Barrow, N. J. *Aust. J. Agric. Res.* **1994**, *45*, 877-887.

(111) Pedrero, Z.; Madrid, Y.; Camara, C. *J. Agric. Food Chem.* **2006**, *54*, 2412-2417.

(112) Taylor, E. W. *Biol. Trace Elem. Res.* **1995**, *49*, 85-95.

(113) Cheng, Y. Y.; Qian, P. C. *Biomed. Environ. Sci.* **1990**, *3*, 422-428.

(114) Hartikainen, H. *J. Trace Elem. Med. Biol.* **2005**, *18*, 309-318.

(115) Vanderpas, J. B.; Contempre, B.; Duale, N. L.; Deckx, H.; Bebe, N.; Longombe, A. O.; Thilly, C. H.; Diplock, A. T.; Dumont, J. E. *Am. J. Clin. Nutr.* **1993**, *57*, 271S-275S.

(116) Vanderpas, J. B.; Contempre, B.; Duale, N. L.; Goossens, W.; Bebe, N.; Thorpe, R.; Ntambue, K.; Dumont, J.; Thilly, C. H.; Diplock, A. T. *Am. J. Clin. Nutr.* **1990**, *52*, 1087-1093.

(117) Chen, L.; Yang, F.; Xu, J.; Hu, Y.; Hu, Q.; Zhang, Y.; Pan, G. *J. Agric. Food Chem.* **2002**, *50*, 5128-5130.

(118) Yang, C.; Niu, C.; Bodo, M.; Gabriel, E.; Notbohm, H.; Wolf, E.; Muller, P. K. *Biochem. J.* **1993**, *289*, 829-835.

(119) Allander, E. *Scand. J. Rheumatol. Suppl.* **1994**, *99*, 1-36.

(120) Arthur, J. R.; Beckett, G. J. *Br. Med. Bull.* **1999**, *55*, 658-668.

(121) Schofield, F. W. *Can. J. Comp. Med.* **1953**, *17*, 422-424.

(122) Schroder, G.; Weissenbock, H.; Baumgartner, W. C.; Truschner, K. *Wiener Tiearztilche Monnatsshrift* **1991**, *80*, 171-176.

(123) Kumar, K.; Bhatia, K. C.; Sadana, J. R. *Ind. J. Anim. Nutr.* **1989**, *6*, 52-55.

(124) Prasad, T.; Arora, S. P. *Br. J. Nutr.* **1991**, *66*, 261-267.

(125) Gupta, R. C.; Kwatra, M. S.; Singh, N. *Ind. Vet. J.* **1982**, *59*, 738-740.

(126) Kiremidjian-Schumacher, L.; Roy, M.; Wishe, H. I.; Cohen, M. W.; Stotzky, G. *Biol. Trace Elem. Res.* **1994**, *41*, 115-127.

(127) Roy, M.; Kiremidjian-Schumacher, L.; Wishe, H. I.; Cohen, M. W.; Stotzky, G. *Biol. Trace Elem. Res.* **1994**, *41*, 103-114.

(128) Look, M. P.; Rockstroh, J. K.; Rao, G. S.; Kreuzer, K. A.; Spengler, U.; Sauerbruch, T. *Biol. Trace Elem. Res.* **1997**, *56*, 31-41.

(129) Singhal, N.; Austin, J. *J. Int. Assoc. Physicians AIDS* **2002**, *1*, 63-75.

(130) Romero-Alvira, D.; Roche, E. *Med. Hypotheses* **1998**, *51*, 169-173.

(131) Campa, A.; Shor-Posner, G.; Indacoche, F.; Zhang, G.; Lai, H.; Asthana, D.; Scott, G. B.; Baum, M. K. *J Acquir. Immune Defic. Syndr. Hum. Retrovirol.* **1999**, *15*, 508-513.

(132) Baum, M. K.; Shor-Posner, G.; Lai, S.; Zhang, G.; Lai, H.; Fletcher, M. A.; Sauberlich, H.; Page, J. B. *J Acquir. Immune Defic. Syndr. Hum. Retrovirol.* **1997**, *15*, 370-375.

(133) Baum, M. K.; Shor-Posner, G.; Lai, S.; Zhang, G.; Lai, H.; Fletcher, M. A.; Sauberlich, H.; Page, J. B. *J Acquir. Immune Defic. Syndr. Hum. Retrovirol.* **1997**, *15*, 370-374.

(134) Chen, C.; Zhou, J.; Xu, H.; Jiang, Y.; Zhu, G. *Biol. Trace Elem. Res.* **1997**, *59*, 187-193.

(135) Olmsted, L.; Schruazer, G. N.; Flores-Acre, M.; Dowd, J. *Biol. Trace Elem. Res.* **1989**, *25*, 89-96.

(136) Schrauzer, G. N.; Sacher, J. *Chem. Biol. Interact.* **1994**, *91*, 199-205.

(137) Giovannucci, E. *Lancet* **1998**, *352*, 755-756.

(138) Harrison, P. R.; Lanfear, J.; Wu, L.; Fleming, J.; McGarry, L.; Blower, L. *Biomed. Environ. Sci.* **1997**, *10*, 235-245.

(139) Clark, L. C.; Combs, G. F., Jr.; Turnbull, B. W.; Slate, E. H.; Chalker, D. K.; Chow, J.; Davis, L. S.; Glover, R. A.; Graham, G. F.; Gross, E. G.; Krongrad, A.; Lesher, J. L., Jr.; Park, H. K.; Sanders, B. B., Jr.; Smith, C. L.; Taylor, J. R. *J. Am. Med. Assoc.* **1996**, *276*, 1957-1963.

(140) Clark, L. C.; Dalkin, B.; Krongrad, A.; Combs, G. F., Jr.; Turnbull, B. W.; Slate, E. H.; Witherington, R.; Herlong, J. H.; Janosko, E.; Carpenter, D.; Borosso, C.; Falk, S.; Rounder, J. *Br. J. Urol.* **1998**, *81*, 730-734.

(141) Bhuvarahamurthy, V.; Balasubramanian, N.; Govindasamy, S. *Mol. Cell Biochem.* **1996**, *158*, 17-23.

(142) Stewart, M. S.; Spallholz, J. E.; Neldner, K. H.; Pence, B. C. *Free Radic. Biol. Med.* **1999**, *26*, 42-48.

(143) Mantovani, G.; Maccio, A.; Madeddu, C.; Serpe, R.; Massa, E.; Gramignano, G.; Lusso, M. R.; Curreli, N.; Rinaldi, A. *J. Exp. Ther. Oncol.* **2004**, *4*, 69-78.

(144) Spyrou, G.; Bjornstedt, M.; Skog, S.; Holmgren, A. *Cancer Res.* **1996**, *56*, 4407-4412.

(145) Vadhanavikit, S.; Ip, C.; Ganther, H. E. *Xenobiotica* **1993**, *23*, 731-745.

(146) Shen, C. L.; Song, W.; Pence, B. C. *Cancer Epidemiol. Biomarkers Prev.* **2001**, *10*, 385-390.

(147) Ip, C. *J. Am. Coll. Toxicol.* **1986**, *5*, 7-20.

(148) Spallholz, J. E. *Free Radic. Biol. Med.* **1994**, *17*, 45-64.

(149) Battin, E. E.; Brumaghim, J. L. Ph.D. Dissertation, Clemson University, 2008.

(150) Berggen, M. M.; Mangin, J. F.; Gasdaska, J. R.; Powis, G. *Biochem. Pharmacol.* **1998**, *57*, 187-193.

(151) Berggren, M.; Gallegos, A.; Gasdaska, J.; Powis, G. *Anticancer Res.* **1997**, *17*, 3377-3380.

(152) El-Bayoumy, K. *Mutat. Res.* **2001**, *475*, 123-139.

(153) Ip, C. *J. Nutr.* **1998**, *128*, 1845-1854.

(154) Young, V. R.; Nahapetian, A.; Janghorbani, M. *Am. J. Clin. Nutr.* **1982**, *35*, 1076-1088.

(155) Lu, J.; Kaeck, M.; Jiang, C.; Wilson, A. C.; Thompson, H. J. *Biochem. Pharmacol.* **1994**, *47*, 1531-1535.

(156) Wilson, A. C.; Thompson, H. J.; Schedin, P. J.; Gibson, N. W.; Ganther, H. E. *Biochem. Pharmacol.* **1992**, *43*, 1137-1141.

(157) Lu, J.; Jiang, C.; Kaeck, M.; Ganther, H.; Vadhanavikit, S.; Ip, C.; Thompson, H. *Biochem. Pharmacol.* **1995**, *50*, 213-219.

(158) Gazi, M. H.; Gong, A.; Donkena, K. V.; Young, C. Y. *Clin. Chim. Acta* **2007**, *380*, 145-150.

(159) Burk, R. F.; Lawrence, R. A.; Lane, J. M. *J. Clin. Invest.* **1980**, *65*, 1024-1031.

(160) Hill, K. E.; Burk, R. F. *Biomed. Environ. Sci.* **1997**, *10*, 198-208.

(161) Holben, D. H.; Smith, A. M. *J. Am. Diet. Assoc.* **1999**, *99*, 836-843.

(162) Yang, J. G.; Hill, K. E.; Burk, R. F. *J. Nutr.* **1989**, *119*, 1010-1012.

(163) Gallegos, A.; Berggren, M.; Gasdaska, J. R.; Powis, G. *Cancer Res.* **1997**, *57*, 4965-4970.

(164) Behne, D.; Kyriakopoeulos, A.; Weiss-Nowak, C.; Kalckloesch, M.; Westphal, C.; Gessner, H. *Biol. Trace Elem. Res.* **1996**, *55*, 99-110.

(165) Singh, M.; Lu, J.; Briggs, S. P.; McGinley, J. N.; Haegele, A. D.; Thompson, H. J. *Carcinogenesis* **1994**, *15*, 1567-1570.

(166) Thirunavukkarasu, C.; Prince Vijeya Singh, J.; Thangavel, M.; Selvendiran, K.; Sakthisekaran, D. *Cell Biochem. Funct.* **2002**, *20*, 347-356.

(167) Thirunavukkarasu, C.; Sakthisekaran, D. *J. Cell. Biochem.* **2003**, *88*, 578-588.

(168) Thompson, H. J.; Wilson, A.; Lu, J.; Singh, M.; Jiang, C.; Upadhyaya, P.; el-Bayoumy, K.; Ip, C. *Carcinogenesis* **1994**, *15*, 183-186.

(169) Kim, T. S.; Yun, B. Y.; Kim, I. Y. *Biochem. Pharmacol.* **2003**, *66*, 2301-2311.

(170) Ganther, H. E. *Biochemistry* **1968**, *7*, 2898-2905.

(171) Ganther, H. E. *Biochemistry* **1971**, *10*, 4089-4098.

(172) Jacob, C. *Nat. Prod. Rep.* **2006**, *23*, 851-863.

(173) Kim, T. S.; Jeong, D. W.; Yun, B. Y.; Kim, I. Y. *Biochem. Biophys. Res. Commun.* **2002**, *294*, 1130-1137.

(174) Seko, Y.; Imura, N. *Biomed. Environ. Sci.* **1997**, *10*, 333-339.

(175) Vaux, D. L.; Korsmeyer, S. J. *Cell* **1999**, *96*, 245-254.

(176) Harrison, W. T. A.; Stucky, G. D.; Morris, R. E.; Cheetham, A. K. *Acta Cryst.* **1992**, *C48*, 1365-1367.

(177) Xiao, D.; An, H.; Wang, E.; Xu, L. *J. Mol. Structure* **2005**, *740*, 249-253.

(178) Cao, G.; Sofic, E.; Prior, L. R. *J. Agric. Food Chem.* **1996**, *44*, 3426-3431.

(179) Gey, K. F. *Biochem. Soc. Trans.* **1990**, *18*, 1041-1045.

(180) Willet, C. W. *Science* **1994**, *264*, 532-537.

(181) Ishikawa, K.; Naganawa, R.; Yoshida, H.; Iwata, N.; Fukuda, H.; Fujino, T.; Suzuki, A. *Biosci. Biotechnol. Biochem.* **1996**, *60*, 2086-2088.

(182) Kyo, E.; Uda, N.; Suzuki, A.; Kakimoto, M.; Ushujima, M.; Kasuga, S.; Itakura, Y. *Phytomedicine* **1998**, *5*, 259-267.

(183) Mirhadi, S. A.; Singh, S.; Gupta, P. P. *Ind. J. Exp. Biol.* **1991**, *29*, 162-168.

(184) Morimitsu, Y.; Morioka, Y.; Kawakishi, S. *J. Agric. Food Chem.* **1992**, *40*, 368-372.

(185) Prasad, K.; Laxdal, V. A.; Yu, M.; Raney, B. L. *Mol. Cell. Biochem.* **1995**, *148*, 183-189.

(186) Siegers, C.-P.; Robke, A.; Pentz, R. *Phytomedicine* **1999**, *6*, 13-16.

(187) Singh, S. V.; Pan, S. S.; Srivastava, S. K.; Xia, H.; Hu, X.; Zaren, H. A.; Orchard, J. L. *Biochem. Biophys. Res. Commun.* **1998**, *244*, 917-920.

(188) Weber, N. D.; Andersen, D. O.; North, J. A.; Murray, B. K.; Lawson, L. D.; Hughes, B. G. *Planta Med.* **1992**, *58*, 417-423.

(189) Briggs, W. H.; Xiao, H.; Parkin, K. L.; Shen, C.; Goldman, I. L. *J. Agric. Food Chem.* **2000**, *48*, 5731-5735.

(190) Edwards, J. S.; Musker, D.; Collin, H. A.; Britton, G. *Phytochem. Anal.* **1994**, *5*, 4-9.

(191) Thomas, D. J.; Parkin, K. L. *J. Agric. Food Chem.* **1994**, *42*, 1632-1638.

(192) Yoo, K. S.; Pike, L. M. *Sci. Hortic.* **1998**, *75*, 1-10.

(193) Hirsch, K.; Danilenko, M.; Giat, J.; Miron, T.; Rabinkov, A.; Wilchek, M.; Mirelman, D.; Levy, J.; Sharoni, Y. *Nutr. Cancer* **2000**, *38*, 245-254.

(194) Rabinkov, A.; Miron, T.; Konstantinovski, L.; Wilchek, M.; Mirelman, D.; Weiner, L. *Biochim. Biophys. Acta* **1998**, *1379*, 233-244.

(195) Ito, Y.; Nakamura, Y.; Nakamura, Y. *Mutat. Res.* **1997**, *393*, 307-316.

(196) Nakamura, Y.; Matsuo, T.; Shimoi, K.; Nakamura, Y.; Tomita, I. *Bio. Pharm. Bull.* **1993**, *16*, 207-209.

(197) Nakamura, Y.; Matsuo, T.; Shimoi, K.; Nakamura, Y.; Tomita, I. *Biosci. Biotech. Biochem.* **1996**, *60*, 1439-1443.

(198) Kim, L. S.; Axelrod, L. J.; Howard, P.; Buratovich, N.; Waters, R. F. *Osteoarthritis Cartilage* **2006**, *14*, 286-294.

(199) Barrager, E.; Veltmann, J. R., Jr.; Schauss, A. G.; Schiller, R. N. *J. Altern. Complement. Med.* **2002**, *8*, 167-173.

(200) Hucker, H. B.; Miller, J. K.; Hochberg, A.; Brobyn, R. D.; Riordan, F. H.; Calesnick, B. *J. Pharmacol. Exp. Ther.* **1967**, *155*, 309-317.

(201) Pryor, W. A.; Jin, X.; Squadrito, G. L. *Proc. Natl. Acad. Sci. USA* **1994**, *91*, 11173-11177.

(202) Schoneich, C.; Zhao, F.; Wilson, G. S.; Borchardt, R. T. *Biochim. Biophys. Acta* **1993**, *1158*, 307-322.

(203) Ali, F. E.; Separovic, F.; Barrow, C. J.; Cherny, R. A.; Fraser, F.; Bush, A. I.; Masters, C. L.; Barnham, K. J. *J. Pept. Sci.* **2005**, *11*, 353-360.

(204) Bush, A. I. *Curr. Opin. Chem. Biol.* **2000**, *4*, 184-191.

(205) Lynch, T.; Cherny, R. A.; Bush, A. I. *Exp. Gerontol.* **2000**, *35*, 445-451.

(206) Gao, J.; Yin, D. H.; Yao, Y.; Sun, H.; Qin, Z.; Schoneich, C.; Williams, T. D.; Squier, T. C. *Biophys. J.* **1998**, *74*, 1115-1134.

(207) Squier, T. C.; Bigelow, D. J. *Front Biosci.* **2000**, *5*, D504-D526.

(208) Berlett, B. S.; Levine, R. L.; Stadtman, E. R. *Proc. Natl. Acad. Sci. USA* **1998**, *95*, 2784-2789.

(209) Brot, N.; Weissbach, H. *Arch. Biochem. Biophys.* **1983**, *223*, 271-281.

(210) Chao, C. C.; Ma, Y. S.; Stadtman, E. R. *Proc. Natl. Acad. Sci. USA* **1997**, *94*, 2969-2974.

(211) Levine, R. L.; Mosoni, L.; Berlett, B. S.; Stadtman, E. R. *Proc. Natl. Acad. Sci. USA* **1996**, *93*, 15036-15040.

(212) Vogt, W. *Free Radic. Biol. Med.* **1995**, *18*, 93-105.

(213) von Eckardstein, A.; Walter, M.; Holz, H.; Benninghoven, A.; Assmann, G. *J. Lipid Res.* **1991**, *32*, 1465-1476.

(214) Levine, R. L.; Moskovitz, J.; Stadtman, E. R. *IUBMB Life* **2000**, *50*, 301-307.

(215) Moskovitz, J.; Flescher, E.; Berlett, B. S.; Azare, J.; Poston, J. M.; Stadtman, E. R. *Proc. Natl. Acad. Sci. USA* **1998**, *95*, 14071-14075.

(216) Tang, X. D.; Daggett, H.; Hanner, M.; Garcia, M. L.; McManus, O. B.; Brot, N.; Weissbach, H.; Heinemann, S. H.; Hoshi, T. *J. Gen. Physiol.* **2001**, *117*, 253-274.

(217) Assmann, A.; Briviba, K.; Sies, H. *Arch. Biochem. Biophys.* **1998**, *349*, 201-203.

(218) Padmaja, S.; Squadrito, G. L.; Lemercier, J. N.; Cueto, R.; Pryor, W. A. *Free Radic. Biol. Med.* **1996**, *21*, 317-322.

(219) Amagase, H.; Petesch, B. L.; Matsuura, H.; Kasuga, S.; Itakura, Y. *J. Nutr.* **2001**, *131*, 955S-962S.

(220) Corzo-Martinez, M.; Corzo, N.; Villamiel, M. *Trends Food Sci. Technol.* **2007**, *18*, 609-625.

(221) Das, S. *Asian Pac. J. Cancer Prev.* **2002**, *3*, 305-311.

(222) Chu, T. C.; Ogidigben, M.; Han, J. C.; Potter, D. E. *J. Ocul. Pharmacol.* **1993**, *9*, 201-209.

(223) Gebhardt, R.; Beck, H. *Lipids* **1996**, *31*, 1269-1276.

(224) Kaye, A. D.; Nossaman, B. D.; Ibrahim, I. N.; Feng, C. J.; McNamara, D. B.; Agrawal, K. C.; Kadowitz, P. J. *Eur. J. Pharmacol.* **1995**, *276*, 21-26.

(225) Makheja, A. N.; Bailey, J. M. *Agents Actions* **1990**, *29*, 360-363.

(226) Chung, L. Y. *J. Med. Food* **2006**, *9*, 205-213.

(227) Kumari, K.; Mathew, B. C.; Augusti, K. T. *Indian J. Biochem. Biophys.* **1995**, *32*, 49-54.

(228) Kumari, K.; Augusti, K. T. *Planta Med.* **1995**, *61*, 72-74.

(229) Kumari, K.; Augusti, K. T. *J. Ethnopharmacol.* **2007**, *109*, 367-371.

(230) Kumari, K.; Augusti, K. T. *Indian J. Exp. Biol.* **2002**, *40*, 1005-1009.

(231) Kawamori, T.; Tanaka, T.; Ohnishi, M.; Hirose, Y.; Nakamura, Y.; Satoh, K.; Hara, A.; Mori, H. *Cancer Res.* **1995**, *55*, 4053-4058.

(232) Nakamura, Y.; Matsuo, T.; Okamoto, S.; Nishikawa, A.; Imai, T.; Park, E. Y.; Sato, K. *Genes Environ.* **2008**, *30*, 41-47.

(233) Nagira, T.; Narisawa, J.; Teruya, K.; Katakura, Y.; Shim, S. Y.; Kusumoto, K.; Tokumaru, S.; Tokumaru, K.; Barnes, D. W.; Shirahata, S. *Cytotechnology* **2002**, *40*, 125-137.

(234) Richmond, V. L. *Life Sci.* **1986**, *39*, 263-268.

(235) Hucker, H. B.; Ahmad, P. M.; Miller, E. A.; Brobyn, R. *Nature* **1966**, *209*, 619-620.

(236) Otsuki, S.; Qian, W.; Ishihara, A.; Kabe, T. *Nutr. Res.* **2002**, *22*, 313-322.

(237) Egorin, M. J.; Rosen, D. M.; Sridhara, R.; Sensenbrenner, L.; Cottler-Fox, M. *J. Clin. Oncol.* **1998**, *16*, 610-615.

(238) Engelke, U. F.; Tangerman, A.; Willemsen, M. A.; Moskau, D.; Loss, S.; Mudd, S. H.; Wevers, R. A. *NMR Biomed.* **2005**, *18*, 331-336.

(239) Lin, A.; Nguy, C. H.; Shic, F.; Ross, B. D. *Toxicol. Lett.* **2001**, *123*, 169-177.

(240) Rose, S. E.; Chalk, J. B.; Galloway, G. J.; Doddrell, D. M. *Mag. Reson. Imag.* **2000**, *18*, 95-98.

(241) Cronin, J. R. *Altern. Compliment. Ther.* **1999**, *5*, 386-390.

(242) Usha, P. R.; Naidu, M. U. *Clin. Drug Investig.* **2004**, *24*, 353-363.

(243) Moskovitz, J.; Berlett, B. S.; Poston, J. M.; Stadtman, E. R. *Proc. Natl. Acad. Sci. USA* **1997**, *94*, 9585-9589.

(244) Ruan, H.; Tang, X. D.; Chen, M. L.; Joiner, M. L.; Sun, G.; Brot, N.; Weissbach, H.; Heinemann, S. H.; Iverson, L.; Wu, C. F.; Hoshi, T. *Proc. Natl. Acad. Sci. USA* **2002**, *99*, 2748-2753.

(245) Moskovitz, J.; Rahman, M. A.; Strassman, J.; Yancey, S. O.; Kushner, S. R.; Brot, N.; Weissbach, H. *J. Bacteriol.* **1995**, *177*, 502-507.

(246) St. John, G.; Brot, N.; Ruan, J.; Erdjument-Bromage, H.; Tempst, P.; Weissbach, H.; Nathan, C. *Proc. Natl. Acad. Sci. USA* **2001**, *98*, 9901-9906.

(247) Moskovitz, J.; Bar-Noy, S.; Williams, W. M.; Requena, J.; Berlett, B. S.; Stadtman, E. R. *Proc. Natl. Acad. Sci. USA* **2001**, *98*, 12920-12925.

(248) Sattler, W.; Christison, J.; Stocker, R. *Free Radic. Biol. Med.* **1995**, *18*, 421-429.

(249) Maier, K.; Leuschel, L.; Costabel, U. *Am. Rev. Respir. Dis.* **1991**, *143*, 271-274.

(250) Petropoulos, I.; Mary, J.; Perichon, M.; Friguet, B. *Biochem. J.* **2001**, *355*, 819-825.

(251) Gabbita, S. P.; Aksenov, M. Y.; Lovell, M. A.; Markesbery, W. R. *J. Neurochem.* **1999**, *73*, 1660-1666.

(252) Michaelis, M. L.; Bigelow, D. J.; Schoneich, C.; Williams, T. D.; Ramonda, L.; Yin, D.; Huhmer, A. F.; Yao, Y.; Gao, J.; Squier, T. C. *Life Sci.* **1996**, *59*, 405-412.

(253) Wells-Knecht, M. C.; Lyons, T. J.; McCance, D. R.; Thorpe, S. R.; Baynes, J. W. *J. Clin. Invest.* **1997**, *100*, 839-846.

(254) Gellman, S. H. *Biochemistry* **1991**, *30*, 6633-6636.

(255) Armitage, B. *Chem. Rev.* **1998**, *98*, 1171-1200.

(256) Mayo, D. J.; Turner, D. P.; Zucconi, B. E.; Predecki, A. H. *Bioorg. Med. Chem. Lett.* **2007**, *17*, 6116-6118.

(257) Wauchope, O. R.; Shakya, S.; Sawwan, N.; Liebman, J. F.; Greer, A. *Sulf. Chem.* **2007**, *28*, 11-15.

(258) Krause, R. J.; Glocke, S. C.; Sicuri, A. R.; Ripp, S. L.; Elfarra, A. A. *Chem. Res. Toxicol.* **2006**, *19*, 1643-1649.

(259) Schrauzer, G. N. *J. Nutr.* **2000**, *130*, 1653-1656.

(260) Kajander, E. O.; Harvima, R. J.; Eloranta, T. O.; Martikainen, H.; Kantola, M.; Karenlampi, S. O.; Akerman, K. *Biol. Trace Elem. Res.* **1991**, *28*, 57-68.

(261) Ziegler, D. M.; Graf, P.; Poulsen, L. L.; Stahl, W.; Sies, H. *Chem. Res. Toxicol.* **1992**, *5*, 163-166.

CHAPTER TWO

EFFECTS OF INORGANIC SELENIUM COMPOUNDS ON OXIDATIVE DNA DAMAGE

Introduction

Generation of reactive oxygen species (ROS) in cells can damage cellular components including nucleic acids, lipids, and proteins.[1] Oxidative damage *in vivo* is caused by ROS such as the hydroxyl radical ($^{\bullet}OH$) produced in the Fenton reaction.[2,3]

$$Fe^{2+} + H_2O_2 \rightarrow Fe^{3+} + [^{\bullet}OH] + OH^-$$

Iron-generated hydroxyl radical is the primary cause of oxidative DNA damage and cell death in both prokaryotes[4] and eukaryotes, including humans.[4,5] This DNA damage can lead to conditions such as aging,[6] cancer,[7] neurodegenerative,[2] and cardiovascular diseases.[8] Since cellular reductants such as NADH reduce Fe^{3+} back to Fe^{2+}, the production of hydroxyl radical is catalytic *in vivo*.[9]

Two kinetically-distinct modes of cell killing exist when *Escherichia coli* or mammalian cells are exposed to H_2O_2. Mode I killing is faster than Mode II and occurs at low peroxide concentrations (1-5 mM), whereas Mode II killing occurs at peroxide concentrations greater than 10 mM and is independent of H_2O_2 concentration.[9,10] Similar kinetics are also observed for *in vitro* DNA damage with maximal damage under Mode I conditions at 50 μM H_2O_2 and under Mode II conditions at H_2O_2 concentrations greater than 10 mM.[9-11] Iron-mediated cleavage of the DNA backbone under Mode I and II conditions occurs selectively at different DNA sequences: RTGR (with cleavage at the thymidine deoxyribose) for Mode I damage and RGGG for Mode II (R = A or G).[11,12]

Under Mode I conditions, hydroxyl radical is likely generated by Fe(II) bound to solvent-accessible sites on the deoxyribose-phosphate backbone or bases of DNA, whereas DNA damage under Mode II conditions occurs when H_2O_2 reacts with more-sterically-hindered Fe(II) bound to DNA bases, particularly guanine.[11]

Antioxidants can prevent or reduce oxidative DNA damage,[13-15] and selenium has been widely studied for its antioxidant and anticancer effects.[16-18] Selenium is also an essential micronutrient for both humans and animals with a RDA ranging from 55-350 μg/day for humans,[19] and it is incorporated as selenocysteine in the active site of antioxidant proteins, including glutathione peroxidases (GPx) and thioredoxin reductases.[16,20,21] Selenium is found in most multivitamins and dietary supplements[19] as selenomethionine, selenite (SeO_3^{2-}), or selenate (SeO_4^{2-}).[22] In addition, selenite and selenate are also incorporated into animal feed, protein mixes, and infant formula.[19] Selenium additives to animal feed, 16.8 tons annually for sheep and cows alone,[23] improve animal performance and increase selenium dietary intake for people consuming meat products.[24]

Initially, the ability of selenium to prevent hydroxyl radical formation by decomposition of H_2O_2 to water via GPx enzymes was proposed as a mechanism for their anticancer activity.[16,25] However, other studies indicate that while selenium is an effective antioxidant, this is not the sole basis for its anticancer activity.[16,26,27] Recently, a new mechanism involving selenometabolites was proposed to explain the anticancer effects of selenium.[16,18] Compounds such as selenite generate hydrogen selenide (H_2Se), used to incorporate selenium into selenocysteine and selenomethionine. Thus, H_2Se produced in

high concentrations may react with oxygen to produce ROS toxic to cells.[20,28,29] Additionally, selenometabolites such as selenodigluthathione have been found to inhibit cell growth and induce apoptosis in tumor cells.[16,18,30]

Although the mechanisms of antioxidant and anticancer activity for selenium compounds are unclear, organoselenium compounds such as selenomethionine have been shown to have antioxidant activity.[26,27,31] In addition, a plethora of anticancer studies have been conducted with sodium selenite (Na_2SeO_3), showing conflicting results.[16-18,30,32-34] Few studies have been conducted with either sodium selenate (Na_2SeO_4) and selenium dioxide (SeO_2). Hamilton *et al.* found that Na_2SeO_4 (6.2 mM) inhibited DNA damage via alkylating agents.[35] Takahashi and coworkers found that both Na_2SeO_3 (10 μM) and SeO_2 (50-100 μM) induced apoptosis in HSC-3 cells, whereas Na_2SeO_4 (100 μM) did not, suggesting that the former compounds are better anticancer agents.[16] In addition, SeO_2 (3-30 μM) was shown to inhibit the growth of lung cancer GLC-82 cells via apoptosis in a dose-dependent and time-dependent manner.[36]

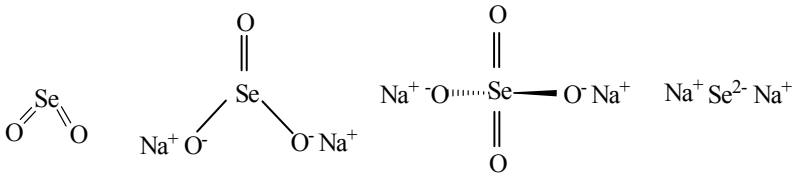

1 **2** **3** **4**

Figure 2.1. Selenium compounds tested: (1) selenium dioxide, SeO_2, (2) sodium selenite, Na_2SeO_3, (3) sodium selenate, Na_2SeO_4, and (4) sodium selenide, Na_2Se.

Despite the widespread use of inorganic selenium compounds in vitamins and animal feed, relatively little work has been done to determine their antioxidant properties. Thus,

we have used gel electrophoresis to study the effects of Na_2SeO_3, Na_2SeO_4, SeO_2, and Na_2Se (Figure 2.1) on DNA damage in the presence of H_2O_2 under both Mode I and II conditions. For the selenium compounds that inhibited DNA damage, the mechanism by which these compounds prevented such damage was also investigated.

Similarly to iron, Cu^+ can also undergo Fenton-like chemistry, producing the DNA-damaging hydroxyl radical. Unlike the bimodal rate of DNA damage observed

$$Cu^+ + H_2O_2 \rightarrow Cu^{2+} + OH^- + {}^{\bullet}OH$$

under Fenton reaction conditions, the rate of copper-mediated DNA damage is linear with increasing hydrogen peroxide concentration.[37] The ability of the inorganic selenium compounds to prevent copper-mediated DNA damage was also studied via gel electrophoresis experiments. The iron work discussed in this chapter is published in *J. Inorg. Biochem.* **2007**, *101*, 1028-1035.[38]

Results

The selenium compounds in Figure 2.1 differ in both oxidation state of the selenium atom and in charge. Selenide, selenite, and selenate are charged species with -2, +4 and +6 selenium oxidation states, respectively. Selenium dioxide, however is neutral with a +4 selenium oxidation state. Our DNA damage studies examine both the ability of these compounds to inhibit iron-mediated DNA damage, and the effects of selenium oxidation state and charge on this activity.

Mode I experiments with inorganic selenium compounds and Fe^{2+}

A gel electrophoresis experiment testing selenite for its ability to inhibit DNA damage under Mode I conditions (50 μM H_2O_2, 10 mM ethanol) is shown in Figure 2.2A. At this H_2O_2 concentration, the rate of Mode I DNA damage is maximal; ethanol was also added to emulate organic molecules in cells that scavenge hydroxyl radical.[11] From the gel in Figure 2.2A, it is clear that both H_2O_2 alone (lane 3) and Na_2SeO_3 with H_2O_2 alone (lane 4) had no effect on DNA damage as compared to the plasmid-only lane (lane 2). Addition of both Fe(II) (2 μM) and H_2O_2 (lane 5) produced 94% damaged (nicked) DNA. Addition of increasing concentrations of Na_2SeO_3 (0.5-5000 μM, all $p < 0.02$)

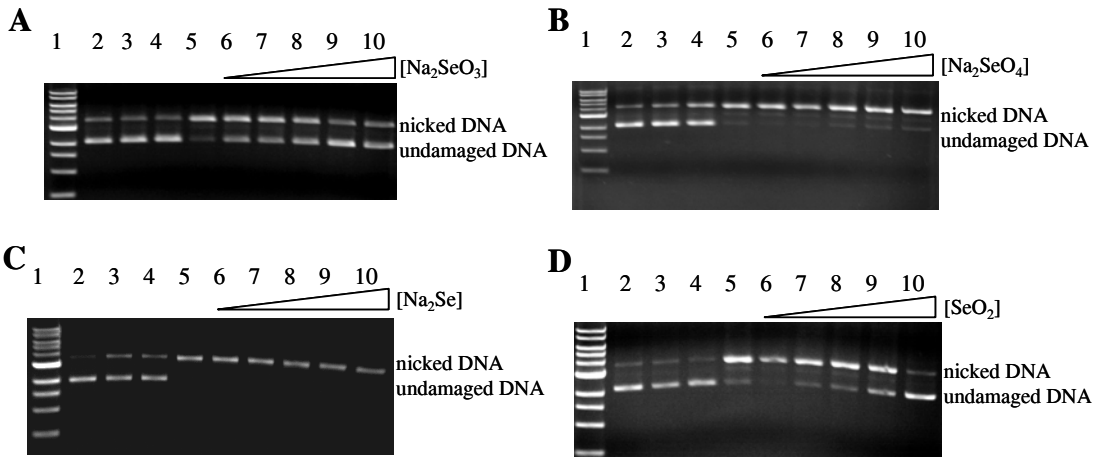

Figure 2.2. DNA gel electrophoresis experiments for (A) Na_2SeO_3, (B) Na_2SeO_4, (C) Na_2Se, and (D) SeO_2 under Mode I conditions. For each gel, lane 1: 1 kb ladder; lanes 2-5: plasmid, H_2O_2 (50 μM), Na_2SeO_3, Na_2SeO_4, SeO_2 (5000 μM) or Na_2Se (200 μM), and Fe^{2+} (2 μM) respectively; lanes 6-10: 0.5, 5, 50, 500 and 5000 μM of Na_2SeO_3, Na_2SeO_4, and SeO_2 respectively, or 0.5, 5, 50, 100 and 200 μM of Na_2Se.

resulted in increased undamaged (closed, circular) DNA (Figure 2.2A, lanes 6-10), indicating that Na_2SeO_3 inhibited oxidative DNA damage. From quantification of these

gel bands, we determined that the highest Na_2SeO_3 concentration (5000 μM) inhibited 91% of iron-mediated DNA damage.

Similar electrophoresis experiments were conducted for Na_2SeO_4, SeO_2 and Na_2Se under identical Mode I conditions. In this case, Na_2SeO_4 (Figure 2.2B) and Na_2Se (Figure 2.2C), showed no inhibition of DNA damage with increasing concentration. In contrast, adding SeO_2 in the presence of Fe(II) and H_2O_2 showed a slight increase in DNA damage (Figure 2.2D, lanes 6-8) at concentrations of 0.5-50 μM compared to the Fe(II)/H_2O_2 lane (lane 5). This corresponds to a 20% increase in DNA damage at 50 μM SeO_2 ($p = 0.02$). At higher concentrations (500 and 5000 μM, lanes 9-10), however, SeO_2 inhibited DNA damage by 17% ($p = 0.01$) and 100% ($p = > 0.0001$), respectively.

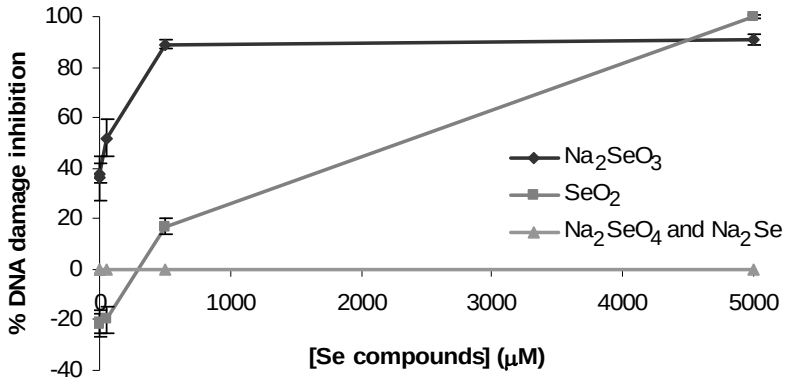

Figure 2.3. Percent DNA damage inhibition graph for Na_2SeO_3, Na_2SeO_4, SeO_2, and Na_2Se under Mode I conditions. Error bars represent standard deviations calculated from the average of three trials.

Figure 2.3 shows a graph of percent DNA damage inhibition vs. concentration of selenium compound for the four inorganic selenium compounds tested. Inhibition of DNA damage is clearly greatest for Na_2SeO_3 and high concentrations of SeO_2, whereas

SeO_2 shows increased DNA damage at lower concentrations, and both Na_2SeO_4 and Na_2Se show no effect on DNA damage.

$[Fe(EDTA)]^{2-}$ experiments under Mode I conditions

Since our studies indicated that both Na_2SeO_3 and SeO_2 inhibit DNA damage at high concentrations (500-5000 μM) under Mode I conditions, we investigated metal coordination as a possible mechanism for the inhibitory effect of these compounds. Iron binding to the selenium compound could prevent the generation or release of the hydroxyl radical upon exposure to H_2O_2. To test this metal coordination hypothesis, we performed gel electrophoresis experiments with the $[Fe(EDTA)]^{2-}$ complex as the iron source. The chelating ligand EDTA (ethylenediaminetetraacetic acid) completely coordinates Fe^{2+}, preventing potential coordination between the selenium compound and iron. Although completely coordinated, $[Fe(EDTA)]^{2-}$ does generate DNA-damaging hydroxyl radical in the presence of H_2O_2.

Gel electrophoresis experiments showed that addition of $[Fe(EDTA)]^{2-}$ (400 μM) and H_2O_2 under Mode I conditions produced approximately 63% nicked DNA (Figure 2.4, lane 5). As the concentration of Na_2SeO_3 was increased, no effect on oxidative DNA damage was observed (lanes 6-10). Similarly, increasing concentrations of SeO_2 had no effect on DNA damage under the same conditions (Figure 2.4B). The lack of DNA damage inhibition by both Na_2SeO_3 and SeO_2 with $[Fe(EDTA)]^{2-}$ instead of $FeSO_4$ as the iron source suggests that metal coordination is required for the effects of both compounds on DNA damage under Mode I conditions.

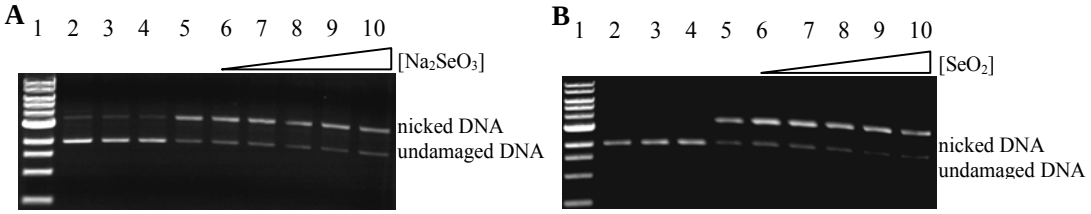

Figure 2.4. DNA gel electrophoresis experiments for (A) Na_2SeO_3 and (B) SeO_2 with $[Fe(EDTA)]^{2-}$ under Mode I conditions. For each gel, lane 1: 1 kb ladder; lanes 2-5: plasmid, H_2O_2 (50 μM), Se compound (5000 μM) and $[Fe(EDTA)]^{2-}$ (400 μM) respectively; lanes 6-10: 0.5, 5, 50, 500, and 5000 μM respectively of either Na_2SeO_3 or SeO_2.

Mode II experiments with inorganic selenium compounds

At higher peroxide concentrations (> 10 mM), *in vitro* iron-mediated DNA damage was shown to occur independently of H_2O_2 concentration.[11] This Mode II DNA damage likely differs from Mode I damage in that the generated hydroxyl radical results from the reaction of H_2O_2 with Fe(II) bound to the bases of DNA.[11] Because Mode I and Mode II DNA damage result from hydroxyl radical being produced at different sites of iron localization on DNA, we also determined the effects of Na_2SeO_3, Na_2SeO_4, SeO_2 and Na_2Se on oxidative DNA damage under Mode II conditions.

Experiments performed under Mode II conditions were identical to those for Mode I except that the concentrations of H_2O_2 (50 mM) and ethanol (100 mM) were increased to ensure that DNA damage was caused only by Mode II radicals.[10,11] Initial experiments with Na_2SeO_3 indicated that this compound increases DNA damage in the presence of H_2O_2 without addition of Fe(II). Therefore, further experiments with selenite under Mode II conditions were conducted at pH 7 in the absence of iron.

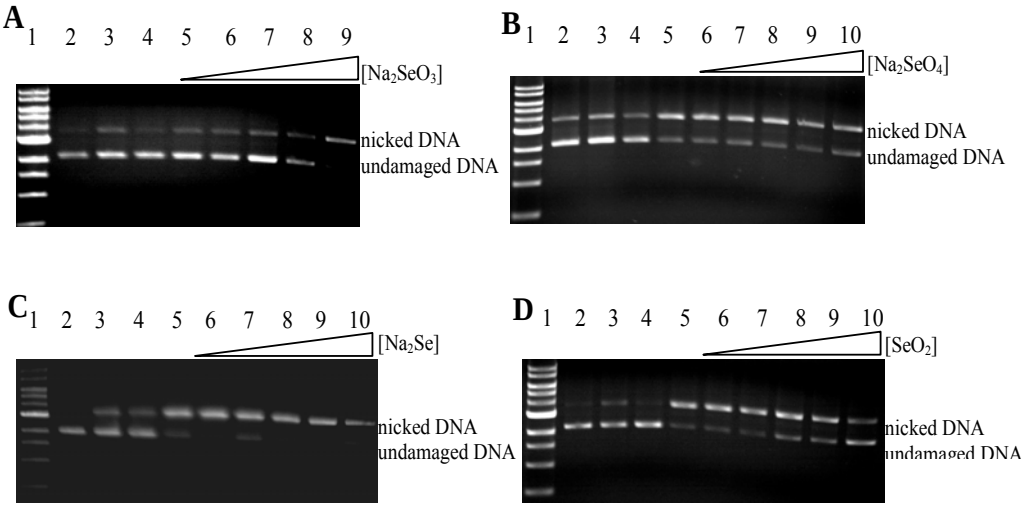

Figure 2.5. DNA gel electrophoresis experiments for (A) Na_2SeO_3, (B) Na_2SeO_4, (C) Na_2Se and (D) SeO_2 under Mode II conditions. For (A) Na_2SeO_3 lane 1: 1 kb ladder; lanes 2-4: plasmid, H_2O_2 (50 mM), and Na_2SeO_3 (5000 μM) respectively; lanes 5-9 have H_2O_2 + 0.5, 5, 50, 500, 5000 μM Na_2SeO_3, respectively. For gels B-D, lane 1: 1 kb ladder; 2-5: plasmid, H_2O_2 (50 mM), H_2O_2 + Na_2SeO_4, SeO_2 (5000 μM) or Na2Se (200 μM), H_2O_2 + Fe^{2+} (2 μM); lanes 6-10: H_2O_2 + Fe^{2+} + 0.5, 5, 50, 500 and 5000 μM of Na_2SeO_4 or SeO_2 respectively. For Na_2Se, lanes 6-10: H_2O_2 + Fe^{2+} + 0.5, 5, 50, 100 and 200 μM Na_2Se, respectively.

Sodium selenate (0.5-5000 μM) was also tested under Mode II conditions with Fe(II) (2 μM) at pH 6. As seen from the gel in Figure 2.5B, Na_2SeO_4 had no effect on DNA damage, regardless of concentration (lanes 6-10). Under similar conditions, addition of Na_2Se also had no effect on DNA damage (Figure 2.5C). In contrast, adding increasing concentrations of SeO_2 (5-5000 μM) under the same Mode II conditions showed inhibition of DNA damage (Figure 2.5D lanes 6-10, all $p < 0.05$).

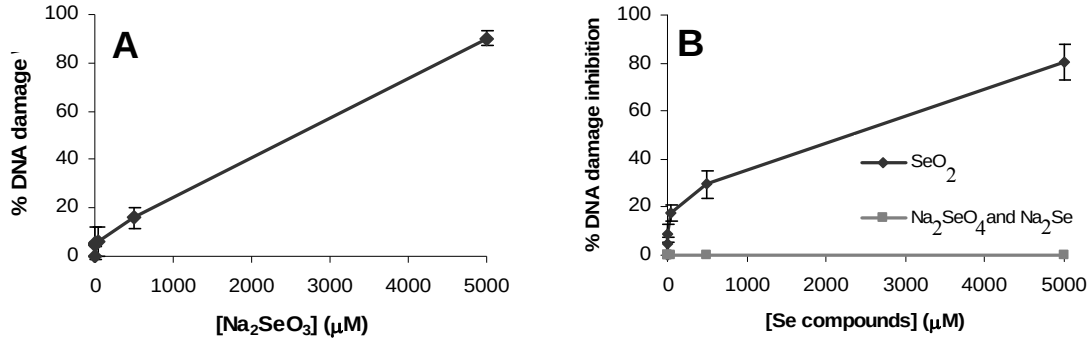

Figure 2.6. A) Percent DNA damage graph for 0.5-5000 μM Na_2SeO_3 under Mode II conditions in the absence of Fe^{2+} B) Percent DNA damage inhibition graph for 0.5-5000 μM Na_2SeO_4 and SeO_2, and 0.5-200 μM Na_2Se under Mode II conditions in the presence of Fe^{2+} (2 μM) and H_2O_2 (50 mM). Error bars for both graphs represent standard deviations calculated from the average of three trials.

Unlike selenite, adding only SeO_2 and H_2O_2 (lane 4) had no effect on DNA damage compared to the DNA control (lane 2). Increasing the concentration of SeO_2 to 5000 μM resulted in inhibition of 81% DNA damage (lane 10; $p = 0.003$). Thus, under Mode II conditions, SeO_2 had an inhibitory effect on DNA that is concentration-dependent. A comparison of DNA damage inhibition by Na_2SeO_4, Na_2Se, and SeO_2 under Mode II conditions is shown in Figure 2.6B.

$[Fe(EDTA)]^{2-}$ experiments under Mode II conditions

Under Mode II conditions, SeO_2 was the only selenium compound to inhibit DNA damage. Experiments similar to those under Mode I conditions, using $[Fe(EDTA)]^{2-}$ as the iron source, were therefore conducted to determine whether metal coordination is required for SeO_2 inhibition of DNA damage under Mode II conditions. The gel shown in

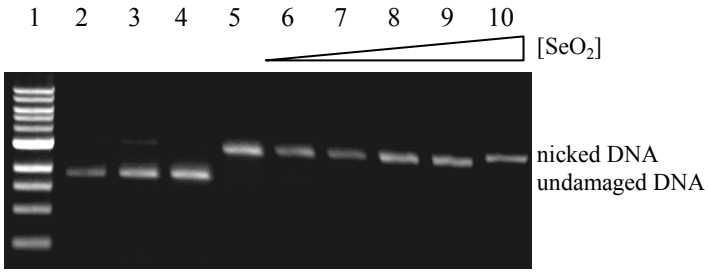

Figure 2.7. DNA gel electrophoresis experiments for SeO_2 with $[Fe(EDTA)]^{2-}$ under Mode II conditions. Lane 1: 1 kb ladder; lanes 2-5: plasmid, H_2O_2 (50 μM), SeO_2 (5000 μM) and $[Fe(EDTA)]^{2-}$ (400 μM), respectively; lanes 6-10: 0.5, 5, 50, 500, and 5000 μM SeO_2, respectively.

Figure 2.7 shows that $[Fe(EDTA)]^{2-}$ combined with H_2O_2 (lane 5) resulted in 100% nicked DNA. Upon addition of increasing concentrations of SeO_2 (lanes 6-10), the percentage of DNA damage did not change. This suggests that iron coordination is required for SeO_2 to prevent DNA damage under Mode II conditions in much the same manner as was found for SeO_2 and Na_3SeO_3 inhibition of DNA damage under Mode I conditions.

^{77}Se NMR Experiments

Several studies indicate that in aqueous solution at pH 6, SeO_2 exists as $HSeO_3^-$ ($SeO_2 + H_2O \rightarrow HSeO_3^- + H^+$),[39-41] a species similar to Na_2SeO_3 in aqueous solution. Since our gel results with Na_2SeO_3 and SeO_2 showed differing effects of these compounds on DNA damage, ^{77}Se NMR experiments were performed to elucidate the speciation of SeO_2. Aqueous solutions of SeO_2 showed singlets at δ 1317 and 1299 (Figure 2.11) at pH 6 and 7, respectively, which did not change over a period of three

days. Under the same conditions, Na_2SeO_3, showed a singlet at δ 1274 at both pH 6 and 7 (Figure 2.12). Thus, our results indicate that aqueous solutions of Na_2SeO_3 and SeO_2 do not form the same compound under these conditions.

DNA nicking experiments with inorganic selenium compounds and Cu^+

Since copper generates the DNA-damaging hydroxyl radical, the antioxidant effects of Na_2SeO_3, Na_2SeO_4, Na_2Se and SeO_2 on copper-mediated DNA damage were investigated via gel electrophoresis. In these experiments Cu^{2+} (6 μM) was reduced to Cu^+ by ascorbic acid (7.5 μM) and hydroxyl radical was generated upon addition of H_2O_2 (50 μM). A gel electrophoresis experiment testing the ability of selenite to inhibit copper-mediated DNA damage is shown in Figure 2.8A.

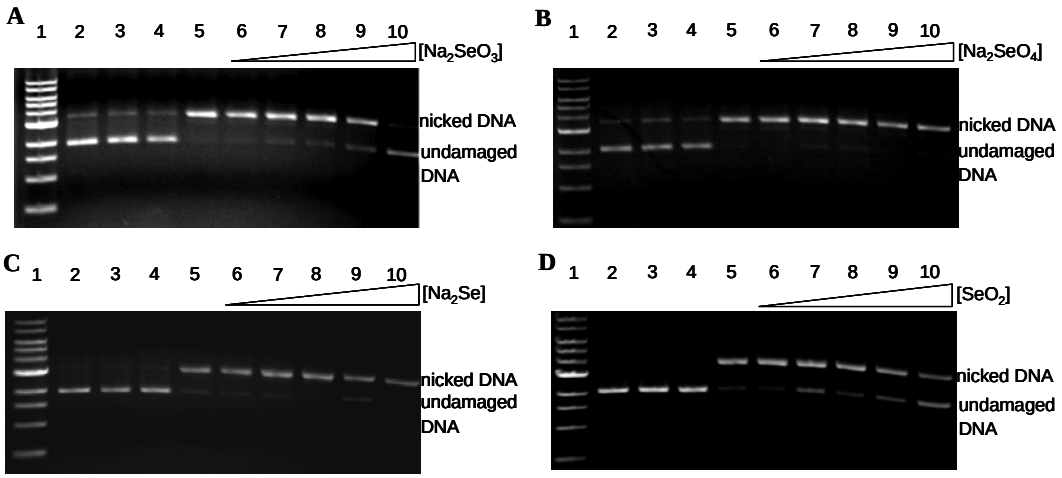

Figure 2.8. DNA gel electrophoresis experiments for (A) Na_2SeO_3, (B) Na_2SeO_4, (C) Na_2Se, and (D) SeO_2 for Cu^+. For each gel, lane 1: 1 kb ladder; lanes 2-5: plasmid, H_2O_2 (50 μM), Na_2SeO_3, Na_2SeO_4, SeO_2 (5000 μM) or Na_2Se (200 μM), Cu^{2+} (6 μM), and ascorbic acid (7.5 μM) respectively; lanes 6-10: 0.5, 5, 50, 500 and 5000 μM of Na_2SeO_3, Na_2SeO_4, and SeO_2 respectively, or 0.5, 5, 50, 100 and 200 μM of Na_2Se.

The gel data show that both H_2O_2 alone (lane 3) or Na_2SeO_3 with H_2O_2 alone (lane 4) have no effect on DNA as compared to the plasmid-only lane (lane 2). Addition of both Cu^+ and H_2O_2 (lane 5) produces 97% damaged DNA, and adding increasing concentrations of Na_2SeO_3 (0.5-5000 μM) results in increased undamaged DNA (Figure 2.8A, lanes 9-10). Na_2SeO_3 (5000 μM) inhibit 95% copper-mediated DNA damage.

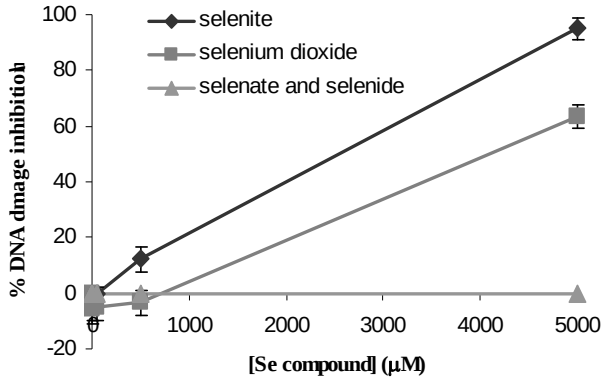

Figure 2.9. Percent DNA damage inhibition graph for Na_2SeO_3, Na_2SeO_4, SeO_2, and Na_2Se with Cu^+. Error bars represent standard deviations calculated from three trials.

Similar electrophoresis experiments performed with SeO_2 (Figure 2.8D) under similar conditions show that this compound inhibits 63% DNA damage at the highest concentration tested (5000 μM; Figure 2.9). Both Na_2SeO_4 (Figure 2.8B) and Na_2Se (Figure 2.8C) show no inhibition of DNA damage upon adding increasing concentrations of these selenium compounds (Figure 2.9).

$[Cu(bipy)_2]^+$ experiments with inorganic selenium compounds

Since Na_2SeO_3 and SeO_2 are the only tested inorganic selenium compounds to inhibit copper-mediated DNA damage, further gel electrophoresis experiments were conducted to determine whether metal coordination is required for their antioxidant activity. In these experiments, however $[Cu(bipy_2)]^+$ (50 μM) was used instead of Cu^{2+} as the metal source because this complex is completely coordinated (similar to the $Fe(EDTA)^{2-}$ experiments previously described). The gel shown in Figure 2.10A indicates that $[Cu(bipy_2)]^+$ combined with H_2O_2 (lane 5) results in 94% nicked DNA, and upon addition of increasing concentrations of Na_2SeO_3 (Figure 2.10; lanes 6-10), the percentage of DNA damage did not change. Similarly, increasing concentrations of SeO_2 have no effect on DNA damage under the same conditions (Figure 2.10B). The lack of DNA damage inhibition by both Na_2SeO_3 and SeO_2 with the completely-coordinated $[Cu(bipy)_2]^+$ suggests that metal binding is required for both selenium compounds to inhibit DNA damage.

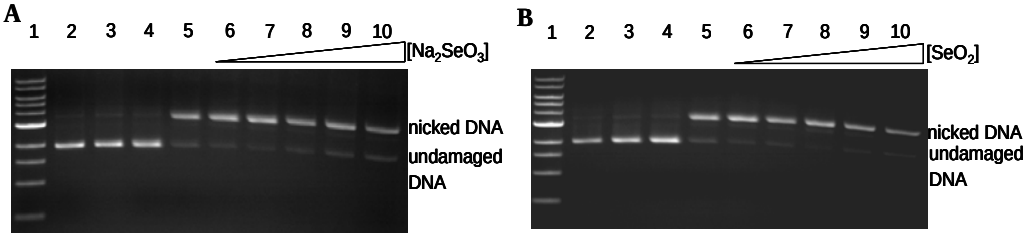

Figure 2.10: DNA gel electrophoresis experiments for (A) Na_2SeO_3 and (B) SeO_2 with $[Cu(bipy)_2]^+$. For each gel, lane 1: 1 kb ladder; lanes 2-5: plasmid, H_2O_2 (50 μM), Se compound (5000 μM), $[Cu(bipy)_2]^{2+}$ (50 μM), ascorbic acid (62.5 μM) and respectively; lanes 6-10: 0.5, 5, 50, 500, and 5000 μM respectively of either Na_2SeO_3 or SeO_2.

Discussion

Selenium compounds are effective at preventing cancer, either due to their antioxidant ability to neutralize ROS,[16,32] or through induction of apoptosis in cancer cells.[18,30,32] Evidence for both prevention of cell death under oxidative stress and promotion of apoptosis has been found for Na_2SeO_3 administered in similar concentrations: Na_2SeO_3 (1 μM) prevented cell death from ROS in hepatoma cells[42] and stimulated benign mesothelial cell growth (7.5 μM),[30] whereas in prostate cancer cells, Na_2SeO_3 (0.5-5 μM) inhibited cell growth via apoptosis.[18] Our results help explain these contradictory chemopreventative (antioxidant) and anticancer effects of selenite, since we have found that for selenite and selenium dioxide, inhibition of oxidative DNA damage by hydroxyl radical is dependent on both the concentration of selenium compound and H_2O_2.

Mode I experiments with inorganic selenium compounds and Fe^{2+}

Experiments conducted with Na_2SeO_3 and SeO_2 show that both compounds inhibit DNA damage under Mode I conditions in a concentration-dependent manner with maximal DNA damage inhibition at 5000 μM. Under the same conditions, Na_2SeO_4 and Na_2Se have no effect on DNA damage (Table 2.1). Although selenium concentrations of 5000 μM are much larger than would be found in cells, plasma selenium concentrations in humans can reach 1.1-1.3 μM after consuming 40 μg of selenium supplement a day.[43] At 0.5 μM, Na_2SeO_3 inhibited 37% of DNA damage ($p = 0.02$), whereas SeO_2 at this concentration acted as a pro-oxidant, increasing DNA damage by 20 % ($p = 0.02$). These

results indicate that Na_2SeO_3 may be a more effective antioxidant *in vivo* than Na_2SeO_4, Na_2Se, or SeO_2.

Table 2.1. Summary of effects of inorganic selenium compounds on DNA damage under Mode I and Mode II conditions.

Compound	**DNA Damage Behavior**
Na_2SeO_4	No antioxidant or pro-oxidant behavior under any conditions
Na_2SeO_3	*Mode I:* Antioxidant at all concentrations (0.5 – 5000 μM) *Mode II:* Pro-oxidant behavior with or without Fe^{2+} at all concentrations (0.5 – 5000 μM)
SeO_2	*Mode I*: Pro-oxidant at low concentrations (0.5 – 250 μM), antioxidant at higher concentrations (250 - 5000 μM) *Mode II*: Antioxidant at all concentrations
Na_2Se	No antioxidant or pro-oxidant behavior under any conditions (0.5 – 200 μM)
All antioxidant behavior requires Fe^{2+} coordination	

It is not clear why SeO_2 acts as a pro-oxidant and an antioxidant depending upon concentration, but the pro-oxidant effect of SeO_2 at low concentrations may be due to its ability to generate radical species. SeO_2 is proposed to react with aqueous H_2O_2 to form peroxyselenenic acid ($SeO_2 + H_2O_2 \rightarrow HOSe(O)OOH$), that then may decompose to yield $^{\bullet}OH$.[44] In addition, it has been reported that SeO_2 in aqueous solution at pH 6 exists as $HSeO_3^-$,[39-41] which can then be reduced to SeO_2^- radical ($SeO_2 + H_2O \rightarrow HSeO_3^- + H^+ \rightarrow SeO_2^- + OH^-$).[39] However, if aqueous SeO_2 is present as $HSeO_3^-$, it is surprising that

we see significantly different effects with SeO_2 as compared to Na_2SeO_3 in our gel electrophoresis studies. Our ^{77}Se NMR studies of SeO_2 and Na_2SeO_3 show different resonance frequencies for both compounds in aqueous solutions, indicating that they do not form the same species. This result correlates well with the different effects of these two compounds on DNA damage. A separate study showed that Na_2SeO_3 was more effective at inducing apoptosis than SeO_2[16] suggesting that these compounds also have different properties *in vivo*.

The four inorganic selenium compounds studied in this work differ by both oxidation state and charge. Both Na_2SeO_3 and SeO_2 with a selenium oxidation state of +4 inhibit DNA damage at high concentrations, whereas Na_2SeO_4 with an oxidation state of +6 and Na_2Se (-2) have no effect on DNA damage. This indicates that inorganic selenium compounds with selenium in the +4 oxidation state are more effective at preventing DNA damage under Mode I conditions than those in either the highest or lowest oxidation states. The lack of DNA damage inhibition with Na_2SeO_4 can be explained if the selenium compound reacts with and neutralizes generated $^{\bullet}OH$. Since Na_2SeO_4 is in its highest oxidation state, it cannot be oxidized by $^{\bullet}OH$. The lack of DNA damage inhibition by Na_2Se is more difficult to explain using charge arguments, since the oxidation state of the selenium is low. In addition, organic selenides (R-Se-R, selenium oxidation state of -2) are well-known for their antioxidant properties.[21,31] However, based on their respective reduction potentials, selenide (0.924 V[45]) cannot be oxidized by H_2O_2 (0.38 V[10]).

From our results, it is clear that charge on the inorganic selenium compounds does not play a significant role in preventing DNA damage. Na_2SeO_3, Na_2SeO_4 and Na_2Se have the same -2 charge, however only Na_2SeO_3 was able to inhibit DNA damage under Mode I conditions. SeO_2, a neutral compound, also inhibits DNA damage at high concentrations, suggesting that oxidation state plays a much more significant role than overall charge in DNA damage inhibition.

Mode II experiments with inorganic selenium compounds and Fe^{2+}

Similar to results observed under Mode I conditions, Na_2SeO_4 and Na_2Se have no effect on DNA damage under Mode II conditions. In contrast to Mode I conditions, however, SeO_2 under Mode II conditions inhibited DNA damage at all concentrations tested, reducing DNA damage by a maximum of 81% at 5000 μM (Table I). At more biologically-relevant concentrations of selenium (0.5 μM), SeO_2 showed weak antioxidant activity under Mode II conditions, in direct opposition to its pro-oxidant activity at the same concentration under Mode I conditions.

Interestingly, when Na_2SeO_3 is combined with H_2O_2 without Fe^{2+} under Mode II conditions, DNA damage is promoted in a concentration-dependent manner. This is very different behavior compared to its inhibitory effect at all concentrations under Mode I conditions. A possible reason for the pro-oxidant activity seen under Mode II conditions is that the Na_2SeO_3 is oxidized by H_2O_2 from +4 to +6 states, producing $^{\bullet}OH$ in the process. Considering the reduction potentials of selenite (-0.05 V [45]) and H_2O_2 (0.38V[10]), selenite is capable of reducing H_2O_2. Additionally, $SeO_3^{\bullet-}$ formed from the one electron

oxidation of Na_2SeO_3 by $^{\bullet}OH$ could also damage DNA.[46] It is unclear, however, why the antioxidant or pro-oxidant behavior of Na_2SeO_3 would be entirely dependent upon H_2O_2 concentration. Calculations indicate that the steady-state H_2O_2 concentration in unstressed *E. coli* is ~20 nM, but with a high generation rate of 9-22 μM/s.[47] Thus, H_2O_2 concentrations may increase quickly if an imbalance between generation and decomposition exists. If the antioxidant or pro-oxidant behavior of Na_2SeO_3 depends on cellular H_2O_2 concentrations, this highlights the need to accurately measure concentrations of H_2O_2 in both unstressed and oxidatively-stressed cells.

Modes I and II $[Fe(EDTA)]^{2-}$ experiments with inorganic selenium compounds

Experiments with $[Fe(EDTA)]^{2-}$ as the iron source were performed to determine whether DNA damage inhibition by inorganic selenium compounds is due to iron coordination. Increasing concentrations of Na_2SeO_3 and SeO_2 using the completely-coordinated $[Fe(EDTA)]^{2-}$ resulted in no change in DNA damage. These experiments indicate that iron coordination by Na_2SeO_3 and SeO_2 is required for inhibition of (or increase in, for lower concentrations of SeO_2) DNA damage inhibition under Mode I conditions. Similarly, under Mode II conditions, iron binding is also important for the inhibitory effect of SeO_2 on DNA damage. In a similar study performed with organic selenium compounds using copper and H_2O_2 to generate $^{\bullet}OH$, metal coordination was also the proposed mechanism for DNA damage inhibition.[31]

Coordination between iron and SeO_3^{2-} or SeO_2 is likely: both Na_2SeO_3 and SeO_2 contain hard oxygen ligands, which can coordinate to Fe^{2+}, a borderline hard Lewis acid.

Because selenium is much softer than oxygen, it less likely that Fe^{2+} would bind to selenium, especially given its positive oxidation state in both Na_2SeO_3 and SeO_2. In fact, characterization of several iron-selenite complexes shows that iron indeed binds selenite through the negatively-charged oxygen atoms.[48,49]

Based on our results, Na_2SeO_3, and to a lesser extent SeO_2, exhibit both antioxidant and pro-oxidant behaviors dependent on H_2O_2 concentration. Understanding this seemingly contradictory behavior may help explain conflicting results seen for anticancer studies using Na_2SeO_3.[20,33,34,50,51] We have clearly demonstrated the ability of inorganic selenium compounds both to prevent and generate DNA damage using a biologically-relevant DNA damage assay, but the complex behaviors of these compounds with regard to their concentration and concentration of H_2O_2 *in vivo* merit further study.

Cu^+ experiments with inorganic selenium compounds

Similar to results observed under Mode I conditions with iron, Na_2SeO_4 and Na_2Se have no effect on copper-mediated DNA damage. Under similar conditions, however, both Na_2SeO_3 and SeO_2 inhibit 95% and 63% DNA damage, respectively at high concentrations (5000 μM). Interestingly, the antioxidant activity observed for Na_2SeO_3 were similar for both Fe^{2+}-mediated DNA damage under Mode I conditions (91%) and Cu^+-mediated DNA damage (95%) at 5000 μM. However, SeO_2 at the same concentration was more effective at inhibiting Fe^{2+}-mediated DNA damage (100%) than Cu^+-mediated DNA damage (63%) under similar reaction conditions. At more biologically-relevant concentrations (0.5 μM), Na_2SeO_3 is a better antioxidant with iron-

mediated DNA damage under Mode I conditions (36%, p = 0.02) when compared to the insignificant activity observed for this compound with copper-mediated DNA damage (-0.5%, p = 0.5). Interestingly, the pro-oxidant activity of SeO_2 (-21%, p = 0.02) at more biologically-relevant concentrations (0.5 μM) under Mode I conditions with iron was unobserved with copper-mediated DNA damage at the same concentration (0.1%, p = 0.2). These results suggest that the metal ion plays a significant role in the antioxidant and pro-oxidant propeties of inorganic selenium compounds. Under Fenton reaction conditions, iron coordination to the selenium compound is novel mechanism for the antioxidant and pro-oxidant activities of both Na_2SeO_3 and SeO_2. Our copper coordination results performed with $[Cu(bipy)]^+$ indicate that this novel metal-binding mechanism is also responsible for the antioxidant activity observed with inorganic selenium compounds with copper-mediated DNA damage. Similar to the results observed for iron-mediated DNA damage, both Na_2SeO_3 and SeO_2 (both with a selenium oxidation state of +4) are much more effective at preventing DNA damage than either Na_2SeO_4 (+6) or Na_2Se (-2). Our results suggest that oxidation state of the selenium atom of the four inorganic selenium compounds tested plays an important role in the antioxidant activity of these compounds on copper-mediated DNA damage.

Conclusions

The essential micronutrient selenium is widely used in over-the-counter supplements, infant formulas, protein mixes, and animal feed, often in the form of its inorganic compounds. Despite having received much attention for their antioxidant and

chemopreventative properties, uncertainties remain with regard to the concentration dependence and mechanism for these behaviors.[16,18,30] We have shown that Na_2SeO_4 and Na_2Se are unable to inhibit both iron-mediated and copper-mediated DNA damage, a surprising result given the ability of organic selenides to inhibit DNA damage under similar conditions.[21,31] Additionally, SeO_2 and Na_2SeO_3 behave as both pro-oxidants and antioxidants depending on the concentrations of selenium compound and H_2O_2 with iron-mediated DNA damage, but were only antioxidants with copper-mediated DNA damage. Identification of these complex antioxidant and pro-oxidant behaviors help to reconcile seemingly conflicting results obtained in cell studies with these compounds,[16,18,32] and also suggest that the more damage-neutral Na_2SeO_4 may be more suitable for use in selenium supplementation. Our results also demonstrate that the formal oxidation state of the selenium atom is the primary determinant of antioxidant behavior for these inorganic selenium compounds, and not their overall charge. In addition, the antioxidant effects of both inorganic and organic selenium compounds have now been attributed to their coordination of the metal ions responsible for the production of reactive radicals,[31] indicating that this novel metal-coordination mechanism for antioxidant behavior may be relevant to antioxidant function *in vivo*.

Materials and Methods

Materials

NaCl (99.999% to avoid trace metal contamination), Na_2SeO_3, SeO_2 $Na_2SeO_4 \cdot 10H_2O$, glacial acetic acid, NaOH, 30% H_2O_2 solution, $FeSO_4 \cdot 7H_2O$,

$CuSO_4 \cdot 5H_2O$, ascorbic acid, 2,2'-bipyridine and bromophenol blue were from Alpha Aesar. Glucose, agarose, and ampicillin were from EMD Chemicals. TRIS hydrochloride and sodium EDTA were from J.T. Baker. HCl was from VWR Scientific; ethidium bromide from Lancaster Synthesis Inc. Xylene cyanol, peptone, and yeast extract came from EM Science. D_2O and DCl were from Acros, and NaOD was from Cambridge Isotope Laboratories, Inc. Water was purified using the NANOpure DIamond water deionization system (Barnstead International, Dubuque, IA). Iron-free microcentrifuge tubes were prepared by washing the tubes in 1 M HCl prior to use and rinsing thoroughly. ^{77}Se NMR data were obtained from a Bruker Avance 500 MHz NMR spectrometer.

Purification of plasmid DNA

DH1 *E. coli* cells were transfected with pBSSK, plated on LB/amp plates, and incubated for 16 h at 37 ^{o}C. Cell cultures were grown in TB/amp medium inoculated with a single colony and incubated for 15 h at 37 ^{o}C. Plasmid DNA was purified from the cell pellets using a QIAprep Spin Miniprep kit, and tris-EDTA (TE) buffer was used to elute the DNA. Dialysis of plasmid DNA was performed against 130 mM NaCl for 24 h at 4 ^{o}C. The resulting DNA concentration was found using UV-vis measurements at A_{260} (1 A_{260} = 50 ng/μL). Purity of plasmid DNA was determined via gel electrophoresis of a digested sample, and all absorbance ratios were within acceptable limits ($A_{250/260} < 0.95$, and $A_{260/280} > 1.8$).

DNA nicking experiments under Mode I conditions with Fe^{2+}

The indicated concentrations of Na_2SeO_3, Na_2SeO_4, SeO_2 and Na_2Se, 0.1 pmol plasmid DNA, 130 mM NaCl, 10 mM ethanol, 2 μM $FeSO_4 \cdot 7H_2O$ at pH 6 were combined and allowed to stand for 5 min at room temperature. H_2O_2 (50 μM)[11] was then added and incubated for 30 min. EDTA (50 μM) was added after this time and a total volume of 10 μL was maintained with ddH_2O. DNA was separated on 1% agarose gels via electrophoresis, stained with ethidium bromide for 30 min, and imaged on an UVIproDBT-8000 gel imager (UVITec, Cambridge, UK). Quantification of closed-circular and nicked DNA was performed using the UviPro software and results were shown in a bar graph. For gels run with $[Fe(EDTA)]^{2-}$ (400 μM) as the iron source, a similar procedure was used substituting $[Fe(EDTA)]^{2-}$ (400 μM) for $FeSO_4 \cdot 7H_2O$.

DNA nicking experiments under Mode II conditions with Fe^{2+}

Similar procedures to Mode I experiments were followed with increases in ethanol (100 mM) and H_2O_2 (50 mM).[11] Experiments with Na_2SeO_3 were performed at pH 7 without iron.

DNA nicking experiments with copper

Similar procedures to Mode I experiments were followed using Cu^+ (6 μM) as the metal source instead of Fe^{2+} at pH 7. For gels run with $[Cu(bipy)]^+$ (50 μM) as the metal source, a similar procedure was used substituting $[Cu(bipy)]^+$ (50 μM) for $FeSO_4 \cdot 7H_2O$.

Data analysis

Percent DNA damage inhibition was determined using the formula 1-[% N / % B]*100, where % N = % nicked DNA in the selenium containing lanes and % B = % of nicked DNA in the Fe^{2+} or Cu^{+}/H_2O_2 lane. Percentages are corrected for residual nicked DNA prior to calculation. Results are the average of three trials, and standard deviations are indicated by error bars. Percent DNA damage was calculated using the formula [% N / % B]*100, where % B = percent of nicked DNA in the H_2O_2 only lane. Statistical significance was determined by calculating p values at 95% confidence ($p < 0.05$ indicates significance) as described by Perkowski *et al*.[52] A complete listing of these values can be found at the end of this Materials and Methods section in Tables 2.2-2.18.

^{77}Se NMR Experiments

^{77}Se NMR samples (0.75 mL) were prepared by adding SeO_2 (2 M) or Na_2SeO_3 (0.6 M) to solutions of NaCl (2 equiv.) in D_2O. Appropriate amounts of NaOD or DCl were added to achieve the desired pD (6.4 or 7.4). Conversion of pH into pD was performed using the formula $p[D^+] = 0.4 + p[H^+]$.[53,54] These experiments were performed using diphenyl diselenide as a reference (δ 850). ^{77}Se NMR spectra obtained for these experiments are shown in Figures 2.11 and 2.12.

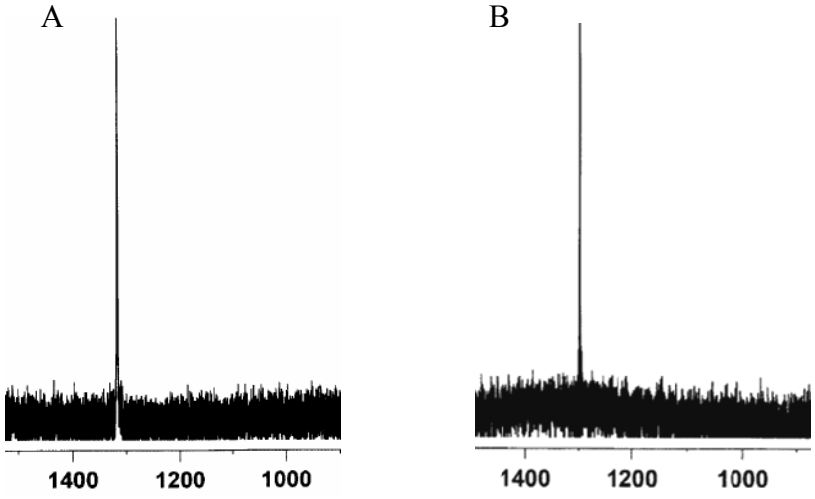

Figure 2.11. ^{77}Se NMR spectra of Na_2SeO_3 at (A) pH 6 and (B) pH 7. Both spectra show a singlet at δ 1274.

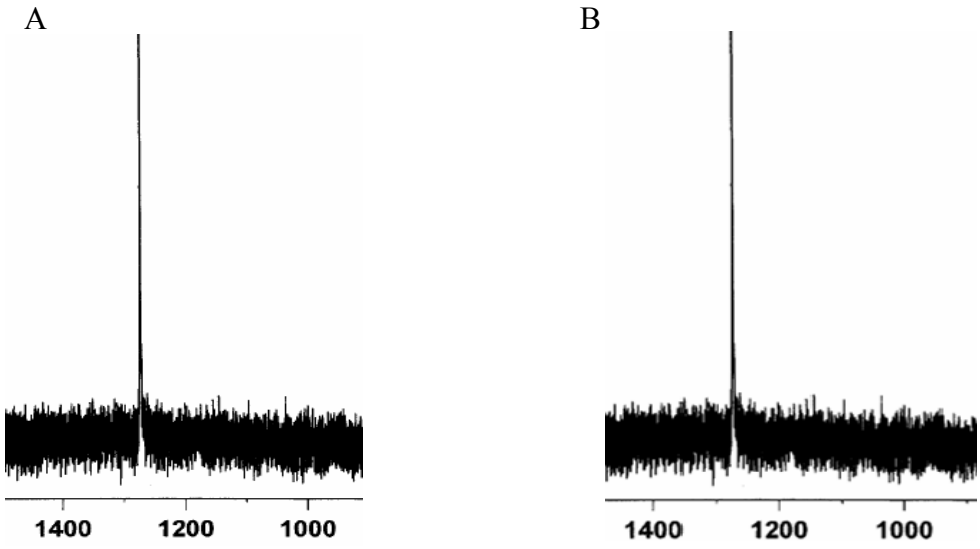

Figure 2.12. ^{77}Se NMR spectra of SeO_2 at (A) pH 6 with a singlet at δ 1317, and (B) pH 7 with a singlet at δ 1299.

Tabular data for gel electrophoresis experiments

Tabulated values for the percentages of closed, circular and nicked DNA bands observed in the gel electrophoresis experiments for Fe^{2+}/H_2O_2 (pH = 6) in Mode I are

given in Tables 2.2-2.5. Tabulated values using $[Fe(EDTA)]^{2-}$ as the iron source instead of Fe^{2+} in Mode I at pH 6 are in Tables 2.6-2.7. Additionally, tabulated values of the compounds tested in the absence or presence of Fe^{2+} (pH = 6) in Mode II are given in Tables 2.8-2.11 and those with $[Fe(EDTA)]^{2-}$ are given in Table 2.12. Tabulated values for the inorganic selenium compounds tested with copper (pH 7) are given in Tables 2.13-2.16 and those with $[Cu(bipy)]^{+}$ are in Tables 2.17-2.18. All reported tabulated values are the average of three experimental trials with the indicated calculated standard deviation.

Table 2.2. Tabulation for electrophoresis results for Na_2SeO_3 with Fe^{2+} (2 μM) and H_2O_2 (50 μM) in Mode I (pH 6).

Lane	Concentration (μM)	% Circular DNA	% Nicked DNA	% Damage Inhibition	p-value
5	0	6.0 ± 3.0	94	0	
6	0.5	37 ± 6.5	63	36 ± 8.8	0.02
7	5	39 ± 1.5	61	38 ± 3.9	0.004
8	50	50 ± 4.7	50	52 ±7.3	0.007
9	500	82 ± 0.96	18	89 ± 1.9	0.0002
10	5000	83 ± 2.3	17	91 ± 2.0	0.0002

Table 2.3. Tabulation for electrophoresis results for Na_2SeO_4 with Fe^{2+} (2 μM) and H_2O_2 (50 μM) in Mode I (pH 6).

Lane	Concentration (μM)	% Circular DNA	% Nicked DNA	% Damage Inhibition	p-value
5	0	2.0 ± 1.5	98	0	
6	0.5	3.7 ± 2.3	96.3	2.1 ± 1.4	0.12
7	5	2.0 ± 0.78	98	-0.05 ± 1.1	0.94
8	50	4.7 ± 3.7	95.3	3.4 ± 3.1	0.20
9	500	2.2 ± 0.61	97.8	0.3 ± 1.4	0.75
10	5000	5.0 ± 3.0	95	3.8 ± 3.1	0.17

Table 2.4. Tabulation for electrophoresis results for Na_2Se with Fe^{2+} (2 μM) and H_2O_2 (50 μM) in Mode I (pH 6).

Lane	Concentration (μM)	% Circular DNA	% Nicked DNA	% Damage Inhibition	p-value
5	0	0.0 ± 0.1	100	0	
6	0.5	0.1 ± 0.1	99.9	0.1 ± 0.1	0.23
7	5	0.2 ± 0.3	99.8	0.2 ± 0.3	0.37
8	50	0.0 ± 0.2	100	0.0 ± 0.2	1.0
9	100	0 .0 ± 0.3	100	0.0 ± 0.3	1.0
10	200	0.2 ± 0.4	99.8	0.2 ± 0.4	0.48

Table 2.5. Tabulation for electrophoresis results for SeO_2 with Fe^{2+} (2 μM) and H_2O_2 (50 μM) in Mode I (pH 6).

Lane	Concentration (μM)	% Circular DNA	% Nicked DNA	% Damage Inhibition	p-value
5	0	22 ± 1.9	78	0	
6	0.5	6.0 ± 1.0	94	-21 ± 4.5	0.015
7	5	5.4 ± 1.2	94.6	-22 ± 4.7	0.015
8	50	6.6 ± 1.5	93.4	-20 ± 5	0.02
9	500	34 ± 1.9	66	17 ± 3.1	0.01
10	5000	97 ± 1.0	3.0	100 ± 0.5	< 0.0001

Table 2.6. Tabulation for electrophoresis results for Na_2SeO_3 with $[Fe(EDTA)]^{2-}$ (400 μM) and H_2O_2 (50 μM) in Mode I (pH 6).

Lane	Concentration (μM)	% Circular DNA	% Nicked DNA	% Damage Inhibition	p-value
5	0	38 ± 0.66	63	0.0	
6	0.5	39 ± 0.54	61	2.5 ± 1.8	0.14
7	5	40 ± 1.9	60	4.8 ± 2.1	0.06
8	50	40 ± 0.82	60	3.7 ± 0.3	0.003
9	500	38 ± 0.82	62	0.2 ± 0.4	0.48
10	5000	41 ± 0.66	59	6.5 ± 1.5	0.02

Table 2.7. Tabulation for electrophoresis results for SeO_2 with $[Fe(EDTA)]^{2-}$ (400 μM) and H_2O_2 (50 μM) in Mode I (pH 6).

Lane	Concentration (μM)	% Circular DNA	% Nicked DNA	% Damage Inhibition	p-value
5	0	25 ± 2.7	75	0	
6	0.5	26 ± 2.1	74	1.7 ± 0.8	0.06
7	5	25 ± 2.1	75	0.99 ± 0.9	0.18
8	50	26 ± 2.9	74	2.6 ± 2.1	0.17
9	500	27 ± 2.7	73	2.8 ± 0.6	0.02
10	5000	26 ± 2.6	74	1.7 ± 1.4	0.17

Table 2.8. Tabulation for electrophoresis results for Na_2SeO_3 and H_2O_2 (50 mM) without Fe^{2+} in Mode II (pH 6).

Lane	Concentration (μM)	% Circular DNA	% Nicked DNA	% DNA Damage	p-value
3	0	98 ± 0.9	2.0	0	
5	0.5	90 ± 3.9	10	1.7 ± 4.4	0.56
6	5	88 ± 1.8	11.7	3.4 ± 1.8	0.04
7	50	90 ± 0.4	9.6	1.1 ± 0.13	0.005
8	500	78 ± 1.6	22.5	15 ± 1.4	0.0006
9	5000	9.1 ± 2.6	90.9	90 ± 3.0	0.0004

Table 2.9. Tabulation for electrophoresis results for Na_2SeO_4 with Fe^{2+} (2 μM) and H_2O_2 (50 mM) in Mode II (pH 6).

Lane	Concentration (μM)	% Circular DNA	% Nicked DNA	% Damage Inhibition	p-value
5	0	19 ± 0.5	81	0	
6	0.5	21 ± 1.0	89	2.7 ± 2.3	0.18
7	5	21 ± 1.3	89	3.7 ± 2.7	0.14
8	50	21 ± 0.8	89	3.0 ± 2.0	0.12
9	500	19 ± 0.7	81	0.6 ± 0.4	0.12
10	5000	19 ± 0.4	81	0.2 ± 0.3	0.37

Table 2.10. Tabulation for electrophoresis results for Na_2Se with Fe^{2+} (2 μM) and H_2O_2 (50 mM) in Mode II (pH 6).

Lane	Concentration (μM)	% Circular DNA	% Nicked DNA	% Damage Inhibition	p-value
5	0	7.5 ± 6.5	93.9	0	
6	0.5	0	100	-9.1 ± 7.9	0.18
7	5	0	100	-9.1 ± 7.9	0.18
8	50	0	100	-9.1 ± 7.9	0.18
9	100	0	100	-9.1 ± 7.9	0.18
10	200	0	100	-9.1 ± 7.9	0.18

Table 2.11. Tabulation for electrophoresis results for SeO_2 with Fe^{2+} (2 μM) and H_2O_2 (50 mM) in Mode II (pH 6).

Lane	Concentration (μM)	% Circular DNA	% Nicked DNA	% Damage Inhibition	p-value
5	0	13 ± 1.1	87	0	
6	0.5	16 ± 2.1	84	4.5 ± 3.1	0.13
7	5	20 ± 3.1	80	9.1 ± 3.8	0.05
8	50	26 ± 2.4	74	18 ± 3.1	0.01
9	500	34 ± 3.4	66	30 ± 5.6	0.01
10	5000	72 ± 1.6	28	81 ± 7.3	0.003

Table 2.12. Tabulation for electrophoresis results for SeO_2 with $[Fe(EDTA)]^{2-}$ (400 μM) and H_2O_2 (50 mM) in Mode II (pH 6).

Lane	Concentration (μM)	% Circular DNA	% Nicked DNA	% Damage Inhibition	p-value
5	0	0.3 ± 0.3	99.7	0	
6	0.5	0.1 ± 0.2	99.9	-0.3 ± 0.2	0.12
7	5	0.2 ± 0.3	99.8	-0.2 ± 0.2	0.23
8	50	0.2 ± 0.3	99.8	-0.2 ± 0.2	0.23
9	500	0.2 ± 0.3	99.8	-0.2 ± 0.2	0.23
10	5000	0.2 ± 0.3	99.8	-0.2 ± 0.2	0.23

Table 2.13. Tabulation for electrophoresis results for Na_2SeO_3 with Cu^+ (6 μM) and H_2O_2 (50 μM) at pH 7.

Lane	Concentration (μM)	% Circular DNA	% Nicked DNA	% Damage Inhibition	p-value
5	0	0.8 ± 0.3	99.2	0	
6	0.5	0.3 ± 0.7	99.7	-0.5 ±1.2	0.55
7	5	0.6 ± 4.7	99.4	-0.2 ± 1.7	0.86
8	50	0.7± 1.2	99.3	-0.1 ±2.2	0.94
9	500	12.6 ± 5.3	88.4	12.2 ± 4.4	0.04
10	5000	93.4 ± 3.7	6.6	95.1 ± 3.9	0.0003

Table 2.14. Tabulation for electrophoresis results for Na_2SeO_4 with Cu^+ (6 μM) and H_2O_2 (50 μM) at pH 7..

Lane	Concentration (μM)	% Circular DNA	% Nicked DNA	% Damage Inhibition	p-value
5	0	2 ± 1.5	98	0	
6	0.5	3 ± 1.1	97	2.1 ± 1.4	0.12
7	5	2 ± 0.7	98	0.02 ± 1.1	0.98
8	50	5 ± 1.3	95	2.5 ± 3.1	0.30
9	500	2.2 ± 0.3	97.8	0.02 ± 1.4	0.98
10	5000	5 ± 3	95	3.8 ± 3.1	0.17

Table 2.15. Tabulation for electrophoresis results for Na_2Se with Cu^+ (6 μM) and H_2O_2 (50 μM) at pH 7.

Lane	Concentration (μM)	% Circular DNA	% Nicked DNA	% Damage Inhibition	p-value
5	0	0 ± 0.1	100	0	
6	0.5	0.1 ± 0.1	99.9	0.1 ± 0.1	0.25
7	5	0.2 ± 0.3	99.8	0.2 ± 0.3	0.37
8	50	0.2 ± 0.2	99.8	0.2 ± 0.2	0.37
9	100	0.1± 0.1	99.9	0.1 ± 0.1	0.25
10	200	0.2 ± 0.4	99.8	0.2 ± 0.4	0.45

Table 2.16. Tabulation for electrophoresis results for SeO_2 with Cu^+ (6 μM) and H_2O_2 (50 μM) at pH 7..

Lane	Concentration (μM)	% Circular DNA	% Nicked DNA	% Damage Inhibition	p-value
5	0	0 ± 0.1	100	0	
6	0.5	0.4 ± 0.7	99.6	0.1 ± 0.1	0.25
7	5	0.7 ± 0.1	99.3	0.2 ± 0.1	0.48
8	50	0.7 ± 0.2	99.3	0.3 ± 0.2	0.12
9	500	2.2 ± 1.5	98.8	3.5 ± 1.2	0.04
10	5000	65.5 ± 4.3	34.5	70.4 ± 3.3	0.0007

Table 2.17. Tabulation for electrophoresis results for Na_2SeO_3 with $[Cu(bipy)_2]^+$ (50 μM) and H_2O_2 (50 μM) at pH 7..

Lane	Concentration (μM)	% Circular DNA	% Nicked DNA	% Damage Inhibition	p-value
5	0	5 ± 0.7	95	0	
6	0.5	5.5 ± 0.5	94.5	1.5 ± 1.2	0.16
7	5	4.2 ± 1.9	95.8	2.1 ± 1.3	0.11
8	50	5.1 ± 0.8	94.9	1.5 ± 0.3	0.01
9	500	2 ± 0.8	98	0.2 ± 0.1	0.07
10	5000	2.3 ± 0.6	97.7	0.3 ± 0.2	0.12

Table 2.18. Tabulation for electrophoresis results for SeO_2 with $[Cu(bipy)_2]^+$ (50 μM) and H_2O_2 (50 μM) at pH 7..

Lane	Concentration (μM)	% Circular DNA	% Nicked DNA	% Damage Inhibition	p-value
5	0	16 ± 0.5	84	0	
6	0.5	10 ± 0.3	90	-4.7 ± 0.9	0.01
7	5	9.5 ± 1.2	90.5	-5.0 ± 1.2	0.02
8	50	8.3 ± 0.9	91.7	- 5.1 ± 0.2	0.003
9	500	8.1 ± 0.7	91.9	-5.5 ± 0.3	0.0009
10	5000	8 ± 0.8	92	-5.6 ± 0.1	0.0001

References

(1) Stewart, M. S.; Spallholz, J. E.; Neldner, K. H.; Pence, B. C. *Free Rad. Biol. Med.* **1999**, *26*, 42-48.

(2) Halliwell, B. *Drugs and Aging* **2001**, *18*, 685-716.

(3) Henle, E. S.; Linn, S. *J. Biol. Chem.* **1997**, *272*, 19095-19098.

(4) Hoffmann, M. E.; Mello-Filho, A. C.; Meneghini, R. *Biochem. Biophys. Acta* **1984**, *781*, 234-238.

(5) Mello-Filho, A. C.; Meneghini, R. *Mutat. Res.* **1991**, *251*, 109-113.

(6) Henle, E. S.; Luo, Y.; Linn, S. *Biochemistry* **1996**, *35*, 12212-12219.

(7) Steinberg, D. J. *Biol. Chem.* **1997**, *272*, 20963-20966.

(8) Singal, P. K.; Khaper, N.; Palace, V.; Kumar, D. *Cardiovasc. Res.* **1998**, *40*, 426-32.

(9) Imlay, J. A.; Chin, S. M.; Linn, S. *Science* **1988**, *240*, 640-642.

(10) Imlay, J. A.; Linn, S. *Science* **1988**, *240*, 1302-1309.

(11) Henle, E. S.; Zhengxu, H.; Tang, N.; Rai, P.; Luo, Y.; Linn, S. *J. Biol. Chem.* **1999**, *274*, 962-971.

(12) Henle, E. S.; Linn, S. *J. Biol. Chem.* **1997**, *272*, 19095-19098.

(13) Warner, D. S.; Sheng, H.; Batinic-Haberle, I. *J. Exp. Biol.* **2004**, *207*, 3221-3231.

(14) Milne, L.; Nicotera, P.; Orrenius, S.; Burkitt, M. J. *Arch. Biochem. Biophys.* **1993**, *304*, 102-109.

(15) El-Bayoumy, K. *Mutat. Res.* **2001**, *475*, 123-139.

(16) Takahashi, M.; Sato, T.; Shinohara, F.; Echigo, S.; Rikiishi, H. *Int. J. Oncol.* **2005**, *27*, 489-495.

(17) Zhong, W.; Oberley, T. D. *Cancer Res.* **2001**, *61*, 7071-7078.

(18) Holmgren, A. *Free Rad. Biol. Med.* **2006**, *41*, 862-865.

(19) Schrauzer, G. N. *J. Am. Coll. Nutr.* **2001**, *20*, 1-4.

(20) Combs, G. F.; Gray, W. P. *Pharmacol. Ther.* **1998**, *79*, 179-192.

(21) Gladyshev, V. N.; Kryukov, G. V. *BioFactors* **2001**, *14*, 87-92.

(22) Finley, J. W.; Ip, C.; Lisk, D. J.; Davis, C. D.; Hintze, K. J.; Whanger, P. D. *J. Agric. Food Chem.* **2001**, *49*, 2679-2683.

(23) Van Houweling, C. D. *Final Environmental Impact Statement on Selenium in Animal Feeds*, 1975.

(24) Spallholz, J. E.; Boylan, L. M.; Rhaman, M. M. *Sci. Tot. Environ.* **2004**, *323*, 21-32.

(25) Mugesh, G.; Singh, H. B. *Chem. Soc. Rev.* **2000**, *29*, 347-357.

(26) Davis, C. D.; Feng, Y.; Hein, D. W.; Finley, D. W. *J. Nutr.* **1999**, *129*, 63-69.

(27) Ip, C.; Hayes, C. *Carcinogenesis* **1989**, *10*, 921-925.

(28) Wilson, A. C.; Thompson, H. J.; Schedin, P. J.; Gibson, N. W.; Ganther, H. E. *Biochem. Pharmacol.* **1992**, *43*, 1137-1141.

(29) Snyder, R. D. *Cancer Lett.* **1987**, *34*, 73-81.

(30) Nilsonne, G.; Sun, X.; Nystrom, C.; Rundlof, A.-K.; Fernandes, A. P.; Bjornstedt, M.; Dobra, K. *Free Rad. Biol. Med.* **2006**, *41*, 874-885.

(31) Battin, E. B.; Perron, N. R.; Brumaghim, J. L. *Inorg. Chem.* **2006**, *45*, 499-501.

(32) Zhou, N.; Xiao, H.; Li, T.-K.; Nur-E-Kamal, A.; Liu, L. F. *J. Biol. Chem.* **2003**, *278*, 29532-29537.

(33) Dorado, R. D.; Porta, E. A.; Aquino, T. M. *Hepatology* **1985**, *5*, 1201-1208.

(34) Perchellet, J. P.; Abney, N. L.; Thomas, R. M.; Guislan, Y. L.; Perchellet, E. M. *Cancer Res.* **1987**, *47*, 447-485.

(35) Hamilton, E. E.; Wilker, J. J. *Biol. Inorg. Chem.* **2004**, *9*, 894-902.

(36) Chen, W.; Cao, X.; Zhu, R.; Lui, W. *Chinese J. Cancer Res.* **2004**, *16*, 162-166.

(37) Prütz, W. A. Z. *Naturforsch* **1990**, *45C*, 1197-1206.

(38) Ramoutar, R. R.; Brumaghim, J. L. *J. Inorg. Biochem.* **2007**, *101*, 1028-1035.

(39) Adhikari, S.; Mukherjee, T.; Janata, E. *Res. Chem. Intermed.* **2005**, *31*, 227-234.

(40) Nazarenk, I. I.; Ermakov, A. N. *Analytical Chemistry of Selenium and Tellurium*; John Wiley and Sons, Inc.: New York, 1972.

(41) Tamba, M.; Dadello, R. *Radiat. Phys. Chem.* **1977**, *10*, 283-288.

(42) Fiskin, K. *Turk. J. Med. Sci.* **2000**, *30*, 230-207.

(43) Duffield, A. J.; Thomson, C. D.; Hill, K. E.; Williams, S. *Am. J. Clin. Nutr.* **1999**, *70*, 896-903.

(44) Mlochowski, J. *Phosphorus, Sulfur, Silicon* **1998**, *136-138*, 191-204.

(45) *CRC Handbook of Chemistry and Physics*; Lide, D. R., Ed.; CRC Press: Boca Raton, FL, 1994.

(46) Milligan, J. R.; Aguilera, J. A.; Paglinawan, R. A.; Ward, J. F. *Int. J. Radiat. Biol.* **2002**, *78*, 359-374.

(47) Seaver, L. C.; Imlay, J. A. *J. Biol. Chem.* **2004**, *279*, 48742-48750.

(48) Xiao, D.; Hou, Y.; Wang, E.; An, H.; Lu, J.; Li, Y.; Xu, L.; Hu, C. *J. Solid State Chem.* **2004**, *177*, 2699-2704.

(49) Xiao, D.; An, H.; Wang, E.; Xu, L. *J. Mol. Structure* **2005**, *740*, 249-253.

(50) Thompson, H. J.; Meeker, L. D.; Becci, P. J.; Kokoska, S. *Cancer Res.* **1982**, *42*, 4954-4958.

(51) Ip, C.; Ip, M. *Carcinogenesis* **1981**, *9*, 915-918.

(52) Perkowski, D. A.; Perkowski, M. *Data and Probability Connections*; Pearson Prentice Hall: New Jersey, 2007, pp 301-321.

(53) Covington, A. K.; Paabo, M.; Robinson, R. A.; Bates, R. G. *Anal. Chem.* **1968**, *40*, 700-706.

(54) Brumaghim, J. L.; Michels, M.; Raynond, K. N. *Eur. J. Org. Chem.* **2004**, *22*, 4552-4559.

CHAPTER THREE

INVESTIGATING THE ANTIOXIDANT PROPERTIES OF OXO-SULFUR COMPOUNDS ON METAL-MEDIATED DNA DAMAGE

Introduction

Reactive oxygen species (ROS) are generated from numerous processes including enzymatic activity, radiation, and metal ion reduction of oxygen compounds.[1,2] ROS such as hydroxyl radical ($^{\bullet}OH$) oxidize biological components including lipids, proteins, and nucleic acids, leading to lipid peroxidation, enzyme deactivation, and oxidative DNA damage.[3,4] Formation of $^{\bullet}OH$ *in vivo* is caused by the reaction of Fe^{2+} or Cu^{+} with H_2O_2 in Fenton or Fenton-like reactions:[5,6] Fe^{2+} or $Cu^{+} + H_2O_2 \rightarrow Fe^{3+}$ or $Cu^{2+} + {}^{\bullet}OH + OH^{-}$.

Metal-generated $^{\bullet}OH$ is the primary cause of DNA damage and cell death under oxidative stress in mammals, including humans.[7,8] Oxidative DNA damage occurs at either the backbone or bases, with base damage primarily occurring at guanine-rich sites.[9] Oxidative stress due to DNA damage has been linked to several pathological conditions including aging,[10] cancer,[2] and cardiovascular[11] and neurodegenerative diseases.[12]

Iron and copper are the most prevalent transition metals in biological systems and are required for the activity of many enzymes and proteins.[13] Although both metals are typically found in proteins, non-protein-bound (labile) pools of Fe^{2+} and Cu^{+} contribute to cellular oxidative stress.[2] It has been reported that the concentration of labile iron in *E. coli* is ~10-20 μM.[14,15] In yeast, the concentration of labile copper was calculated to be less than 10^{-18} M,[16,17] but recent studies indicate a significant labile copper pool in mouse

mitochondria.[18] Studies have also shown that copper levels vary according to location, with copper concentrations in blood serum ranging from 10-25 μM, 0.5-2.5 μM in cerebrospinal fluid, and 30 μM in the synaptic cleft.[19,20] Copper concentrations are significantly higher in the brain with concentrations ranging from 1.3 mM to 0.4 mM.[19,20]

Even if normal levels are not sufficient to cause significant oxidative damage, mildly-elevated iron levels are linked to increased cancer incidence in humans,[21] and increases in cellular iron and copper concentrations are associated with oxidative stress in neurodegenerative diseases, as well as increased risk of cardiovascular disease.[22-28]

Antioxidants from fruits and vegetables have been widely studied for their ability to reduce or prevent the effects of oxidative DNA damage.[2,29-31] Garlic has been shown to have many health benefits, including antioxidant and antibacterial activities, cholesterol lowering activity, and tumor growth inhibition.[32] The medicinal properties of garlic are mainly due to allicin, the organosulfur compound responsible for its pungent odor (Figure 3.1). Allicin is generated when alliin, produced from the crushing of garlic, reacts with the enzyme alliinase.[33] Rabinkov *et al.* used spin trapping techniques to determine that allicin scavenged $^{\bullet}$OH produced by the Fenton reaction.[32] However, in spectrophotometric investigations also using iron-generated $^{\bullet}$OH, allicin was an inefficient $^{\bullet}$OH scavenger.[4] Disparities concerning the antioxidant activity of allicin may be due to the use of crude garlic extracts in these experiments, since the observed antioxidant activity may be attributed to other endogenous components.[34,35]

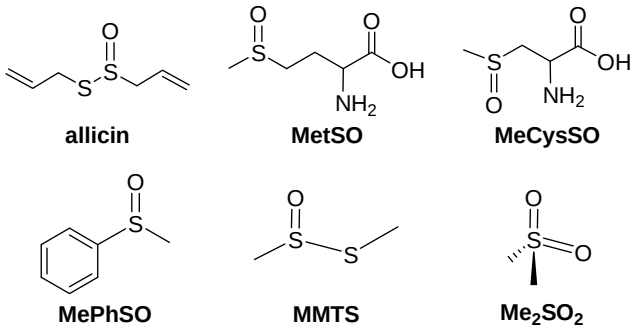

Figure 3.1. Structures of oxo-sulfur compounds discussed in this chapter: allicin, methionine sulfoxide (MetSO), methylcysteine sulfoxide (MeCysSO), methyl phenyl sulfoxide (MePhSO), methyl methanethiosulfonate, (MMTS), and dimethyl sulfone (Me_2SO_2).

Oxidation of biological sulfur compounds is an active area of research for reasons extending beyond their role as antioxidants. ROS oxidation of methionine (Met) produces methionine sulfoxide (MetSO, Figure 3.1), and oxidation of this residue may alter protein structure and function.[36-40] Further oxidation of methionine sulfoxide by ROS has been reported to produce sulfones or radicals that induce oxidative DNA damage.[41] To reverse this oxidation, methionine sulfoxide reductases reduce MetSO back to Met.[42-45] In contrast, recent studies indicate that oxidized methionine residues in proteins do not contribute to loss of protein function and, in fact, show antioxidant behavior.[46,47] Only a few studies have investigated the antioxidant activity of methylcysteine sulfoxide (MeCysSO), but Nishimura *et al.* found that MeCysSO prevents formation of lipid hydroperoxides in human low-density lipoprotein (LDL).[48]

Organosulfur compounds such as methionine and methylcysteine (MeCys) effectively prevent Cu^{+}-mediated oxidative DNA damage from $^{\bullet}OH$, but are not effective at preventing Fe^{2+}-mediated DNA damage.[49] In addition, gel electrophoresis experiments

performed on inorganic selenium compounds indicate that oxidation state of the selenium atom may play a role in preventing metal-mediated DNA damage,[50] and that metal coordination is a possible mechanism by which sulfur and selenium compounds exert their antioxidant activities.[49-51] Despite their proven antioxidant properties, little work has been done to similarly examine analogous oxidized sulfur compounds for antioxidant activity. This work has been previously published in *Main Group Chem.* **2007**, *6*, 143-153.[52]

Results and Discussion

Inhibition of Cu^+-mediated DNA damage by oxo-sulfur compounds

Using DNA gel electrophoresis, we have examined five oxo-sulfur compounds for their ability to inhibit copper- and iron-mediated DNA damage: MetSO, MeCysSO, methyl phenyl sulfoxide (MePhSO), methyl methanethiosulfonate (MMTS), and dimethyl sulfone (Me_2SO_2; Figure 3.1). For these experiments, Cu^+ or Fe^{2+} and H_2O_2 are combined to generate $^{\bullet}OH$ in the presence of plasmid DNA. Hydroxyl radical oxidatively cleaves one strand of the DNA backbone, resulting in unwinding of the supercoiled plasmid into the circular, nicked form. The damaged and undamaged forms of DNA are then separated by gel electrophoresis and the resulting bands are quantified to determine the percentage of damaged and undamaged DNA. By addition of increasing concentrations of oxo-sulfur compound to these reactions, DNA damage inhibition by the compound can be quantified.

The gel image in Figure 3.2A shows the effect of methylcysteine sulfoxide (MeCysSO) on DNA damage produced by freshly-prepared Cu^{+} and H_2O_2 at pH 7. Hydrogen peroxide alone (lane 3) and MeCysSO with H_2O_2 (lane 4) do not generate DNA damage as compared to the plasmid DNA control (lane 2). In contrast, addition of both H_2O_2 and Cu^{+} produced 74% damaged (nicked) DNA (lane 5), and upon adding increasing concentrations of MeCysSO (0.1-1500 μM, lanes 6-15), this DNA damage significantly decreases. Quantification of the band intensities indicates that MeCysSO inhibits 100% of copper-mediated DNA damage at 1500 μM (Table 3.2). The results of

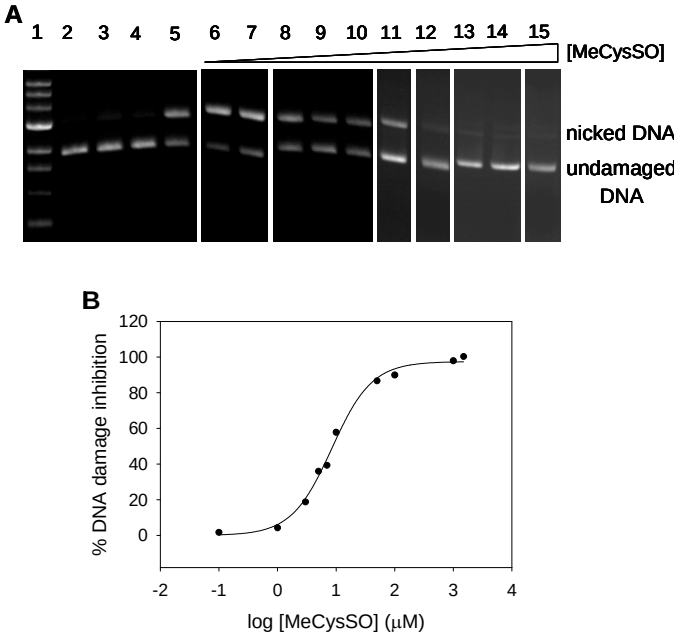

Figure 3.2. A) Agarose gel showing the effect of MeCysSO on Cu+-mediated DNA damage. Lanes: 1) 1 kb DNA ladder; 2) plasmid DNA (p); 3) p + H_2O_2; 4) p + H_2O_2 + MetSO; 5) p + H_2O_2 + Cu^{2+}/ascorbate; 6-15) same as lane 5 with increasing [MeCysSO]: 0.1, 1, 3, 5, 7, 10, 50, 100, 1000, 1500 μM, respectively. B) Plot of DNA damage inhibition vs. log concentration of MeCysSO. The line indicates the best-fit sigmoidal dose-response curve, and error bars show the standard deviation of three duplicate trials (error bars are smaller than symbols).

these gel studies were plotted and fit to a sigmoidal dose-response curve to determine the concentration required to inhibit 50% of copper-mediated DNA damage (IC_{50}; Figure 3.2B). For MeCysSO, this IC_{50} concentration is 8.1 ± 1 μM (Hillslope = 1.27).

MetSO, MePhSO, MMTS, and Me_2SO_2 were also tested for prevention of copper-mediated DNA damage using the same method, and the results are given in Table 3.1. MetSO inhibits 100% of DNA damage at 2000 μM ($p < 0.001$; Figure 3.3A), but its IC_{50} value of 18 ± 3 μM (Hillslope = 1.12, Figure 3.4) is significantly higher than that of MeCysSO. MePhSO and Me_2SO_2 have no effect on oxidative DNA damage, even at 5000 μM, whereas MMTS is a pro-oxidant at the highest concentration tested (5000 μM), further damaging DNA by 35% ($p = 0.005$) under these conditions (Figure 3.3). From these results, it is clear that the nature of the oxo-sulfur compound significantly contributes to the observed antioxidant (or pro-oxidant) activity observed for copper-mediated DNA damage.

Comparing the antioxidant ability of MeCysSO and MetSO to similar experiments with copper-mediated DNA damage inhibition of the non-oxidized amino acids Met and MeCys, it is clear that all four of these compounds are strong antioxidants, with IC_{50} values in the low micromolar range (Table 3.1). While the IC_{50} values for MeCys and MeCysSO are similar (8.9 and 8.1 μM, respectively), the IC_{50} value for Met is significantly lower than that of MetSO (11.2 and 18 μM, respectively; $p = 0.01$ for both compounds), indicating that the reduced form of this amino acid is a more potent antioxidant under these conditions.

Table 3.1. IC_{50} values and λ_{max} for oxo-sulfur compounds with Cu^{+} and H_2O_2 and maximal DNA damage inhibition for Fe^{2+} and H_2O_2.

Compound	IC_{50} (μM) with Cu^{+} [a]	λ_{max} (nm) [b]	Maximum DNA damage inhibition (%) with Fe^{2+}	Reference
MeCysSO	8.1 ± 1.0	237	17 ± 3 at 1000 μM	this work
MetSO	18 ± 3.0	236	-	this work
MMTS	35 ± 4 % DNA damage at 1000 μM	-	20 ± 4 at 1000 μM	this work
MePhSO	-	-	-	this work
Me_2SO_2	-	-	-	this work
Met	11.2 ± 0.02	235	-	47, 56
MeCys	8.9 ± 0.02	239	13 ± 4 % DNA damage at 1000 μM	47, 56

[a] IC_{50} is defined as the concentration at which the compound inhibits 50% of DNA damage.

[b] λ_{max} was determined from the difference in absorbance between the Cu^{+}/oxosulfur compound spectrum and the separate Cu^{+} and oxo-sulfur spectra.

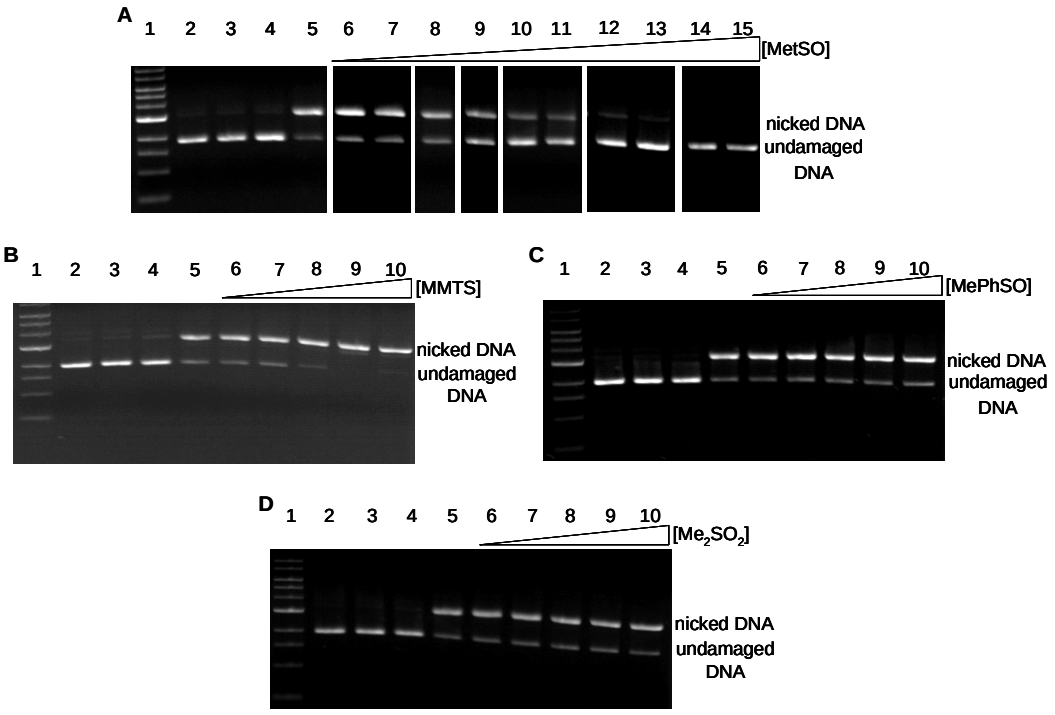

Figure 3.3. Gel images showing the ability of oxo-sulfur compounds to inhibit Cu^{+}-mediated DNA damage using 6 μM Cu^{2+}, 7.5 μM ascorbate and 50 μM H_2O_2 in 10 mM MOPS buffer (pH 7). Tabulated data (Tables 3.3-3.3.6) give the concentrations for each oxo-sulfur compound. A) methionine sulfoxide (MetSO); B) methyl methanethiosulfonate (MMTS); C) methyl phenyl sulfoxide; and D) dimethyl sulfone (Me_2SO_2).

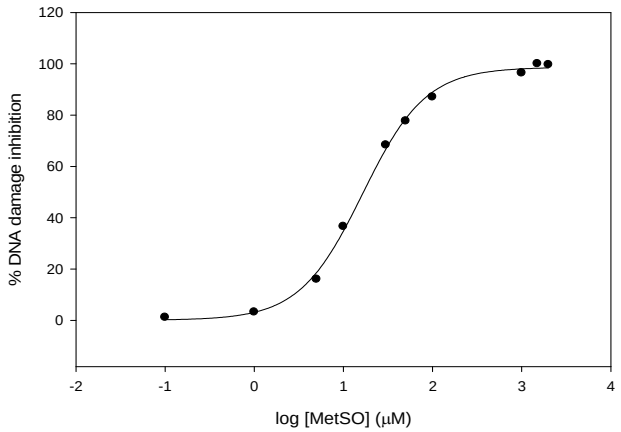

Figure 3.4. Best-fit sigmoidal dose-response curve of percent DNA damage inhibition with Cu^{+}/H_2O_2 versus log concentration of methionine sulfoxide (μM) to determine the concentration required to inhibit 50% of DNA damage (IC_{50}). Error bars show the standard deviation of three duplicate trials (error bars are smaller than symbol).

Inhibition of Fe^{2+}-mediated DNA damage by oxo-sulfur compounds

For gel electrophoresis experiments with iron-generated $^{\bullet}OH$, freshly-prepared $FeSO_4$ solutions are used as the Fe^{2+} source, and the reactions are carried out at pH 6 due to the insolubility of iron at higher pH. Figure 3.5 shows the gel results when increasing concentrations of MeCysSO are added to Fe^{2+} and H_2O_2 in the presence of DNA.

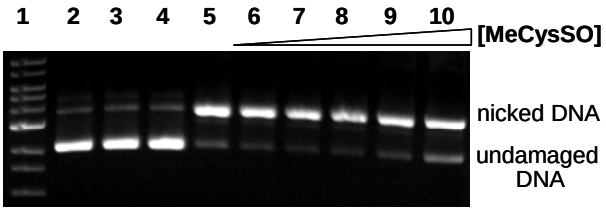

Figure 3.5. Agarose gel showing the effect of MeCysSO on Fe^{2+}-mediated DNA damage. Lanes: 1) 1 kb DNA ladder; 2) plasmid DNA (p); 3) p + H_2O_2; 4) p + H_2O_2 + MeCysSO; 5) p + H_2O_2 + Fe^{2+}, 6-10) same as lane 5 with increasing [MeCysSO]: 0.1, 1, 10, 100, 1000 μM, respectively.

Although some DNA damage inhibition is observed at the highest concentration tested (17 ± 3 % at 1000 μM; p = 0.01), the antioxidant activity in the iron system is much less than that seen for copper-mediated DNA damage.

MMTS also shows a small amount of antioxidant activity (20 ± 4 % at 1000 μM; p = 0.01), comparable to the antioxidant activity of MeCysSO. MetSO, MePhSO and Me_2SO_2 had no effect on iron-mediated DNA damage (Table 3.1; Figure 3.6). Interestingly, no activity is observed for MetSO, in contrast to its significant antioxidant behavior in the copper system, and MMTS promotes copper-mediated DNA damage but decreases iron-mediated damage. Once again, it is clear that not all oxidized sulfur compounds have similar activities with iron-mediated DNA damage.

Under iron-mediated DNA damage conditions, Met shows no significant DNA damage inhibition with iron, similar to its oxidized analog MetSO, whereas MeCys promoted DNA damage by 13% in contrast to the 17% DNA damage inhibition observed for MeCysSO.[49] In this case, oxidation of the amino acid changes the behavior of the compound from pro-oxidant to antioxidant. Xiao and Parkin determined that compounds with the thiosulfonate group (R-S(O)S-R) including MMTS and allicin, effectively scavenge iron-generated $^{\bullet}OH$.[34] MMTS prevents iron-mediated DNA damage by $^{\bullet}OH$, but notably *promotes* copper-mediated DNA damage. The differences between the results for iron- and copper-mediated damage indicate that the nature of the metal ion plays a crucial role in antioxidant or pro-oxidant activity of these compounds.

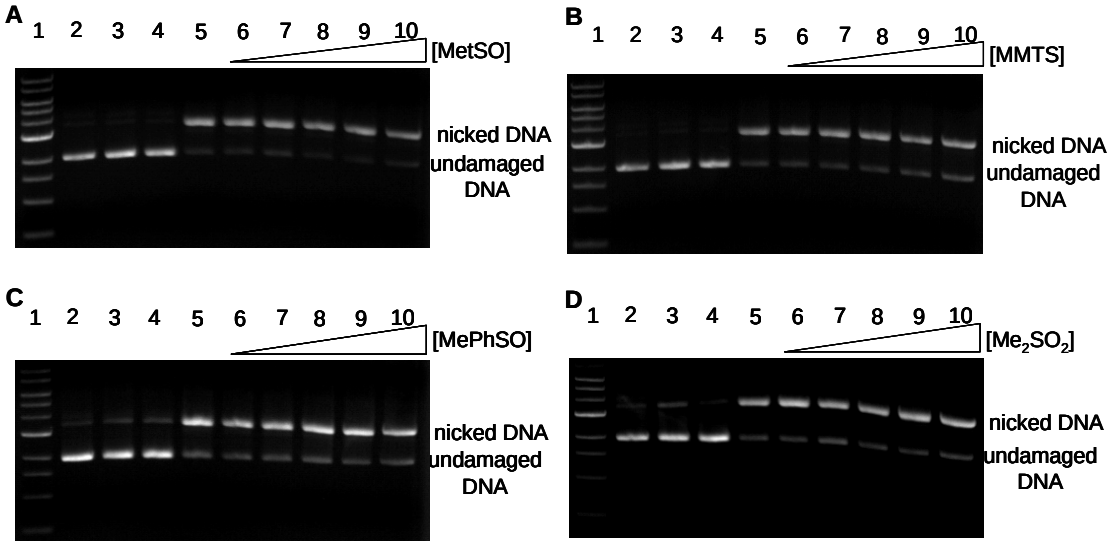

Figure 3.6. Gel images showing the ability of oxo-sulfur compounds to inhibit Fe^{2+}-mediated DNA damage using 2 μM $Fe^{2+}$and 50 μM H_2O_2 in 10 mM MES buffer (pH 6). Tabulated data (Tables 3.11-3.14) give the concentrations for each oxo-sulfur compound. A) methionine sulfoxide (MetSO); B) methyl methanethiosulfonate (MMTS); and C) methyl phenyl sulfoxide; and D) dimethyl sulfone (Me_2SO_2).

Antioxidant activity and metal coordination

Battin *et al.* report that Cu-S charge-transfer bands around 240 nm in the UV-vis spectrum are observed for all the antioxidant sulfur-containing compounds tested, and that this charge transfer band is absent for the sulfur compounds lacking antioxidant activity (Table 3.1).[49] Similarly, addition of MetSO (Figure 3.7) and MeCysSO (Figure 3.11) to Cu^{2+}/ascorbate solution also results in Cu-S charge transfer bands around 240 nm that were not present for the other oxo-sulfur compounds. These UV-vis results indicate that these two oxo-sulfur compounds coordinate the copper, and it is likely that this interaction plays a role in their observed antioxidant activity.

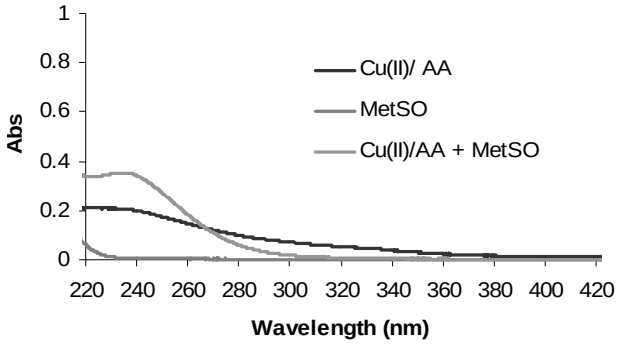

Figure 3.7. UV-vis spectra of MetSO (116 μM), Cu^{2+}/ascorbic acid (AA; 58 μM and 72.5 μM, respectively), and Cu^{2+}/ascorbic acid + MetSO in water at pH 7.

To test this copper-coordination hypothesis of antioxidant activity, plasmid DNA electrophoresis experiments were conducted by substituting $[Cu(bipy)_2]^+$ for Cu^+ as the copper source. Since 2,2'-bipyridine (bipy) ligands completely coordinate Cu^+, no free site for binding of an oxo-sulfur compound is available. $[Cu(bipy)_2]^+$ reduces H_2O_2 to yield DNA-damaging $^{\bullet}OH$ (Figure 3.8, lane 5), but if copper coordination is required for

the antioxidant properties of oxo-sulfur compounds, no inhibition of DNA damage should be observed.

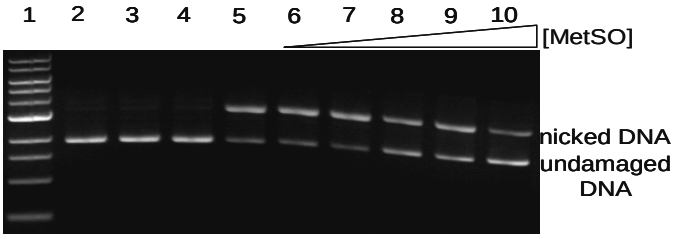

Figure 3.8. Agarose gel showing the effect of MetSO with $[Cu(bipy)_2]^+$. Lanes: 1) 1 kb DNA ladder; 2) plasmid DNA (p); 3) p + H_2O_2; 4) p + H_2O_2 + MetSO; 5) p + H_2O_2 + $[Cu(bipy)_2]^{2+}$/ascorbate; 6-10) same as lane 5 with increasing [MetSO]: 0.1, 1, 10, 100, 1000 μM, respectively.

As can be seen in lanes 6-10 of the gel in Figure 3.8, increasing MetSO concentration from 0.1 to 1000 μM results in some antioxidant activity, but at 1000 μM, DNA damage was inhibited by 43 ± 3 % ($p = 0.002$) compared to 100% with Cu^+ alone (Figure 3.8). MeCysSO also exerted antioxidant activity in the presence of $[Cu(bipy)_2]^+$ and H_2O_2, inhibiting 88 ± 4 % damage DNA at 1000 μM ($p < 0.001$) compared to 100% with Cu^+ alone (Figure 3.9A). Since coordination of the copper by the bipyridine ligands significantly reduces antioxidant activity for both these compounds, copper coordination is likely one factor in their antioxidant activity. However, since some antioxidant activity is still observed under these conditions, a second mechanism, such as $^{\bullet}OH$ scavenging, is likely responsible for the observed antioxidant effects. This is in direct contrast to similar experiments with Met and MeCys that show a complete inhibition of antioxidant behavior when $[Cu(bipy)_2]^+$ is used as the copper source in similar experiments.[49]

MMTS was again a pro-oxidant under these conditions with $[Cu(bipy)_2]^+$, increasing DNA damage by 44 ± 7 % at 1000 μM ($p = 0.007$; Figure 3.9B), a slightly-higher percentage than observed with uncoordinated Cu^+ (35 ± 4 % at 1000 μM). Thus, copper coordination is not required for the observed pro-oxidant activity of MMTS.

UV-vis studies on the five oxo-sulfur compounds resulted in no new absorption band upon addition of Fe^{2+}, suggesting that no Fe-S coordination occurs, consistent with the generally weak activity seen for the oxo-sulfur compounds with iron compared to copper. Experiments were also conducted to determine whether iron coordination is required for the antioxidant activity of oxo-sulfur compounds by using $[Fe(EDTA)]^{2-}$ instead of Fe^{2+} to generate DNA-damaging $^{\bullet}OH$ (Figure 3.10). As with $[Cu(bipy)_2]^+$, EDTA coordinates to Fe^{2+}, leaving no space for the coordination of an oxo-sulfur compound. Surprisingly, the slight antioxidant activity of both MeCysSO and MMTS observed with Fe^{2+} is completely unobserved in the $[Fe(EDTA)]^{2-}/H_2O_2$ system,

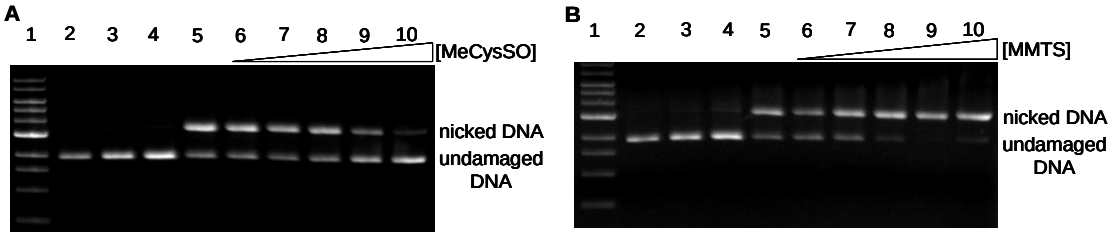

Figure 3.9. Gel images showing the ability of oxo-sulfur compounds to inhibit $[Cu(bipy)_2]^+$-mediated DNA damage using 50 μM $[Cu(bipy)_2]^+$, 62.5 μM ascorbate and 50 μM H_2O_2 in 10 mM MOPS buffer (pH 7). Tabulated data (Tables 3.8-3.9) give the concentrations for each oxo-sulfur compound. A) methylcysteine sulfoxide (MeCysSO) and B) methyl methanethiosulfonate (MMTS).

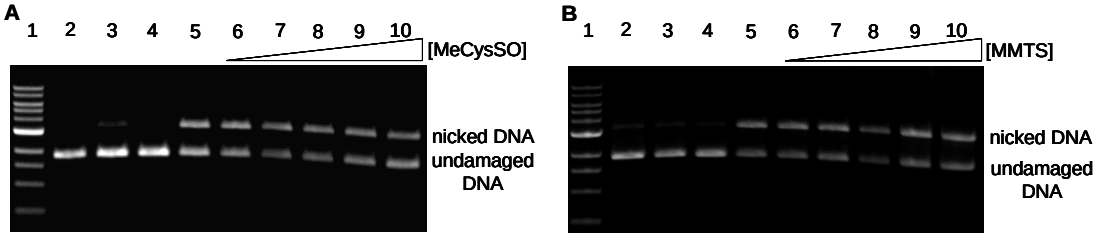

Figure 3.10. Gel images showing the ability of oxo-sulfur compounds to inhibit $[Fe(EDTA)]^{2-}$-mediated DNA damage using 400 μM $[Fe(EDTA)]^{2-}$ and 50 μM H_2O_2 in 10 mM MES buffer (pH 6). Tabulated data (Tables 3.15-3.16) give the concentrations for each oxo-sulfur compound A) methyl-cysteine sulfoxide (MeCysSO) and B) methyl methanethiosulfonate (MMTS).

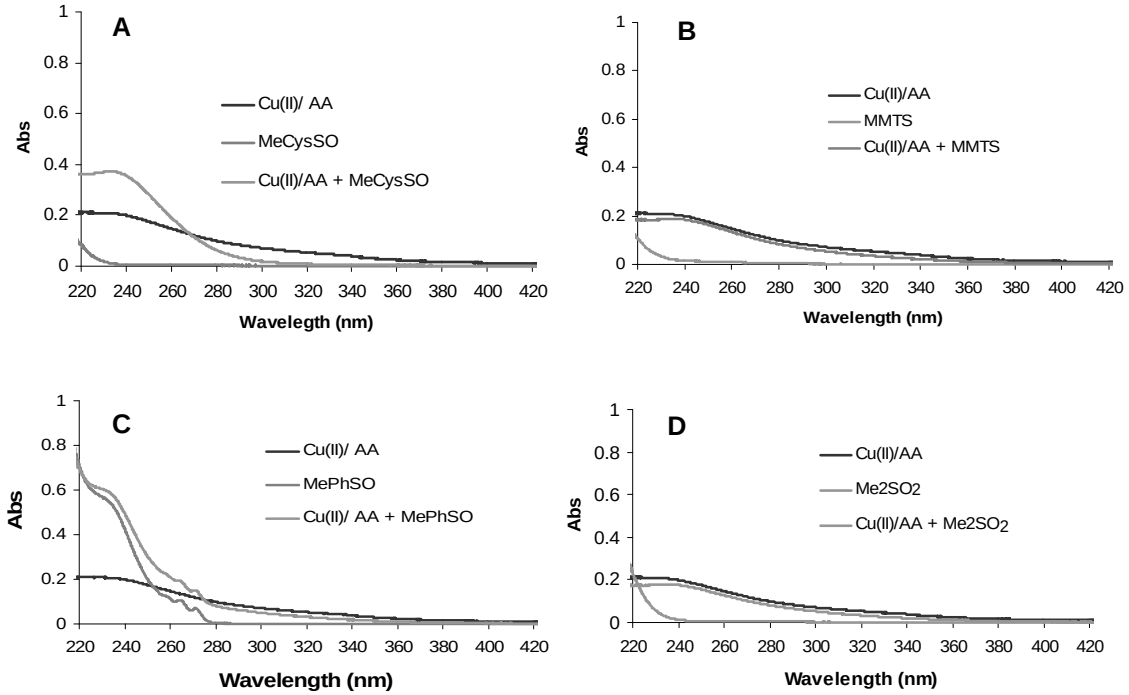

Figure 3.11. UV-vis spectra of oxo-sulfur compounds (116 μM), Cu^{2+} (58 μM)/ascorbate (72.5 μM), and oxo-sulfur compound + Cu^{2+}/ascorbate with MOPS buffer (pH 7, 10 mM): A) methylcysteine sulfoxide (MeCysSO) B) methyl methanethiosulfonate (MMTS); and C) methyl phenyl sulfoxide; and D) dimethyl sulfone (Me_2SO_2).

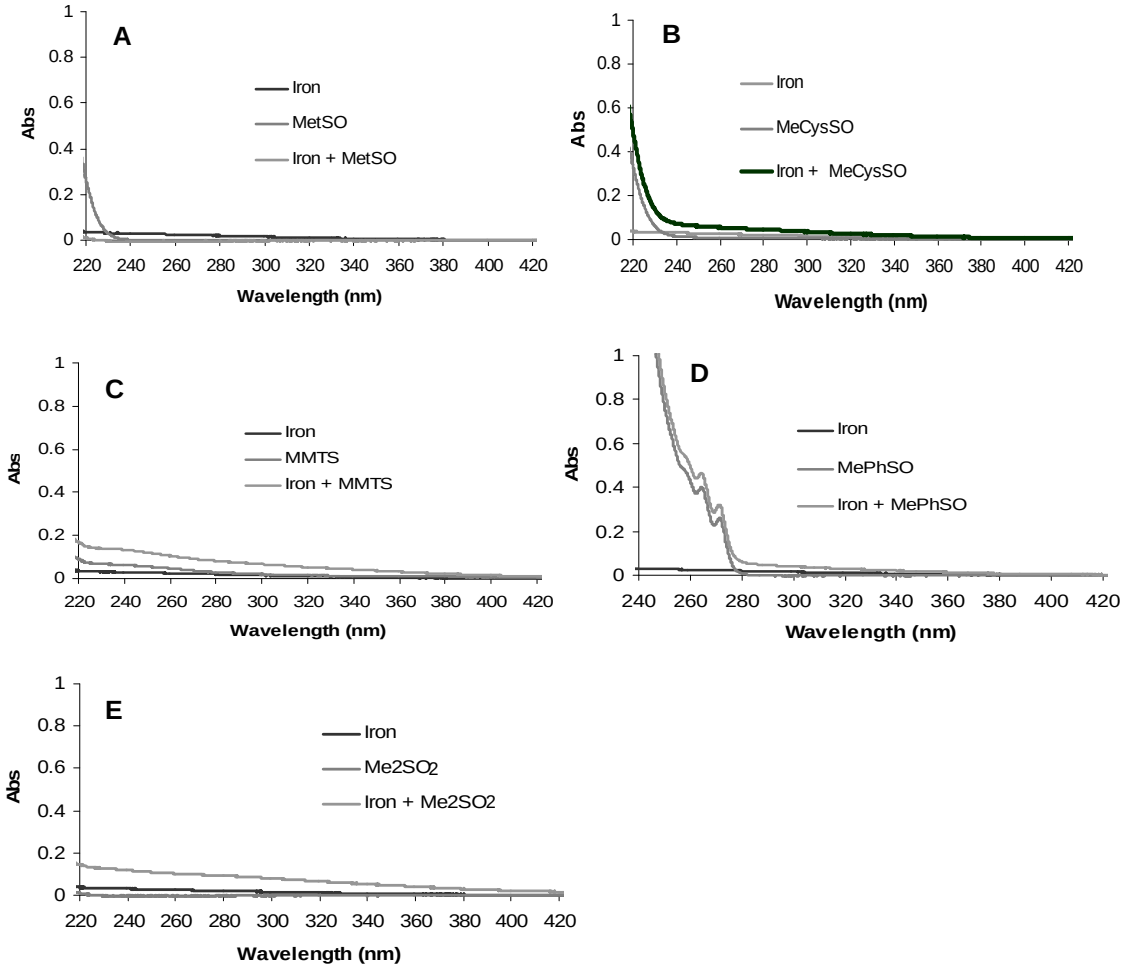

Figure 3.12. UV-vis spectra of oxo-sulfur compounds (300 μM), Fe^{2+} (150 μM), and oxo-sulfur compound + Fe^{2+} maintained at pH 6 with MES buffer (10 mM): **A:** methionine sulfoxide (MetSO); **B:** methyl-cysteine sulfoxide (MeCysSO) **C:** methyl methanethiosulfonate (MMTS); and **D:** methyl phenyl sulfoxide; and **E:** dimethyl sulfone (Me_2SO_2).

indicating that a weak interaction between these compounds and iron may be responsible for their observed antioxidant effects.

Oxidation state and antioxidant activity

Previous work with inorganic selenium compounds suggests that oxidation state of the selenium atom may play a role in their antioxidant activity. Sodium selenite and selenium dioxide both have selenium oxidation states of +4, and both are effective at inhibiting Fe^{2+}-mediated DNA damage. In contrast, compounds with selenium oxidation states of +6 (sodium selenate) and –2 (sodium selenide) exhibited no antioxidant activity under the same conditions. The five oxo-sulfur compounds tested also differ in oxidation state of the sulfur atom: MetSO, MeCysSO, and MePhSO have an oxidation state of 0, the oxidized sulfur of MMTS has an oxidation state of +1, whereas that of the sulfide is –1, and in Me_2SO_2 the sulfur oxidation state is +2. Comparing the results in Table 3.1, no definitive trend can be identified due to the limited number of compounds tested, but the ability of oxo-sulfur compounds to inhibit copper-mediated DNA damage may decrease as the oxidation state of the thiolate sulfur atom increases. Further systematic testing of the antioxidant properties of oxo-sulfur compounds is needed to firmly establish this result.

Mass spectrometry evidence for metal binding to sulfur and selenium antioxidants

Recently, sulfur and selenium containing compounds were tested for their ability to prevent copper-mediated oxidative damage (Figure 3.12).[49,53] Eight of the sulfur compounds tested, including cystine (Cys_2), cysteine (Cys), and methionine sulfoxide (MetSO) were potent antioxidants, with IC_{50} values ranging from 3.3-18 μM.[49,52]

Interestingly, only three of the ten selenium compounds tested prevented copper-mediated DNA damage, with IC_{50} values between 3.3 and 25 μM.[53]

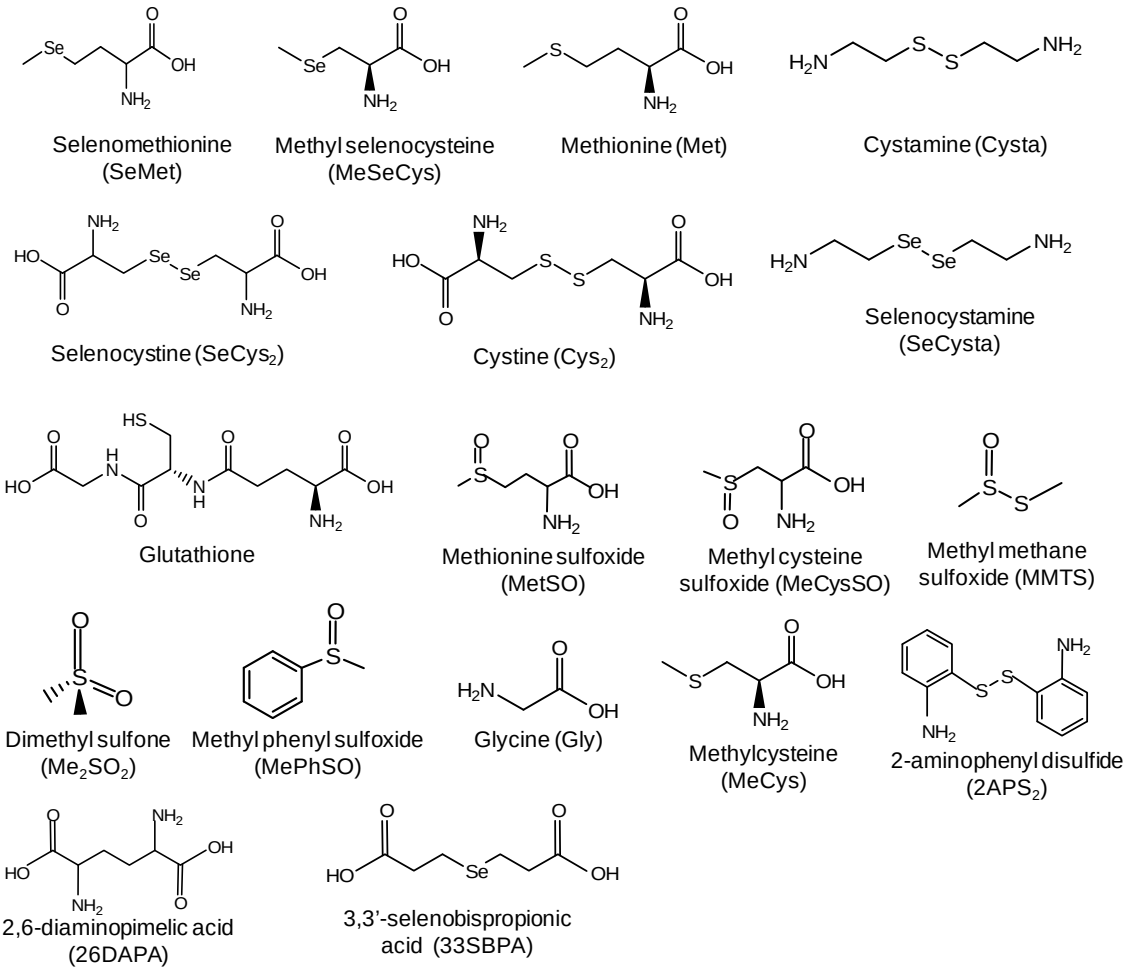

Figure 3.13. Structures of selenium and sulfur compounds studied for metal binding using mass spectroscopy.

Additional gel electrophoresis experiments established that copper binding to most selenium and sulfur compounds is the primary mechanism for their antioxidant activity.[49,53] Experiments with MetSO and methyl cysteine sulfoxide (MeCysSO) indicate

that copper coordination is only partly responsible for their antioxidant activity since both compounds also prevented DNA damage by $[Cu(bipy)_2]^+/H_2O_2$.[52]

As previously described, UV-vis spectroscopy was also used to examine copper binding to selenium and sulfur compounds. Adding antioxidant sulfur compounds (Figure 3.13) to Cu^+ results in a new absorption band at 240 nm, indicative of Cu-S charge transfer.[49,51,52] Similarly, adding selenium antioxidants (Figure 3.13) to Cu^+, results in new absorption bands between 226 and 240 nm, indicative of Cu-Se coordination.[53] These charge transfer bands were unobserved for compounds that had no antioxidant activity in the presence of Cu^+ and H_2O_2.[49,52,53]

Electrospray ionization mass spectroscopy (ESI-MS) is a widely used technique for analysis of metal coordination complexes and covalent organometallic compounds.[54,55] To confirm metal coordination as the mechanism for antioxidant activity of selenium and sulfur compounds, ESI-MS was utilized. This technique was also used to examine stoichiometric ratios of copper binding to the antioxidant compounds. In these experiments, Cu^{2+} was reduced to Cu^+ by ascorbic acid *in situ*, and the combined with either selenium or sulfur compounds in Cu^+:antioxidant compound ratios of 1:1, 1:2, or 1:3. Analysis of the mass spectra obtained indicates that copper generally coordinates to the selenium or sulfur compounds with 1:1 stoichiometry (Table 3.2). Furthermore, nearly all of the compounds that showed antioxidant activity also showed copper coordination, confirming the metal-coordination results obtained in gel electrophoresis and UV-vis experiments.

Selenomethionine (SeMet) was found to be an effective antioxidant with an IC_{50} of 25.1 ± 0.01 μM.[49,56] Mass spectra obtained using different ratios of Cu^+:SeMet showed a signal at m/z 259.8 Da, suggesting that copper binds to SeMet only in a 1:1 stiochiometric ratio. Similarly, methyl selenocysteine (MeSeCys), a more potent antioxidant (IC_{50} = 10.0 ± 0.02 μM)[49,56] than SeMet, has a peak envelope at m/z 245.8

Table 3.2. IC_{50} and ESI-MS values of selenium and sulfur compounds discussed in this chapter.

Compound	IC_{50} (μM)[a] with Cu^+	Cu^+ : Se or S compound	m/z (Da)	Reference[b]
SeMet	25.1 ± 0.01	1:1	259.8	53
MeSeCys	10.0 ± 0.02	1:1	245.8	53
$SeCys_2$	3.34 ± 0.08	-	-	53
SeCysta	-	-	-	53
33SBPA	-	-	-	53
MeCys	8.90 ± 0.02	1:1	197.9	49, 56
Met	11.20 ± 0.02	1:1	211.9	49, 56
Cys_2	3.34 ± 0.07	-	-	49, 56
Cysta	-	-	-	49, 56
GSH	12.98 ± 0.01	1:1	369.0	49, 56
GSSG	6.82 ± 0.03	1:1	674.0	49, 56
$2APS_2$	-	-	-	49, 56
MetSO	18 ± 3.0	1:1	228.0	52, 56
MeCysSO	8.1 ± 1.0	1:1, 1:2	213.9, 363.9	52, 56
MMTS	35 ± 4% DNA damage at 5000 μM	1:1, 1:2	189.9, 314.9	52, 56
MePhSO	-	1:1, 1:2	202.9, 342.9	52, 56
Me_2SO_2	-	-	-	52, 56
26DAPA	5.84 ± 0.05	1:1	253.0	53
Gly	22.04 ± 0.01	1:1	138.0	53

[a] IC_{50} is defined as the compound concentration that inhibits 50% copper-mediated DNA damage.
[b] References are for the IC_{50} values.

Da, also indicating 1:1 binding. Similar results were observed for the sulfur analogs, methionine (Met) and methyl cysteine (MeCys), with m/z values of 211.9 Da and 197.9 Da, respectively (Table 3.2).

Interestingly, cystine and selenocystine are potent antioxidants, with similar IC_{50} values of 3.34 ± 0.07 μM and 3.34 ± 0.08 μM, respectively; however no clear copper coordination signals are observed at any Cu^{+}:antioxidant compound ratio tested (Table 3.2). These two compounds are the only two that have IC_{50} values but do not exhibit copper coordination by mass spectrometry. It is possible that the Cu-disulfide or Cu-diselenide interactions are somewhat weak and do not survive conditions of the mass spectrometry However, oxidized glutathione, another disulfide with potent antioxidant activity, does show copper coordination. The absence of observed copper coordination for cystine and selenocystine also contradict results obtained from UV-vis experiments, showing Cu-S and Cu-S charge transfer bands due to copper binding.[49]

A previous study observed copper binding to cystine and glutathione in a 2:1 molar ratio (m/z 603 Da) and a 1:1 (m/z 672 Da), respectively, using ESI-MS.[57] The stability of these copper complexes was found to change over time, and complexation of copper with oxidized glutathione is more stable than with cystine.[57] This stability factor may also contribute to the lack of observed copper coordination with cystine and selenocystine.

Interestingly, complexation between copper and oxo-sulfur compounds extends to both antioxidant and pro-oxidant activities. MeCysSO, an effective antioxidant against copper-mediated DNA damage (IC_{50} = 8.1 ± 1.0 μM)[52,56] showed stoichiometries of 1:1

(m/z 213.9 Da) and 1:2 (m/z 363.9) upon addition of two equivalents of MeCysSO to one equivalent of copper. The less potent antioxidant, MetSO (IC_{50} = 18 ± 3.0 μM)[52,56] showed only 1:1 copper binding regardless of the Cu^+:MetSO molar ratio used. Surprisingly, although MePhSO and MMTS do not prevent copper-mediated DNA damage, both coordinate to copper. MePhSO binds to copper in both a 1:1 (m/z 202.9 Da) and 1:2 (m/z 342.9 Da) Cu^+ to MePhSO ratio. MMTS is a pro-oxidant at high concentrations, and binds copper in both 1:1 and 1:2 ratios, with m/z 189.9 Da and 314.9 Da, respectively (Table 3.2). However, UV-vis experiments with MMTS and Cu^+ resulted in no observed Cu-S charge transfer band.[52] These experiments indicate that copper binding is necessary but not sufficient for the antioxidant activity of sulfur compounds, and additional studies are required to fully determine the factors involved in sulfur and selenium antioxidant activity in addition to copper binding.

The disparities in the mass spectroscopy, UV-vis, and gel electrophoresis for sulfur compounds suggest that the copper-binding mechanism for the antioxidant and pro-oxidant activity of these compounds is complex. Results may be dependent on differences in Cu^+:sulfur compound ratio, concentration, or copper complex stability in aqueous solutions. In addition, the structural characteristics of these sulfur and selenium compounds likely play a significant role in both copper coordination and the resulting antioxidant activity of these compounds.

Conclusions

The DNA damage inhibition abilities of several oxo-sulfur compounds were examined for both copper- and iron-mediated $^{\bullet}OH$ damage. Both MetSO and MeCysSO were found to be effective at preventing copper-mediated DNA damage, with IC_{50} values in the low micromolar range. Overall, the results ranged from potent antioxidant activity to pro-oxidant activity, indicating that the nature of the oxo-sulfur compounds is an important factor for antioxidant activity. All of the oxo-sulfur compounds tested showed less pronounced antioxidant or pro-oxidant activity with iron-mediated DNA damage. UV-vis spectroscopy indicated that Cu-S coordination occurs only for the oxo-sulfur compounds that prevent copper-mediated DNA damage, and electrophoresis experiments confirm that copper coordination is required for a substantial amount of the observed antioxidant activity of these compounds, although a second antioxidant mechanism is also responsible for additional antioxidant activity. Studies are currently being performed to correlate these gel electrophoresis results with the ability of oxidized sulfur compounds to inhibit metal-mediated cell death *in vivo*. Additional studies on how metal coordination promotes the observed antioxidant activity are also underway to provide mechanistic details on the effects of protein oxidation and the antioxidant effects of garlic, onions, and other sulfur-containing foods.

These ESI-MS experiments performed confirm copper binding for the majority of sulfur and selenium antioxidant compounds, with a 1:1 stoichiometry being predominant. Interestingly, copper coordination as observed by ESI-MS seems to be necessary but not sufficient for antioxidant (or pro-oxidant) activity. For example, antioxidant compounds

such as MMTS and MePhSO show copper coordination, but have little or no observed DNA damage prevention abilities. To further understand how copper binding results in antioxidant behavior, experiments showing how copper binds to the sulfur and selenium compounds are essential. These experiments may include extended X-ray absorption fine structure (EXAFS) analysis to determine the coordination environment of copper-selenium or -sulfur complexes, if suitable crystals cannot be grown for X-ray structural analysis. Additionally, synthesis of related copper-selenium or -sulfur complexes may also be useful in further exploring the copper coordination to sulfur and selenium compounds. These experiments, in addition to the studies presented in this chapter, will help in understanding the antioxidant mechanisms of selenium and sulfur compounds.

Materials and Methods

Materials

NaCl (99.999% to avoid trace metal contamination), selenomethionine, reduced and oxidized glutathione, and methyl-selenocysteine were purchased from Acros. Selenocystamine, methyl-cysteine, 2,6-diaminopimelic acid, selenocysteine, methionine sulfoxide, methyl cysteine sulfoxide, methyl phenyl sulfoxide, methyl methane thiosulfonate, and dimethyl sulfone were from Sigma-Aldrich. Glycine and ascorbic acid were purchased from J. T. Baker, and cysteine came from Alfa Aesar. Cystamine, methionine, and 2-aminophenyl disulfide were purchased from TCI America, and cystine came from Lancaster.. H_2O_2 solution (30%), $FeSO_4 \cdot 7H_2O$, and $CuSO_4 \cdot 5H_2O$ were from Fisher. EDTA (disodium salt) and ascorbic acid were from J.T. Baker. MES and MOPS

were from Acros and 2,2'-bipyridine came from Alfa Aesar. Water was purified using the NANOpure DIamond water deionization system (Barnstead International, Dubuque, IA). Iron-free microcentrifuge tubes were prepared by washing the tubes in 1 M HCl prior to use and rinsing thoroughly with ddH_2O. Degassed ddH_2O was used for all mass spectroscopy experiments and was prepared by bubbling nitrogen gas into deionized water for 12 h prior to use.

DNA purification

Plasmid DNA was purified from DH1 *E. coli* cells using a QIAprep Spin Miniprep kit (Qiagen, Chatsworth, CA), eluted using Tris-EDTA (TE) buffer, and then dialyzed against 130 mM NaCl for 24 h at 4 ^{o}C. The resulting DNA concentration was determined using UV-vis measurements at A_{260} (1 A_{260} = 50 ng/μL) with a Shimadzu UV-3101 PC spectrophotometer. Purity of plasmid DNA was determined via gel electrophoresis of a digested sample, all DNA samples had absorbance ratios of $A_{250/260} < 0.95$ and $A_{260/280} > 1.8$.

DNA nicking experiments with Fe^{2+} and H_2O_2

The indicated concentrations of MetSO, MeCysSO, MePhSO, MMTS or Me_2SO_2, 0.1 pmol plasmid DNA, 130 mM NaCl, 10 mM ethanol, freshly-prepared 2 μM $FeSO_4 \cdot 7H_2O$ maintained at pH 6 with MES buffer were combined and allowed to stand for 5 min at room temperature. H_2O_2 (50 μM) was then added and incubated for 30 min to produced sufficient nicked (damaged) DNA with the iron concentration used in these

experiments. EDTA (50 μM) was added after this time and a total volume of 10 μL was maintained with ddH_2O. DNA was separated on 1% agarose gels via electrophoresis, stained with ethidium bromide for 30 min, and imaged on an UVIproDBT-8000 gel imager (UVITec, Cambridge, UK). Quantification of closed-circular and nicked DNA was performed using the UviPro software and results were shown in a bar graph. Ethidium stains Circular DNA less efficiently than nicked DNA, so Circular DNA band intensities were multiplied by 1.24 prior to comparison.[58] For gels run with $Fe(EDTA)^{2-}$ (400 μM) as the iron source, a similar procedure was used substituting $Fe(EDTA)^{2-}$ (400 μM) for $FeSO_4•7H_2O$.

DNA nicking experiments with Cu^+ and H_2O_2

Similar procedures to the Fe^{2+}/H_2O_2 experiments were followed using $CuSO_4•5H_2O$ (6 μM) and ascorbic acid (7.5 μM) instead of iron to produce sufficient DNA damage upon addition of H_2O_2. The pH was maintained at pH 7 with MOPS buffer. For gels run with $[Cu(bipy)_2]^+$ as the copper source, a similar procedure was followed substituting $[Cu(bipy)_2]^+$ (50 μM) for $CuSO_4•5H_2O$ and increasing ascorbic acid concentration to 62.5 μM.

Gel analysis and IC_{50} determination

Percent DNA damage inhibition was determined using the formula 1-[% N / % B]*100, where % N = % nicked DNA in the oxo-sulfur containing lanes and % B = % of nicked DNA in the Fe^{2+}/H_2O_2 or Cu^+/H_2O_2 lane. Percentages are corrected for residual

nicking prior to calculation. Results are the average of three trials, and standard deviations are indicated by error bars. Calculation of p values at 95% confidence as described by Perkowski *et al*. was used to determine statistical significance.[59] Sigma Plot (v.9.01, Sysat Software, Inc., San Jose, CA) was used to plot percent DNA damage inhibition as a function of log concentration of oxo-sulfur compound and fit to a variable-slope sigmoidal dose response curve using the equation:

$$f = \min + [(\max - \min) / (1 + 10^{(\log IC_{50} - x)H})]$$

where f = percent DNA damage inhibition, min = minimum DNA damage inhibition, max = maximum DNA damage inhibition, x = log concentration of compound, and H = Hillslope. Results are the average of the fits of three trials, and errors are reported as standard deviations from error propagation calculations of the gel data.

UV-vis measurements

$FeSO_4 \cdot 7H_2O$ (300 μM) and the oxo-sulfur compound (600 μM) were combined in MES buffer (10 mM) at pH 6. For experiments with Cu^+, $CuSO_4 \cdot 5H_2O$ (58 μM), ascorbic acid (72.5 μM) and the oxo-sulfur compound (116 μM) were combined in MOPS buffer (10 mM). The indicated concentrations are final concentrations in a volume of 3 mL.

Electrospray ionization mass spectroscopy (ESI-MS) measurements

For 1:1 mole ratio of Cu^+:selenium or sulfur compound, $CuSO_4$ (100 μM) and ascorbic acid (125 μM) were combined in a 3:1 ratio of methanol : water, and allowed to

stand for 3 min at room temperature. The sulfur or selenium compound (100 μM) was added to the solution to obtain a final volume of 1 mL, and allowed to stand for 5 min at room temperature. Mass spectra were obtained using the QSTAR XL Hybrid MS/MS System (Applied Biosystems), with direct injection of the sample (flow rate = 0.05 mL/min) into the Turbo Ionspray ionization source. Samples were run under positive mode, with ionspray voltage of 5500 V, and time of flight (TOF) scan mode. The QSTAR instrument was operated by Carolyn Quarles from Dr. R. Kenneth Marcus group at Clemson University. For a 1:2 mole ratio of Cu^{+}:selenium or sulfur compound, a similar procedure was followed, using $CuSO_4$ (50 μM) and ascorbic acid (62.5 μM). For a 1:3 ratio, $CuSO_4$ (25 μM), ascorbic acid (33 μM), and selenium or sulfur compound (75 μM) were used. All reported m/z peak envelopes (Table 3.2) matched theoretical peak envelopes.

Tabular data for gel electrophoresis experiments

Tabulated values for the percentages of closed, circular (undamaged) and nicked (damaged) DNA bands observed in the gel electrophoresis experiments for Cu^{+}/H_2O_2 (pH = 7) are given in Tables 3.2-3.6. Tabulated values using $[Cu(bipy)_2]^{+}$ as the copper source instead of Cu^{+} at pH 7 are in Tables 3.7-3.9. Additionally, tabulated values of the compounds tested with Fe^{2+}/H_2O_2 (pH = 6) are given in Tables 3.10-3.14 and those with $[Fe(EDTA)]^{2-}$ are given in Table 3.15-3.16. All reported tabulated values are the average of three experimental trials with the indicated calculated standard deviation.

Table 3.2. Tabulation for electrophoresis results for MeCysSO with Cu^{2+} (6 μM), ascorbate (7.5 μM) and H_2O_2 (50 μM) at pH 7.

Lane	Concentration (μM)	% Circular DNA	% Nicked DNA	% Damage Inhibition	p-value
5	0	27 ± 1.5	73	0	
6	0.1	30 ± 1.9	70	3.1 ± 1.4	0.06
7	1	31 ± 1.4	69	4.5 ± 0.40	0.003
8	3	40 ± 1.4	60	20 ± 1.2	0.001
9	5	52 ± 1.1	48	37 ± 1.8	< 0.001
10	7	31 ± 1.4	69	42 ± 3.4	0.002
11	10	56 ± 3.5	30	60 ± 2.0	< 0.001
12	50	89 ± 0.37	69	86 ± 0.73	< 0.001
13	100	92 ± 0.37	8.0	90 ± 1.0	< 0.001
14	1000	99 ± 0.97	1.0	99 ± 1.8	< 0.001
15	1500	99 ± 1.5	1.0	99 ± 1.5	< 0.001

Table 3.3. Tabulation for electrophoresis results for MetSO with Cu^{2+} (6 μM), ascorbate (7.5 μM) and H_2O_2 (50 μM) at pH 7.

Lane	Concentration (μM)	% Circular DNA	% Nicked DNA	% Damage Inhibition	p-value
5	0	27 ± 2.2	73	0	
6	0.1	29 ± 0.24	71	3.7 ± 2.9	0.16
7	1	29 ± 0.96	71	2.7 ± 2.8	0.23
8	5	37 ± 1.6	63	15 ± 4.7	0.03
9	10	50 ± 2.3	50	34 ± 2.4	0.002
10	30	77 ± 2.1	23	69 ± 3.5	< 0.001
11	50	81 ± 2.5	19	75 ± 3.2	< 0.001
12	100	86 ± 1.9	14	86 ± 2.0	< 0.001
13	1000	95 ± 2.7	5.0	100 ± 2.8	< 0.001
14	1500	99 ± 0.83	1.0	100 ± 1.1	< 0.001
15	2000	99 ± 0.17	1.0	100 ± 0.5	< 0.001

Table 3.4. Tabulation for electrophoresis results for MMTS with Cu^{2+} (6 μM), ascorbate (7.5 μM) and H_2O_2 (50 μM) at pH 7.

Lane	Concentration (μM)	% Circular DNA	% Nicked DNA	% Damage Inhibition	p-value
5	0	26 ± 2.2	74	0	
6	0.5	25 ± 1.8	75	-1.1 ± 1.1	0.23
7	5	19 ± 0.59	81	-9.0 ± 2.7	0.03
8	50	5.0 ± 3.3	95	-27 ± 6.1	0.02
9	500	0 ± 0.16	100	-35 ± 4.4	0.005
10	5000	0 ± 0.10	100	-35 ± 4.1	0.005

Table 3.5. Tabulation for electrophoresis results for MePhSO with Cu^{2+} (6 μM), ascorbate (7.5 μM) and H_2O_2 (50 μM) at pH 7.

Lane	Concentration (μM)	% Circular DNA	% Nicked DNA	% Damage Inhibition	p-value
5	0	21 ± 1.2	79	0	
6	0.5	23 ± 1.5	77	1.9 ± 2.3	0.29
7	5	23 ± 1.7	77	2.1 ± 0.78	0.04
8	50	22 ± 1.3	79	1.8 ± 0.11	0.001
9	500	26 ± 3.4	74	5.7 ± 4.9	0.18
10	5000	25 ± 0.90	75	4.4 ± 1.6	0.04

Table 3.6. Tabulation for electrophoresis results for Me_2SO_2 with Cu^{2+} (6 μM), ascorbate (7.5 μM) and H_2O_2 (50 μM) at pH 7.

Lane	Concentration (μM)	% Circular DNA	% Nicked DNA	% Damage Inhibition	p-value
5	0	23 ± 1.6	77	0	
6	0.5	25 ± 2.4	75	3.2 ± 2.4	0.15
7	5	26 ± 2.5	74	4.1 ± 2.8	0.13
8	50	25 ± 2.4	75	3.9 ± 3.1	0.16
9	500	26 ± 2.3	74	4.0 ± 2.3	0.09
10	5000	25 ± 1.2	75	3.9 ± 1.0	0.02

Table 3.7. Tabulation for electrophoresis results for MetSO with $[Cu(bipy)_2]^{2+}$ (50 μM), ascorbate (62.5 μM) and H_2O_2 (50 μM) at pH 7.

Lane	Concentration (μM)	% Circular DNA	% Nicked DNA	% Damage Inhibition	p-value
5	0	23 ± 0.96	77	0	
6	0.1	25 ± 3.0	75	3.5 ± 4.2	0.28
7	1	29 ± 3.1	71	9.1 ± 3.7	0.05
8	10	37 ± 4.7	63	20 ± 7.2	0.04
9	100	36 ± 5.6	64	18 ± 6.6	0.04
10	1000	55 ± 2.0	45	43 ± 3.2	0.002

Table 3.8. Tabulation for electrophoresis results for MeCysSO with $[Cu(bipy)_2]^{2+}$ (50 μM), ascorbate (62.5 μM) and H_2O_2 (50 μM) at pH 7.

Lane	Concentration (μM)	% Circular DNA	% Nicked DNA	% Damage Inhibition	p-value
5	0	36 ± 2.5	64	0	
6	0.1	36 ± 5.1	64	0.62 ± 11	0.9
7	1	38 ± 4.9	62	3.4 ± 10	0.62
8	10	39 ± 1.8	61	5.0 ± 6.6	0.32
9	100	65 ± 2.6	35	46 ± 4.8	0.004
10	1000	92 ± 2.0	8.0	88 ± 3.3	<0.001

Table 3.9. Tabulation for electrophoresis results for MMTS with $[Cu(bipy)_2]^{2+}$ (50 μM), ascorbate (62.5 μM) and H_2O_2 (50 μM) at pH 7.

Lane	Concentration (μM)	% Circular DNA	% Nicked DNA	% Damage Inhibition	p-value
5	0	32 ± 2.9	68	0	
6	0.1	33 ± 1.5	67	-0.24 ± 3.4	0.91
7	1	22 ± 3.6	77	-14 ± 4.8	0.04
8	10	8.0 ± 1.4	92	-36 ± 4.2	0.005
9	100	0.2 ± 1.9	99.8	-48 ± 6.4	0.006
10	1000	3.0 ± 1.7	97	-44 ± 6.5	0.007

Table 3.10. Tabulation for electrophoresis results for MetSO with Fe^{2+} (2 μM) and H_2O_2 (50 μM) at pH 6.

Lane	Concentration (μM)	% Circular DNA	% Nicked DNA	% Damage Inhibition	p-value
5	0	11 ± 3.8	89	0	
6	0.1	14 ± 9.2	86	3.7 ± 6.6	0.43
7	1	9.0 ± 0.73	91	-1.6 ± 4.7	0.61
8	10	10 ± 2.4	90	-0.55 ± 1.6	0.62
9	100	92 ± 0.70	8.0	-3.3 ± 4.2	0.31
10	1000	91 ± 1.3	9.0	-1.5 ± 3.3	0.52

Table 3.11. Tabulation for electrophoresis results for MeCysSO with Fe^{2+} (2 μM) and H_2O_2 (50 μM) at pH 6.

Lane	Concentration (μM)	% Circular DNA	% Nicked DNA	% Damage Inhibition	p-value
5	0	11 ± 4.2	89	0	
6	0.1	11 ± 5.9	89	0.18 ± 4.9	0.96
7	1	91 ± 5.3	9.0	-2.3 ± 5.5	0.53
8	10	12 ± 6.1	88	1.3 ± 7.6	0.80
9	100	13 ± 4.4	87	2.2 ± 1.5	0.13
10	1000	25 ± 1.1	75	17 ± 3.0	0.01

Table 3.12. Tabulation for electrophoresis results for MMTS with Fe^{2+} (2 μM) and H_2O_2 (50 μM) at pH 6.

Lane	Concentration (μM)	% Circular DNA	% Nicked DNA	% Damage Inhibition	p-value
5	0	12 ± 2.8	88	0	
6	0.5	15 ± 2.4	85	3.0 ± 2.9	0.009
7	5	17 ± 1.6	83	5.5 ± 4.8	0.19
8	50	21 ± 0.74	79	9.5 ± 2.5	0.02
9	500	22 ± 1.7	78	12 ± 1.4	0.005
10	5000	30 ± 0.72	70	20 ± 3.5	0.01

Table 3.13. Tabulation for electrophoresis results for MePhSO with Fe^{2+} (2 μM) and H_2O_2 (50 μM) at pH 6.

Lane	Concentration (μM)	% Circular DNA	% Nicked DNA	% Damage Inhibition	p-value
5	0	16 ± 1.3	84	0	
6	0.5	20 ± 2.7	80	4.4 ± 2.4	0.09
7	5	21 ± 1.9	79	5.9 ± 1.0	0.01
8	50	21 ± 2.4	79	5.4 ± 1.8	0.03
9	500	20 ± 1.8	80	4.5 ± 1.8	0.05
10	5000	21 ± 1.6	79	6.0 ± 1.0	0.01

Table 3.14. Tabulation for electrophoresis results for Me_2SO_2 with Fe^{2+} (2 μM) and H_2O_2 (50 μM) at pH 6.

Lane	Concentration (μM)	% Circular DNA	% Nicked DNA	% Damage Inhibition	p-value
5	0	14 ± 2.9	86	0	
6	0.5	16 ± 1.7	84	3.2 ± 2.8	0.19
7	5	21 ± 5.7	79	8.6 ± 7.1	0.17
8	50	17 ± 1.7	83	4.2 ± 2.0	0.07
9	500	18 ± 0.62	82	4.6 ± 2.8	0.10
10	5000	18 ± 1.4	82	5.5 ± 3.6	0.12

Table 3.15. Tabulation for electrophoresis results for MetSO with $[Fe(EDTA)]^2$ (400 μM) and H_2O_2 (50 μM) at pH 7.

Lane	Concentration (μM)	% Circular DNA	% Nicked DNA	% Damage Inhibition	p-value
5	0	49 ± 0.10	51	0	
6	0.1	49 ± 0.20	51	1.2 ± 0.23	0.29
7	1	49 ± 0.19	51	1.8 ± 0.46	0.04
8	10	49 ± 0.98	51	1.7 ± 1.9	0.001
9	100	51 ± 1.4	49	4.6 ± 3.0	0.18
10	1000	51 ± 0.30	49	5.5 ± 0.65	0.04

Table 3.16. Tabulation for electrophoresis results for MMTS with $[Fe(EDTA)]^2$ (400 μM) and H_2O_2 (50 μM) at pH 7.

Lane	Concentration (μM)	% Circular DNA	% Nicked DNA	% Damage Inhibition	p-value
5	0	21 ± 1.2	79	0	
6	0.5	23 ± 1.5	77	1.9 ± 2.3	0.29
7	5	23 ± 1.7	77	2.1 ± 0.78	0.04
8	50	22 ± 1.3	79	1.8 ± 0.11	0.001
9	500	26 ± 3.4	74	5.7 ± 4.9	0.18
10	5000	25 ± 0.90	75	4.4 ± 1.6	0.04

References

(1) Cadenas, E. *Ann. Rev. Biochem.* **1989**, *58*, 79-110.

(2) Valko, M.; Rhodes, C. J.; Moncol, J.; Izakovic, M.; Mazur, M. *Chemico-Biological Interactions* **2006**, *160*, 1-40.

(3) Stewart, M. S.; Spallholz, J. E.; Neldner, K. H.; Pence, B. C. *Free Radic. Biol. Med.* **1999**, *26*, 42-48.

(4) Chung, L. Y. *J. Med. Food* **2006**, *9*, 205-213.

(5) Halliwell, B. *Drugs Aging* **2001**, *18*, 685-716.

(6) Henle, E. S.; Linn, S. *J. Biol. Chem.* **1997**, *272*, 19095-19098.

(7) Hoffmann, M. E.; Mello-Filho, A. C.; Meneghini, R. *Biochim. Biophys. Acta* **1984**, *781*, 234-238.

(8) Mello-Filho, A. C.; Meneghini, R. *Mutat. Res.* **1991**, *251*, 109-113.

(9) Henle, E. S.; Zhengxu, H.; Tang, N.; Rai, P.; Luo, Y.; Linn, S. *J. Biol. Chem.* **1999**, *274*, 962-971.

(10) Karanjawala, Z. E.; Lieber, M. R. *Mech. Ageing Dev.* **2004**, *125*, 405-415.

(11) van Schooten, F. J.; Knappen, A. M.; Izzotti, A. *Mutat. Res.* **2007**, *621*, 1-4.

(12) Emerit, J.; Edeas, M.; Bricaire, F. *Biomed. Pharmacother.* **2004**, *58*, 39-46.

(13) Lippard, S. J.; Berg, J. M. *Principles of Bioinorganic Chemistry*; University Science Books: Mill Valley, 1994.

(14) Park, S.; Imlay, J. A. *J. Bacteriol.* **2003**, *185*, 1942-1950.

(15) Keyer, K.; Imlay, J. A. *Proc. Nat. Acad. Sci. USA* **1996**, *93*, 13635-13640.

(16) Rae, T. D.; Schmidt, P. J.; Pufahl, R. A.; Culotta, V. C.; O'Halloran, T. V. *Science* **1999**, *284*, 27402-27411.

(17) Lippard, S. J. *Science* **1999**, *284*, 748-749.

(18) Yang, L.; McRae, R.; Henary, M. M.; Patel, R.; Lai, B.; Vogt, S.; Fahrni, C. J. *Proc. Nat. Acad. Sci. USA* **2005**, *102*, 11179-11184.

(19) Brown, D. R.; Qin, K. F.; Herms, J. W.; Madlung, A.; MAnson, J.; Strome, R.; Fraser, P. E.; Kruck, T.; vonBohlen, A.; Schulz-Schaeffer, W.; Giese, A.; Weataway, D.; Krestzschmar, H. *Nature* **1997**, *390*, 684-687.

(20) Que, E. L.; Domaille, D. W.; Chang, C. J. *Chem. Rev.* **2008**, *106*, 1517-1549.

(21) Huang, X. *Mutat. Res.* **2003**, *533*, 153-171.

(22) Ke, Y.; Qian, Z. M. *Lancet Neurol.* **2003**, *2*, 246-253.

(23) Moreira, P. I.; Siedlak, S. L.; Aliev, G.; Zhu, X.; Cash, A. D.; Smith, M. A.; Perry, G. *J. Neural Transm.* **2005**, *112*, 921-932.

(24) Valavanidis, A.; Vlahoyianni, T.; Fiotakis, K. *Free Rad. Res.* **2005**, *39*, 1071-1081.

(25) Selima, M. H.; Ratan, R. R. *Ageing Res. Rev.* **2004**, *3*, 345-353.

(26) Wood, R. J. *Ageing Res. Rev.* **2004**, *3*, 355–367.

(27) Giurgea, N.; Constantinescu, M. I.; Stanciu, R.; Suciu, S.; Muresan, A. *Med. Sci. Monit.* **2005**, *11*, RA48-51.

(28) Swaminathan, S.; Fonseca, V. A. *Diabetes Care* **2007**, *30*, 1926-1934.

(29) Moon, H. K.; Yang, E. S.; Park, J. W. *Arch. Pharm. Res.* **2006**, *29*, 213-217.

(30) Sachidanandam, K.; Fagan, S.; Ergul, A. *Cardiovasc. Drug Rev.* **2005**, *23*, 115-132.

(31) Thirunavukkarasu, C.; Sakthisekaran, D. *J. Cell. Biochem.* **2003**, *88*, 578-588.

(32) Rabinkov, A.; Miron, T.; Konstantinovski, L.; Wilchek, M.; Mirelman, D.; Weiner, L. *Biochim. Biophys. Acta* **1998**, *1379*, 233-244.

(33) Stoll, A.; Seebeck, E. *Adv. Enzymol.* **1951**, *11*, 377-400.

(34) Xiao, H.; Parkin, K. *J. Agric. Food. Chem.* **2002**, *50*, 2488-2493.

(35) Yin, M.-C.; Cheng, W.-S. *J. Agric. Food. Chem.* **1998**, *46*, 4097-4101.

(36) Jacob, C.; G.I.Giles; Giles, N. M.; Sies, H. *Angew. Chem. Int. Ed.* **2003**, *42*, 4742-4758.

(37) Brot, N.; Weissbach, H. *Arch. Biochem. Biophys.* **1983**, *223*, 271-281.

(38) Vogt, W. *Free Radic. Biol. Med.* **1995**, *18*, 93-105.

(39) Levine, R. L.; Moskovitz, J.; Stadtman, E. R. *IUBMB Life* **2000**, *50*, 301-307.

(40) Gonias, S. L.; Swaim, M. W.; Massey, M. F.; Pizzo, S. V. *J. Biol. Chem.* **1988**, *263*, 393-397.

(41) Nakao, L. S.; Iwai, L. K.; Kalil, J.; Augusto, O. *FEBS Lett.* **2003**, *547*, 87-91.

(42) Moskovitz, J. *Biochim. Biophys. Acta* **2005**, *1703*, 213-219.

(43) Weissbach, H.; Resnick, L.; Brot, N. *Biochim. Biophys. Acta* **2005**, *1703*, 203-212.

(44) Kim, H.-Y.; Cheng, W.-S. *Biochem. J.* **2007**, *407*, 321-329.

(45) Moskovitz, J.; Berlett, B. S.; Poston, J. M.; Stadtman, E. R. *Proc. Natl. Acad. Sci. U.S.A.* **1997**, *94*, 9585-9589.

(46) Levine, R. L.; Mosoni, L.; Berlett, B. S.; Stadtman, E. R. *Proc. Natl. Acad. Sci. U.S.A.* **1996**, *93*, 15036-15040.

(47) Levine, R. L.; Berlett, B. S.; Moskovitz, J.; Mosoni, L.; Stadtman, E. R. *Mech. Ageing Develop.* **1999**, *107*, 323-332.

(48) Nishimura, H.; Higuchi, O.; Tateshita, K. *BioFactors* **2004**, *21*, 277-280.

(49) Battin, E. E.; Brumaghim, J. L. *J. Inorg. Biochem.* **2008**, *102*, 2036-2042.

(50) Ramoutar, R. R.; Brumaghim, J. L. *J. Inorg. Biochem.* **2007**, *101*, 1028-1035.

(51) Battin, E. E.; Perron, N. R.; Brumaghim, J. L. *Inorg. Chem.* **2006**, *45*, 499-501.

(52) Ramoutar, R. R.; Brumaghim, J. L. *Main Group Chem.* **2007**, *6*, 143-153.

(53) Battin, E. E.; Ramoutar, R. R.; Brumaghim, J. L. *in preparation*.

(54) Schramel, O.; Michalke, B.; Kettrup, A. *Fresenius J. Anal. Chem.* **1999**, *363*, 452-455.

(55) Michalke, B.; Schramel, O.; Kettrup, A. *Fresenius J. Anal. Chem.* **1999**, *363*, 456-459.

(56) Note: The reported IC_{50} and error values have been refined since publication.[49,52]

(57) Polec-Pawlak, K.; Ruzik, R.; Lipiec, E. *Talanta* **2007**, *72*, 1564-1572.

(58) Hertzberg, R. P.; Dervan, P. B. *J. Am. Chem. Soc.* **1982**, *104*, 313-315.

(59) Perkowski, D. A.; Perkowski, M. *Data and Probability Connections*; Pearson Prentice Hall: New Jersey, 2007, pp 318-337.

CHAPTER FOUR

INVESTIGATING THE ABILITY OF π-CONJUGATED POLYMER NANOPARTICLES TO PROMOTE OXIDATIVE DNA DAMAGE

Introduction

Photodynamic therapy (PDT) is fast becoming a new approach for the treatment of cancerous cells and tumors.[1,2] The mechanistic action of photodynamic therapy requires three components: light, oxygen, and a photosensitizing agent that localizes in or near diseased cells or tissues.[1-4] Upon activation by light (photons) at specific wavelengths, the photosensitizer is excited from the singlet ground state (S_0) to a triplet state (T_1) via an intermediate excited singlet state (S_1).[1-3,5,6] The excited singlet state is short-lived, with a lifetime in the nanosecond range, and decays either through radiative or non-radiative processes to the ground or triplet states, which have much longer lifetimes, ranging from micro- to milliseconds.[1,2,5,6]

From the excited triplet state, the photosensitizer can undergo two processes (Type I and Type II), which generate reactive oxygen species (ROS) in the presence of molecular oxygen (O_2). In the Type I process, the photosensitizer in its triplet state transfers an electron to, or abstracts a hydrogen atom from, biomolecules such as lipids in cell membranes to form radical cations or anions. These radical species then react with molecular oxygen to generate ROS such as the superoxide anion radical ($O_2^{-\bullet}$).[1-3,5-7] The second process (Type II) involves the direct transfer of energy from the triplet state to oxygen to form singlet oxygen ($^1O_2$).[1-3,5,6,8-10] While both of these processes occur

simultaneously, Type II generation of singlet oxygen typically predominates over Type I production of radicals since the rate constant for generation of singlet oxygen ($k \sim 1\text{-}3 \times 10^9$ dm^{-1} mol^{-1} s^{-1}) is usually higher than that for generation of $O_2^{-\bullet}$ ($k \leq 1 \times 10^7$ dm^{-1} mol^{-1} s^{-1}).[7]

Singlet oxygen is a highly reactive species that directly oxidatively damages biological targets, thus making it ideal for photodynamic therapy.[2,9,11-13] $^1O_2$ reacts with electron-rich molecules and cellular components such as DNA, in particular guanine bases, resulting in oxidized bases, strand breaks, mutagenesis, and cell death.[10,11,13-18] *In vivo*, cells are protected from such mutations by repair systems that use endonucleases such as the formamidopyrimidine-DNA glycosylase (Fpg) enzyme, which cleaves oxidized purine bases for removal or replacement.[19,20] Other biological targets for singlet oxygen include RNA, lipids, sterols, and proteins.[6,7,21,22] In biological systems, $^1O_2$ has a short half-life (< 0.04 μs) with a small radius of action (< 0.02 μm), therefore only target cells in close proximity to the photosensitizer are affected by photodynamic therapy.[1,2,23]

Many factors influence the efficiency and effectiveness of PDT, including oxygen availability; the type, chemistry, light absorption, and bioavailability properties of the photosensitizer; the location and dosage of the photosensitizer in diseased cells; and the light dosage and timing of light activation after administration of the sensitizer.[1,2,24] Several types of photosensitizer molecules have been examined, including organic dyes, porphyrins and their derivatives, and various organometallic species.[2,3,25,26] Although there are several highly selective sensitizers,[2,27-29] the FDA has approved the use of Photofrin®, a haematoporphyrin derivative, and Verteporfin, a derivative of

benzoporphyrin, to be used in PDT.[1,3] While effective in clinical applications, several problems are associated with existing photosensitizers.[3] These include the hydrophobicity of most sensitizer molecules that causes aggregation in aqueous media and make intravenous administration difficult, as well as a lack of selective accumulation in diseased tissue.[2,3] Although a few selective-targeting sensitizers have been reported, their low selectivity hinders their testing in clinical trials.[3] This lack of effective sensitizers for PDT is of great concern for the advancement of photodynamic therapy. Therefore, significant research efforts have focused on the development of photosensitizer carriers to obtain effective sensitizers that generate more ROS upon irradiation with enhanced localization on or near cancer cells.[1,3,30-37]

Nanotechnology is currently being implemented in the development of such photosensitizer carriers.[3,38,39] Nanoparticles are colloidal particles of various sizes in the nanometer (nm) range and have been used for many applications in catalysis,[40] optics,[41]electronics,[42] clinical diagnostic assays, drug delivery systems, histology studies, and separation techniques.[3,43-45] Recently, a new class of π-conjugated polymer nanoparticles (CP dots) was synthesized by the McNeill group at Clemson University using the conjugated polymer poly(9,9-dihexyl)flourene (PDHF); the efficiency of these CP dots to produce singlet oxygen when doped with the photosensitizer tetraphenyl porphyrin (TPP) was measured.[37,46,47] CP dot nanoparticles vary in size from 5-50 nm, and the McNeill lab has synthesized TPP-doped CP dots with a diameter of 5 ± 1 nm that are comparable to other spherical, nanoparticle-based photosensitizers.[37] These TPP-

doped CP dot nanoparticles are considered to be efficient photosensitizers because of the high yields of singlet oxygen produced upon photoexcitation.

Using spectrophometric analysis to measure the depletion of *p*-nitrosodimethylaniline (RNO) after irradiation, the singlet oxygen quantum yield for CP dots doped with TPP was determined to be between 0.6 and 0.8, which is high compared to the yield produced from undoped PDHF (0.2-0.3).[37] The high absorptivity of doped CP dots (10^7-10^9 $M^{-1}cm^{-1}$), coupled with the high quantum yield of singlet oxygen generated upon irradiation, make these TPP-doped nanoparticles promising photosensitizers for photodynamic therapy cancer treatment.[37] Since the potential use of these doped CP dots to treat cancer is of great interest, it is necessary to determine the effects of TPP-doped CP dot-generated singlet oxygen on cellular components such as DNA.

Gel electrophoresis assays have been previously employed by the Brumaghim group to determine the antioxidant activity of several selenium, sulfur, and polyphenol compounds by prevention of metal-mediated oxidative DNA damage.[48-51] In these studies, DNA damage results from the generation of hydroxyl radical ($^{\bullet}OH$) upon addition of either copper(I) or iron(II) and hydrogen peroxide (H_2O_2).[48-51] In collaboration with the McNeill group, similar gel electrophoresis assays were employed to quantify the amount of DNA backbone and base damage produced by singlet oxygen generated from doped CP dot nanoparticles upon irradiation.

Toxicity of nanoparticles

Apart from PDT, nanomaterials are widely used in the pharmaceutical, biomedical, electrical, cosmetic, and environmental fields.[52] Metals or metal oxides of iron, titanium, and silicon are used as nanomaterials in imaging techniques, sunscreens, and cosmetics.[52,53] To increase solubility, the surfaces of nanoparticles are often functionalized. Nanoparticles functionalized with polyethylene glycol (PEG) and polysorbates to facilitate solubility in drug delivery systems are also known to generate ROS, which can damage cellular components in biological systems.[54-56] In addition, PEG used to functionalize nanoparticles undergo light- or metal-induced decomposition via auto-oxidation to produce peroxides.[54,55]

Production of peroxides from PEG, coupled with metals found in biological systems, may result in potential cellular damage from $^{\bullet}OH$ generated in Fenton and Fenton-like reactions.[57-60] As a result, it is important to understand the toxic effects of such functionalized nanomaterials before they can be used for biomedical applications. It has been reported that PEG stored at different temperatures (25-40 °C) in the dark or exposed to light generates different levels of peroxide (1.5-9.0 μM).[54] In collaboration with the McNeill group, the Brumaghim group has examined the production of H_2O_2 by PEG and PEG-trimethoxysilane (PEG-TMS) under similar conditions. For these experiments, the ferrous oxidation-xylenol orange (FOX) assay was used to determine hydrogen peroxide concentrations.

Functionalized nanoparticles may also localize metal ions in addition to generating ROS species with or without photoexcitation.[32-34,61] Metal ions such as iron(II)

and copper(I) are present in cells, and react with H_2O_2 to produce oxidative DNA damage via $^{\bullet}OH$ generation leading to several health conditions such as cancer, aging, and cardiovascular and neurodegenerative diseases.[57,60,62-65] Functionalized nanoparticles may have surface charges that may cause association with cellular metals such as iron and copper.[57-60] It is therefore important to determine the amount of metal that is associated with these nanoparticles and functional groups to understand potential nanoparticle toxicity *in vivo*. Working with the McNeill group, induced coupled plasma mass spectroscopy (ICP-MS) was utilized in experiments to determine iron association to both PEG and PEG-TMS. The results of these experiments are preliminary, and additional studies will be required to fully understand the chemical behavior of functionalized nanoparticles for use in biomedical applications.

Results and Discussion

Photodynamic therapy and the use of nanomaterials as carriers for photosensitizer molecules is a new approach for the disease treatment. McNeill and coworkers at Clemson University have recently synthesized π-conjugated polymer nanoparticles (CP dots) with large one and two photon cross-sections.[37,46,47,66] These TPP-doped CP dot nanoparticles generate high yields of singlet oxygen upon UV irradiation (0.6-0.8), which may have great potential in the treatment of cancer by PDT.[37] Since singlet oxygen damages both the backbone and bases of DNA, damage that is critical for PDT treatment and cell death, gel electrophoresis experiments were conducted to quantify the amount of DNA damage produced upon irradiation of the doped CP dots.

DNA backbone and base damage experiments with doped CP dot nanoparticles

TPP-doped CP dot nanoparticles were combined with plasmid DNA and irradiated for 0, 50, 100, and 200 min using a fluorescence spectrometer at 377 nm. Gel electrophoresis was used to quantify DNA backbone damage using previously reported methods.[52-55] To determine DNA base damage, the Fpg enzyme was used to digest the DNA after irradiation, prior to running the gel assay. The Fpg enzyme nicks the DNA backbone both 3′ and 5′ to damaged bases such as 8-oxoguanine, 8-oxoadenine, 5-hydroxy-cytosine, and 5-hydroxy-uracil.[70,71] This enzyme was chosen since oxidative damage by $^1O_2$ primarily causes oxidation of guanine and adenine to form 8-oxoguanine and 8-oxoadenine.[67,68]

Figure 4.1 shows the gel images from these DNA damage experiments. The band intensities in lanes 2-8 (Figure 4.1A) are undigested plasmid samples and indicate that DNA backbone damage increases as irradiation time of the TPP-doped CP dot nanoparticles increases. Lanes 2 and 3 (Figure 4.1A) are control lanes indicating that the plasmid (lane 2) is of high quality and that H_2O_2 alone (lane 3) does not damage DNA. Lane 4 shows the DNA damage produced when Fe^{2+} reacts with H_2O_2 to generate $^{\bullet}OH$. Lanes 5-8 show the extent of DNA damage upon irradiation of the TPP-doped CP dots for 0, 50, 100, and 200 min, respectively, as seen by the increase in band intensity from undamaged to damaged DNA upon increasing irradiation time. Preliminary results for base damage experiments are seen in Figure 4.1B. Lane 2 is a control lane with DNA digested by the Fpg enzyme, showing that the enzyme has no effect on undamaged DNA.

Lanes 3-6 show that base damage increases with increasing irradiation times of 0, 50, 100, and 200 min, respectively, of TPP-doped CP dots (Figure 4.1B).

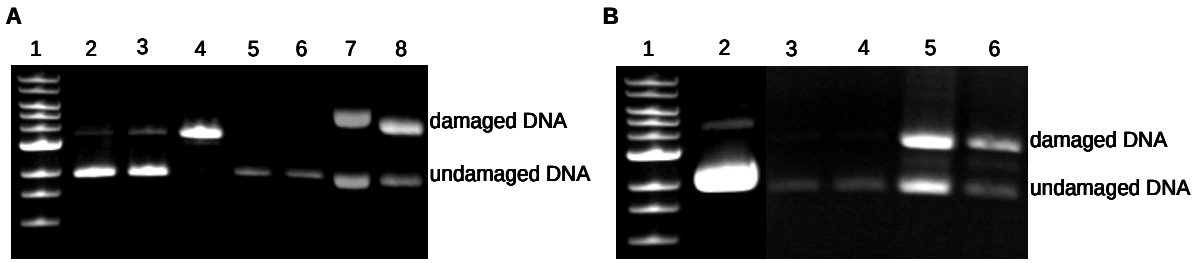

Figure 4.1. Agarose gel image showing DNA backbone and base damage after irradiation of TPP-doped CP dot nanoparticles over time. (A) For DNA backbone damage, lanes: 1) 1 kb DNA ladder; 2) plasmid DNA (p); 3) p + H_2O_2 (50 μM); 4) p + Fe^{2+} (2 μM); 5-8) p + TPP-doped CP dot nanoparticles irradiated for 0, 50, 100, and 200 min, respectively. (B) For DNA base damage, lanes: 1) 1 kb DNA ladder; (2) p + Fpg enzyme; 3-6) lane 2 + TPP-doped CP dot nanoparticles irradiated for 0, 50, 100, and 200 min, respectively, prior to Fpg digestion.

Quantification of the normalized band intensities from the gel images are shown as a bar graph in Figure 4.2. Figure 4.2A shows that non-irradiated TPP-doped CP dots (lane 5) do not damage plasmid DNA. This is expected since photoexcitation of the nanoparticles is required to generate the DNA-damaging singlet oxygen. Similarly, irradiation for 50 min did not produce measurable DNA damage (Figure 4.2A, lane 6). However, 100 min irradiation produced 50% DNA damage, with 70% DNA damage occurring after 200 min (lanes 7 and 8, respectively).

Similar results were obtained for the DNA base damage experiments (Figure 4.2B), where non-irradiated TPP-doped CP dots produced negligible DNA damage (lane 3). Irradiation of TPP-doped CP dots for 50 min (Figure 4.2B, lane 4) also produced a negligible amount of base damage indicating little production of singlet oxygen. As the

irradiation time increased to 100 and 200 min, base damage also increased to ~ 55% (lane 12) and ~75% (lane 13), respectively.

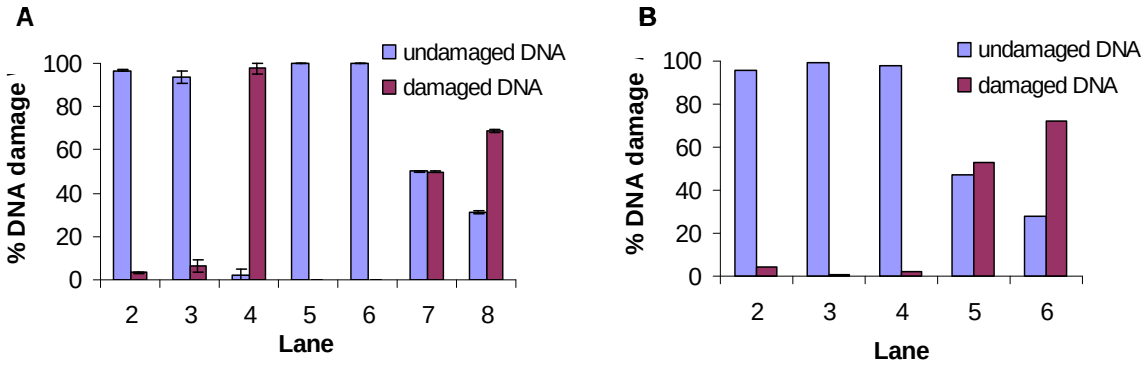

Figure 4.2. Bar graph showing the effect of TPP-doped CP dot nanoparticles on DNA backbone and base damage upon irradiation at different time intervals. (A) Lanes for DNA backbone damage: 2) plasmid DNA (p); 3) p + H_2O_2 (50 μM); 4) p + Fe^{2+} (2 μM) + H_2O_2; and 5-8) p + TPP-doped CP dot nanoparticles irradiated for 0, 50, 100, and 200 min, respectively. (B) Lanes for DNA base damage: 2) p + Fpg enzyme; and 3-6) lane 2 + TPP-doped CP dot nanoparticles irradiated for 0, 50, 100, and 200 min, respectively, prior to Fpg digestion.

As expected, singlet oxygen generated by TPP-doped CP dots produces both backbone and base DNA damage after 50 min of light exposure. In addition, DNA backbone and base damage increases with increased irradiation time, suggesting that more singlet oxygen is continually generated during irradiation. Although these data are preliminary, they suggest the TPP-doped CP dot nanoparticles developed by the McNeill lab may be effective and efficient photosensitizers for PDT. To properly validate the use of the TPP-doped CP dot nanoparticles for PDT, experiments using Fpg digestion should be performed in triplicate to accurately quantify base damage produced from irradiation of these particles. In addition, the Nth (endonuclease III) and 8-oxoG-DNA glycosylase (OGG) enzymes can be used to further determine types of DNA base damage. The Nth

enzyme cleaves damaged pyrimidine bases such as thymine glycol, uracil glycol, and 6-hydroxy-5,6-dihydrothimine.[69,70] The OGG enzyme is specific for 8-oxoguanine.[71] From these base damage experiments, DNA damage at specific bases could be quantified and compared, which would allow for further understanding of DNA damage mechanisms by irradiated TPP-doped CP dot nanoparticles.

Determining hydrogen peroxide formation from PEG and PEG-TMS

Polyethylene glycols (PEGs) are water soluble synthetic polymers with many applications in the pharmaceutical and biotechnological industries.[54] They are used as lubricants, stabilizers, cosolvents and as chemical agents for the PEGylation of proteins.[54] Despite many benefits, PEG and its derivatives can produce low levels of peroxides under various conditions.[54,55] Since PEG-functionalized nanomaterials have potential use in biological systems to increase nanoparticle solubility, nanotoxicity becomes a great concern since peroxides can react with metal ions found in cells to generate damaging $^{\bullet}OH$.[58-60,68]

Since nanoparticles are often functionalized with PEG, and PEG-TMS is used to facilitate such functionalization, determination of peroxide formation from both PEG and PEG-TMS groups was undertaken. To determine peroxide formation from solutions of PEG (MW 950-1050) and PEG-TMS (MW= 460-590), the FOX assay was used. The FOX method is an analytical technique widely used to measure peroxides based on the peroxide oxidation of iron(II) to iron(III) ions, with subsequent binding of iron(III) to the

xylenol-orange dye.[67,72,73] This results in a color change from orange to blue/purple, which can be measured via UV-vis spectroscopy.[67,72,73]

To generate the calibration curve, various concentrations of H_2O_2 (0.01-100 μM) were added to the FOX reagent, and upon appearance of the blue/purple color, the absorbance at each peroxide concentration was taken from 540-650 nm to obtain the wavelength at which the highest absorbance was achieved (λ_{max}). The H_2O_2 calibration curve (Figure 4.3) was fit with a best fit line as indicated ($R^2 = 0.982$).

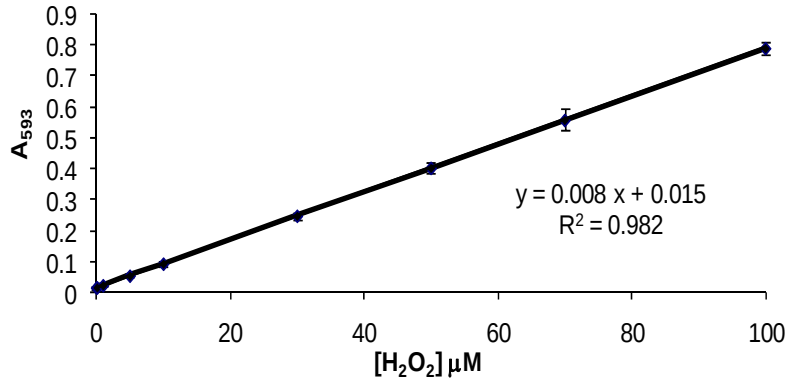

Figure 4.3. Calibration curve of absorbance at 593 nm (A_{593}) vs. hydrogen peroxide concentration as measured by the FOX assay.

The FOX assay was then used to measure H_2O_2 concentrations formed from both PEG and PEG-TMS solutions incubated at 37 °C under light and dark conditions over a one-week period. Aliquots were taken every 24 h, treated with the FOX reagent, and measured via UV-vis. The H_2O_2 concentration was then obtained by measuring the absorbance at 593 nm and calculating the concentration using the calibration curve.

Similar experiments were also performed at 80 °C since peroxide levels are reported to increase as temperature increases.[54]

Figure 4.4 shows a graph of the concentration of peroxide formed by each sample over several days. At 80 °C, PEG exposed to light and PEG-TMS in the dark produced only trace amounts (< 0.1 μM) over the course of the week. PEG incubated at 80 °C in the dark produced the highest concentration of H_2O_2 (~31 μM) after 6 days. For all other samples besides PEG-TMS exposed to light at 80 °C, the highest concentration of H_2O_2 produced was 2-4 μM.

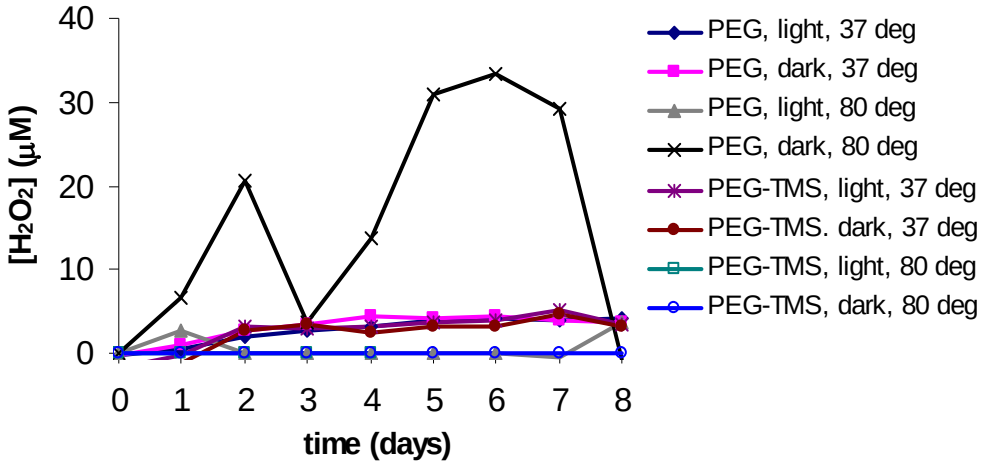

Figure 4.4. Graph showing the amount of peroxide formed from PEG and PEG-TMS under light and dark conditions at 37 °C and 80 °C.

In this investigation, PEG-TMS incubated at 80 °C with exposure to light became viscous with a pungent odor after 4 days, but showed no formation of peroxide after this time (Figure 4.4). Upon addition of the FOX reagent, PEG-TMS in the dark at 80 °C turned a magenta color instead of the blue/purple color observed for all other samples with absorbance measured at λ_{max} = 560 nm. Peroxide concentration for this sample

calculated from the calibration curve generated at 560 nm was found to be ~0.4 μM after 4 days.

The preliminary results from these experiments contradict similar studies performed with PEG 1450 and PEG 20000. Kuman and Kalonia reported that both PEG 1450 and PEG 20000 produced high levels of peroxide at 40 °C after 6 days when stored in ambient light (1.5 and 4.8 μM, respectively).[54] Samples stored in the dark for 20 days at room temperature (25 °C) showed elevated peroxide levels in both PEG 1450 and PEG 20000 (2.7 and 9.0 μM, respectively).[54] The lower levels of peroxides formed in our experiments may be due the low molecular weight PEG used (950-1050) significantly shorter than the PEGs of higher molecular weights (1450 or 20000) used by Kuman and Kalonia. In addition, differences in the experimental design such as lighting and storage conditions may also contribute to the differences observed in peroxide formation.

A study using PEG 400 to enhance the solubility of drug formulations reported that this PEG provided a highly oxidizing environment resulting in radical chain degradation and two-electron nucleophilic reactions.[74] These processes may explain the viscous appearance of the PEG-TMS exposed to light at 80°C and the magenta color of this sample in the FOX assay. In addition, water may play a role in the formation of peroxides by PEG, as reports indicate that peroxide formation is related to the fraction of water in solution, and therefore the amount of dissolved oxygen.[54,75,76]

Preliminary experiments using PEG and PEG-TMS indicate that under most conditions peroxide (~2-4 μM) is formed under conditions of light, dark, and elevated temperature, with the exception of PEG stored in the dark at 80°C. Peroxide

concentrations of 2-4 μM are much higher than the steady-state H_2O_2 concentration calculated for unstressed *E. coli* cells (~20 nM). In addition, *in vivo* studies have shown that peroxide concentrations of 1-3 μM result in cell death due to oxidative DNA damage,[58,59] indicating that peroxide generation by functionalized nanoparticles, even at low concentrations, may be toxic to cells.

Iron association with silica and PEG-functionalized silica beads

PEG-functionalized nanoparticles may facilitate localization of metal ions on their surface since they contain oxygen donor groups that can bind metals. Iron localization on or near PEG is possible due to interactions between the positively charged iron and the electron-rich ether oxygen atoms of PEG. The generation of peroxides either *in vivo* or from the PEG functional groups can react with redox-active metals such as iron to produce the DNA damaging hydroxyl radical.[57,60,68] The ability of metal ions such as iron to associate with functionalized nanoparticles is therefore of considerable relevance to potential nanoparticle toxicity. Studies of PEG-functionalized and non-functionalized silica microspheres (beads) were performed to determine whether iron can associate to PEG-functionalized nanoparticles.

In collaboration with the McNeill group at Clemson University, silica microspheres (0.3 μm) and PEG-functionalized silica microspheres were prepared for analysis by agitation with HCl (1M), centrifugation, and washing with deionized water to ensure the bead surface was metal-free. To determine whether iron associated with the functionalized or non-functionalized silica beads, a calibration curve using various

concentrations of $[Fe(EDTA)]^{2-}$ (0-500 μM) was generated via ICP-MS measurements of iron intensities (Figure 4.5). The calibration curve obtained was found to be linear within the concentration range of 0-500 μM ($R^2 = 0.99$).

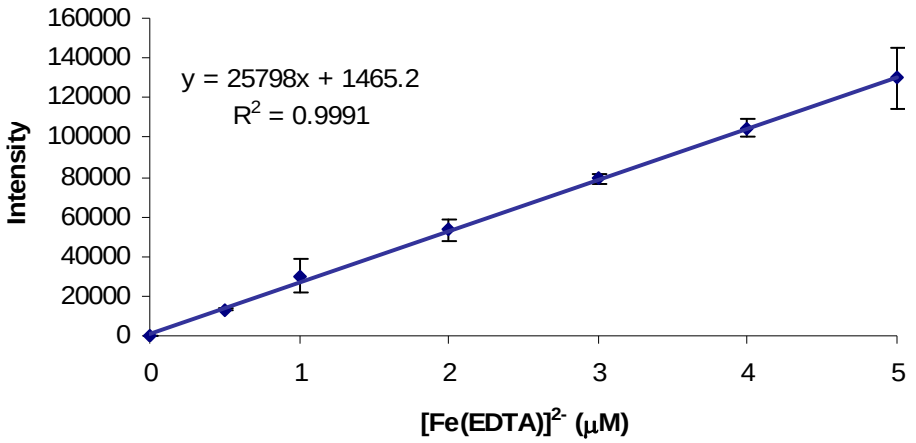

Figure 4.5. Calibration curve for iron intensity vs. $[(Fe(EDTA)]^{2-}$ concentrations (μM) as measured by ICP-MS.

To determine iron association, both PEGylated and non-functionalized silica beads were treated with the indicated volumes of iron (50 μM) and centrifuged. The isolated beads were then washed with EDTA to bind and remove any iron associated with the beads, centrifuged, and the EDTA supernatant was collected for analysis. The iron intensity of each EDTA wash was then measured using ICP-MS, and the concentration of iron was determined from the calibration curve.

Figure 4.6 is a graph of bead-associated iron with and without PEG-functionalization. For the non-functionalized silica beads, the concentration of associated iron was the same (~1.17 ± 0.03 μM) regardless of the amount of iron used (50, 100, and 200 μL of 50 μM solution). However, iron has a greater association with PEG-

functionalized microspheres, with iron concentrations increasing to ~2.2 ± 0.2 μM (p = 0.003), 2.7 ± 0.2 μM (p = 0.002) and 5.0 ±1.0 μM (p = 0.005)at 50, 100, and 200 μL, respectively.

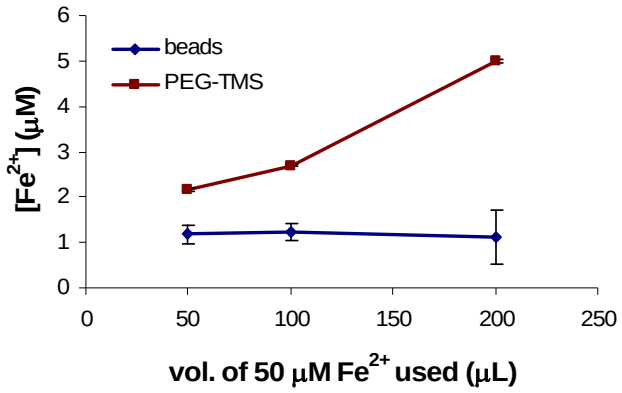

Figure 4.6. Graph showing the concentration of iron associated with PEGylated silica and unfunctionalized silica microspheres. All differences between beads and PEG-TMS are statistically significant ($p \leq 0.005$). Error bars for PEG-TMS are smaller than the data points.

In biological systems, iron is known to generate reactive oxygen species that can damage DNA and result in cell death.[58,59] Therefore, the interaction of iron ions with PEG-functionalized nanoparticles may be an important factor to consider as a source of nanotoxicity. In these iron association experiments, PEG-functionalized beads associated more iron (~2-4 μM) than with the non-functionalized beads. This amount of localized iron is a significant fraction of non-protein-bound cellular iron concentrations (~10-30 μM).[77] Gel electrophoresis experiments with plasmid DNA show that iron at similar concentrations (2 μM) significantly damages DNA in the presence of H_2O_2.[48-51] Combined with the observed peroxide generation, iron association to PEG-functionalized

nanoparticles may lead to formation of the damaging hydroxyl radical and significant cellular damage *in vivo*.

These preliminary experiments highlight the importance of understanding nanotoxicity if nanomaterials are to be used for biomedical applications. To fully comprehend the effects of such toxicity on biological systems, further studies to evaluate the formation of peroxides from functional groups used in nanotechnology or nanomaterials are necessary. In addition, it is also important to determine the association of other cellular metal ions such as iron and copper to functionalized nanoparticles since the combination of peroxide formation and metal association in cells may lead to oxidative DNA damage, cell death, and adverse health effects.

Conclusions

TPP-doped CP dot nanoparticles have a great potential for use as photosensitizers due to their high molar absorptivity (10^7-10^9 M^{-1} cm^{-1}) and production of high yields of singlet oxygen upon irradiation.[37] Studies also show that the generated reactive oxygen species produce both DNA backbone and base damage by irradiation in a time-dependent manner, suggesting that TPP-doped CP dot nanoparticles may be effective photosensitizers to be used in PDT. With the widespread use of nanomaterials for medical purposes, the toxicity of these materials becomes a significant concern. Preliminary results indicate that functionalization of nanoparticles with PEG may be toxic to cells due PEG's ability to form peroxides and associate iron. Iron can react with peroxide to generate $^{\bullet}OH$ that damages cellular components such as DNA, lipids, and

proteins and may cause significant nanotoxicity. Further studies are therefore warranted to further understand the effects of metal localization and peroxide formation on PEG-functionalized nanoparticles in biological systems.

Materials and Methods

Materials

NaCl (99.999% to avoid trace metal contamination), glacial acetic acid, NaOH, 30% H_2O_2 solution, $FeSO_4 \cdot 7H_2O$, and bromophenol blue were purchased from Alpha Aesar. Glucose, agarose, and ampicillin were from EMD Chemicals. TRIS hydrochloride and sodium EDTA were from J.T. Baker. HCl was from VWR Scientific; ethidium bromide was from Lancaster Synthesis, Inc. Xylene cyanol, peptone, and yeast extract was from EM Science. Butylated hydroxytoluene, xylenol orange, HCl (≥ 99%), ammonium hydroxide, H_2O_2 (30%), NaCl (99.999%), methanol (≥ 99%), polyethylene glycol (PEG, MW 950-1050) were purchased from Sigma-Aldrich. H_2SO_4 was from Fisher Scientific. Silica microspheres (0.3 μm) were from Polysciences, Inc. and 2-[methoxy(polyethyleneoxy)propyl] trimethoxy silane (PEG-TMS, 460-590) from Gelest, Inc. Concentrated plasmid DNA in TE buffer (4 mg/mL) was purchased from Aldevron, Fpg enzyme, BSA buffer (10×) and NEB buffer were from New England BioLabs, Inc. Water was purified using the NANOpure DIamond water deionization system (Barnstead International, Dubuque, IA). Iron-free microcentrifuge tubes, bottles and glass vials were prepared by washing the tubes in 1 M HCl prior to use and rinsing thoroughly with

ddH_2O. MES buffer was treated with Chelex resin for 24 h and then filtered into an iron-free bottle. π-Conjugated polymer nanoparticles (CP dots) for gel experiments were obtained from the McNeill group at Clemson University.

Purification of plasmid DNA

Concentrated plasmid DNA (300 μL of 4 mg/mL) purchased from Aldevron was dialyzed against 130 mM NaCl for 24 h at 4 ^oC. The resulting DNA concentration was found using UV-vis measurements at A_{260} (1 A_{260} = 50 ng/μL). Purity of plasmid DNA was determined via gel electrophoresis of a digested sample, and all absorbance ratios were within acceptable limits ($A_{250/260} < 0.95$, and $A_{260/280} > 1.8$).

DNA backbone and base damage gel electrophoresis experiments with TPP-doped CP dot nanoparticles

For control lanes, 0.1 pmol plasmid DNA, 130 mM NaCl (99.999% to avoid metal contamination) and 2 μM $FeSO_4 \cdot 7H_2O$ maintained at pH 6 with MES buffer (10 mM) were combined and allowed to stand for 5 min at room temperature. H_2O_2 (50 μM) was then added and incubated for 30 min. EDTA solution (50 μM) was added after this time for a total volume of 10 μL. For experimental lanes, plasmid DNA (0.1 pmol) was added to TPP-doped CP dot nanoparticles to a final volume of 300 μL. A fluorescence spectrometer (Quantamaster, PTI, Inc.) was used to irradiate the nanoparticles at a wavelength of 377 nm. Aliquots (10 μL) were taken at various time intervals after irradiation (0, 50, 100, and 200 min) to determine DNA damage by the TPP-doped CP

dot nanoparticles. DNA was separated on 1% agarose gels via electrophoresis, stained with ethidium bromide for 30 min, and imaged on an UVIproDBT-8000 gel imager (UVITec, Cambridge, UK). Quantification of undamaged and damaged DNA was performed using the UviPro software. A similar procedure was performed to quantify the amount of DNA base damage by adding the Fpg enzyme to aliquots (10 μL) of doped CP dots after irradiation for 50, 100, and 200 min. The Fpg enzyme cleaves the DNA backbone at damaged bases such as 8-oxoguanine, 5-hydroxy-cytosine 8-oxoadenine, and 5-hydroxy-uracil.[70,78] For these experiments, 0.5 μL of a 10× BSA buffer (2 μL)/NEB buffer 1 (8 μL) solution, Fpg enzyme (0.5 μL) and plasmid DNA irradiation for the indicated time periods were incubated for 1 h at 37 °C. After this time, gel electrophoresis was performed.

H_2O_2 calibration curves using the FOX assay

FOX reagent was prepared by dissolving xylenol orange (7.60 mg), $FeSO_4 \cdot 7H_2O$ (6.95 mg), butylated hydroxytoluene (92.14 mg) and 25 mM H_2SO_4 in a methanol : water (9:1 v/v) solution. The reagent was kept refrigerated until used. H_2O_2 solutions (0-100 μM) were prepared in ddH_2O using MES buffer (90 mM) to maintain pH 6. For the calibration curve, an aliquot of 100 μL of H_2O_2 solution was mixed with 500 μL of the FOX reagent and allowed to stand at room temperature for 30 min. After this time the absorbance of each sample was measured from 540-600 nm using a Shimadzu UV-3101 PC spectrophotometer. The calibration curves for A_{593} vs. [H_2O_2] (μM) and A_{560} vs. [H_2O_2] (μM) were fit with a best-fit line. Determination of a calibration curve at 560 nm

was necessary to calculate the H_2O_2 concentration of PEG-TMS exposed to light at 80°C, since this sample turned magenta (λ_{max} = 560 nm) instead of the blue/purple color observed for the other samples (λ_{max} = 593 nm). Averages and standard deviations were determined from triplicate trials with the exception of the DNA base damage experiments.

H_2O_2 formation from PEG and PEG-TMS

PEG (250 mg) and PEG-TMS (250 mg) were dissolved in ddH_2O and maintained at pH 6 using MES buffer (90 mM) to a final volume of 4 mL in iron-free glass vials. Samples of each compound were tested for formation of H_2O_2 at various temperatures in both the absence and presence of light. Temperatures of 37 °C and 80 °C were maintained using water baths covered with plastic wrap to ensure light permeability. For experiments conducted in the dark, vials for each sample were covered with foil to ensure the absence of light. Aliquots (100 μL) of each sample were taken every 24 h for 8 days and mixed with FOX reagent (500 μL) in 1.5 mL acid-washed microcentrifuge tubes. Upon standing at room temperature for 30 min, the absorbance of each sample was measured from 540-600 nm using a Shimadzu UV-3101 PC spectrophotometer.[67,72,73] The H_2O_2 concentration for samples that turned blue/purple upon addition of the FOX reagent was calculated from the H_2O_2 calibration curve at 593 nm. The H_2O_2 concentration for PEG-TMS exposed to light at 80 °C was calculated from the calibration curve at 560 nm since it turned magenta upon addition of the FOX reagent.

Iron calibration curve from ICP-MS measurements

$[Fe(EDTA)]^{2-}$ solutions (10 mL, 50 μM-500 μM) were prepared and maintained at pH 6 using MES buffer (90 mM). Iron intensity of each sample was measured using inductively coupled plasma optical emission spectroscopy (ICP-OES, JY Horiba Ultima 2, Longjumeau, France) and a calibration curve was then obtained by fitting a best fin line through the experimental data.

Preparation of silica and PEGylated silica beads

The surface of 0.30 μm silica microspheres (beads) was prepared by addition of 1 M HCl with agitation, centrifugation at 13,500 rpm, washing with deionized water. The PEG-silane encapsulation of silica microspheres was performed as follows: 1 mL of a 10% aqueous dispersion of silica microspheres was added to a 4:1 mixture of methanol and ammonium hydroxide (28 wt % ammonia). After mixing for 5 min, PEG-TMS (200 μL) was added to yield a total volume of 11.2 mL and stirred overnight at room temperature. The resulting suspension was then centrifuged and washed with deionized water. Both silica and PEGylated beads were prepared and obtained from the McNeill group.

Iron association with silica and PEGylated beads

Various volumes (0, 50, 100, and 200 μL) of $FeSO_4 \cdot 7H_2O$ (50 μM) maintained at pH 6 with MES buffer (90 mM) was added to silica beads (50 μL), vortex mixed for 2

min, and centrifuged for 5 min at 13,000 rpm. The supernatant was discarded and the procedure was repeated. EDTA solution (500 μL of 400 μM) maintained at pH 6 with MES buffer (90 mM) was then added to the beads and centrifuged as above. The supernatant was saved and the procedure repeated to obtain a total wash volume of 1 mL. Iron content of this solution was then measured using ICP-MS, and the iron concentration was determined from the iron calibration curve. A similar procedure was performed to determine the concentration of iron associated with silica beads using PEG-functionalized beads instead of the silica beads.

Tabular data for gel electrophoresis experiments

Tabulated values for the percentages of closed, circular (undamaged) and nicked DNA (damaged) bands observed in the DNA backbone and base damage gel electrophoresis experiments are given in Tables 4.1 and 4.2. Tabulated values for DNA backbone damage are the average of three experimental trials with the indicated calculated standard deviation and p-value. Tabulated values for iron association with silica beads and PEG-TMS are given in Tables 4.3 and 4.4. Tabulated values for the iron association experiments are from one trial with the indicated standard deviation calculated from the error obtained from the $[Fe(EDTA)]^{2-}$ calibration curve.

Table 4.1. Tabulation for electrophoresis results for DNA backbone damage upon irradiation of TPP-doped CP dot nanoparticles.

Lane	Content	% Circular DNA	% Nicked DNA	p-value
2	plasmid DNA (p)	96.7 ± 0.2	3.3	-
3	p + H_2O_2	93.5 ± 2.5	6.5	-
4	p + H_2O_2 + Fe^{2+}	2.5 ± 2.3	97.5	-
5	p + CP dot (irr for 0 min)	97.5 ± 0.09	2.5	<0.0001
6	p + CP dot (irr for 50 min)	99.9 ± 0.08	0.1	<0.0001
7	p + CP dot (irr for 100 min)	50.0 ± 0.5	50.0	<0.0001
8	p + CP dot (irr for 200 min)	31.0 ± 0.5	69.0	<0.0001

Table 4.2. Tabulation for electrophoresis results for DNA base damage upon irradiation of TPP-doped CP dot nanoparticles.

Lane	Content	% Circular DNA	% Nicked DNA
2	plasmid (p) + Fpg	96.0	4.0
3	p + Fpg + CP dot (irr for 0 min)	99.3	0.7
4	p + Fpg + CP dot (irr for 50 min)	98.0	2.0
5	p + Fpg + CP dot (irr for 100 min)	47.0	53
6	p + Fpg + CP dot (irr for 200 min)	28.0	72

Table 4.3. Tabulation for iron concentration associated to silica beads as determined from the $[Fe(EDTA)]^{2-}$ calibration curve.

Volume of 50 μM Fe^{2+} used (μL)	Concentration of Fe^{2+} associated to beads (μM)	p-value
50	1.17 ± 0.03	0.0002
100	1.24 ±0.03	0.0002
200	1.12 ± 0.03	0.0002

Table 4.4. Tabulation for iron concentration associated to PEG-TMS as determined from the $[Fe(EDTA)]^{2-}$ calibration curve.

Volume of 50 μM Fe^{2+} used (μL)	Concentration of Fe^{2+} associated to PEG-TMS (μM)	p-value
50	2.16 ± 0.22	0.003
100	2.70 ±0.19	0.002
200	5.00 ± 0.60	0.005

References

(1) Dolmans, D. E.; Fukumura, D.; Jain, R. K. *Nat. Rev. Cancer* **2003**, *3*, 380-387.

(2) Dougherty, T. J.; Gomer, C. J.; Henderson, B. W.; Jori, G.; Kessel, D.; Korbelik, M.; Moan, J.; Peng, Q. *J. Natl. Cancer Inst.* **1998**, *90*, 889-905.

(3) Wang, S.; Gao, R.; Zhou, F.; Selke, M. *J. Mater. Chem.* **2004**, *14*, 487-493.

(4) Pass, H. I. *J. Natl. Cancer Inst.* **1993**, *85*, 443-456.

(5) Henderson, B. W.; Dougherty, T. J. *Photochem. Photobiol.* **1992**, *55*, 145-157.

(6) Wilkinson, F. H., W. P.; Ross, A. B. *J. Phys. Chem. Ref. Data* **1993**, *22*, 113-262.

(7) Davies, M. J. *Biochem. Biophys. Res. Commun.* **2003**, *305*, 761-770.

(8) Schweitzer, C.; Schmidt, R. *Chem. Rev.* **2003**, *103*, 1685-1757.

(9) Arnbjerg, J.; Johnsen, M.; Nielsen, C. B.; Jorgensen, M.; Ogilby, P. R. *J. Phys. Chem. A* **2007**, *111*, 4573-4583.

(10) Devasagayam, T. P.; Steenken, S.; Obendorf, M. S.; Schulz, W. A.; Sies, H. *Biochemistry* **1991**, *30*, 6283-6289.

(11) Ravanat, J.-L.; Saint-Pierre, C.; Di Mascio, P.; Martinez, G. R.; Medeiros, M. H. G.; Cadet, J. *Helv. Chim. Acta.* **2001**, *84*, 3702-3709.

(12) Floyd, R. A.; Schneider, J. E.; Watson, J. J.; Maildt, M. L. *Free Radic. Biol. Med.* **1990**, *9*, 76-83.

(13) Ravanat, J.-L.; Cadet, J. *Chem. Res. Toxicol.* **1995**, *8*, 379-388.

(14) Lutgerink, J. T.; van den Akker, E.; Smeets, I.; Pachen, D.; van Dijk, P.; Aubry, J. M.; Joenje, H.; Lafleur, M. V.; Retel, J. *Mutat. Res.* **1992**, *275*, 377-386.

(15) Scurlock, R. D.; Wang, B.; Ogilby, P. R. *J. Am. Chem. Soc.* **1996**, *118*, 388-392.

(16) Epe, B. *Chem. Biol. Interact.* **1992**, *80*, 239-260.

(17) Piette, J. *Photochem. Photobiol. B* **1990**, *4*, 335-339.

(18) Ravanat, J.-L.; Di Mascio, P.; Martinez, G. R.; Medeiros, M. H. G.; Cadet, J. *J. Biol. Chem.* **2000**, *275*, 40601-40604.

(19) Boiteux, S. *J. Photochem. Photobiol. B* **1993**, *19*, 87-96.

(20) Melvin, T.; Cummiffe, S. M. T.; O'Neill, P.; Parker, A. W.; Roldan-Arjona, T. *Nucl. Acids Res.* **1998**, *26*, 4935-4942.

(21) Michaeli, A.; Feitelson, J. *Photochem. Photobiol.* **1997**, *65*, 309-315.

(22) Cadet, J.; Berger, M.; Douki, T.; Morin, B.; Raoul, S.; Ravanat, J. L.; Spinelli, S. *Biol. Chem.* **1997**, *378*, 1275-1286.

(23) Moan, J.; Berg, K. *Photochem. Photobiol.* **1991**, *53*, 549-553.

(24) Peng, Q.; Moan, J.; Nesland, J. M. *Ultrastruct. Pathol.* **1996**, *20*, 109-129.

(25) Redmond, R. W.; Gamlin, J. N. *Photochem. Photobiol.* **1999**, *70*, 391-475.

(26) Gao, R.; Ho, D. G.; Hernandez, B.; Selke, M.; Murphy, D.; Djurovich, P. I.; Thompson, M. E. *J. Am. Chem. Soc.* **2002**, *124*, 14828-14829.

(27) Kessel, D.; Luo, Y. *J. Photochem. Photobiol. B* **1998**, *42*, 89-95.

(28) Kessel, D.; Woodburn, K.; Gomer, C. J.; Jagerovic, N.; Smith, K. M. *J. Photochem. Photobiol. B* **1995**, *28*, 13-18.

(29) Kessel, D.; Woodburn, K.; Henderson, B. W.; Chang, C. K. *Photochem. Photobiol.* **1995**, *62*, 875-881.

(30) Gao, D.; Xu, H.; Philbert, M. A.; Kopelman, R. *Angew. Chem. Int. Ed. Engl.* **2007**, *46*, 2224-2227.

(31) Chen, C. Y.; Tian, Y.; Cheng, Y. J.; Young, A. C.; Ka, J. W.; Jen, A. K. *J. Am. Chem. Soc.* **2007**, *129*, 7220-7221.

(32) Roy, I.; Ohulchanskyy, T. Y.; Pudavar, H. E.; Bergey, E. J.; Oseroff, A. R.; Morgan, J.; Dougherty, T. J.; Prasad, P. N. *J. Am. Chem. Soc.* **2003**, *125*, 7860-7865.

(33) Kim, S.; Ohulchanskyy, T. Y.; Pudavar, H. E.; Pandey, R. K.; Prasad, P. N. *J. Am. Chem. Soc.* **2007**, *129*, 2669-2675.

(34) McCarthy, J. R.; Perez, J. M.; Bruckner, C.; Weissleder, R. *Nano Lett.* **2005**, *5*, 2552-2556.

(35) Samia, A. C. S.; Chen, X. B.; Burda, C. *J. Am. Chem. Soc.* **2003**, *125*, 15736-15737.

(36) Gao, D.; Agayan, R. R.; Xu, H.; Philbert, M. A.; Kopelman, R. *Nano Lett.* **2006**, *6*, 2383-2386.

(37) Grimland, J. L.; Wu, C.; Ramoutar, R. R.; Aristizabal, K.; Brumaghim, J.; McNeill, J. **2009**, in preparation.

(38) DeRosa, M. C.; Crutchley, R. J. *Coord. Chem. Rev.* **2002**, *234*, 351-371.

(39) Zeitouni, N. C.; Oseroff, A. R.; Shieh, S. *Mol. Immunol.* **2003**, *39*, 1133-1136.

(40) Johnson, B. F. G. *Coord. Chem. Rev.* **1999**, *190-192*, 1269-1285.

(41) Fedorovich, R. D.; Naumovets, A. G.; Tomchuk, P. M. *Phys. Rep.* **2000**, *328*, 73-179.

(42) Trinsdale, T. *Chem. Mater.* **2001**, *13*, 3843-3858.

(43) Brigger, I.; Dubernet, C.; Couvreur, P. *Adv. Drug Del. Rev.* **2002**, *54*, 631-651.

(44) Panyam, J.; Labhasetwar, V. *Adv. Drug Deliv. Rev.* **2003**, *55*, 329-347.

(45) Tibbe, A. G.; de Grooth, B. G.; Greve, J.; Liberti, P. A.; Dolan, G. J.; Terstappen, L. W. *Nat. Biotechnol.* **1999**, *17*, 1210-1213.

(46) Wu, C. F.; Peng, H. S.; Jiang, Y. F.; McNeill, J. *J. Phys. Chem. B* **2006**, *110*, 14148-14154.

(47) Szymanski, C. F.; Wu, C.; Hooper, J.; Salazar, M. A.; Perdomo, A.; Dukes, A.; McNeill, J. *J. Phys. Chem. B* **2005**, *109*, 8543-8546.

(48) Ramoutar, R. R.; Brumaghim, J. *Main Group Chem.* **2007**, *6*, 143-153.

(49) Ramoutar, R. R.; Brumaghim, J. L. *J. Inorg. Biochem.* **2007**, *101*, 1028-1035.

(50) Battin, E. E.; Brumaghim, J. *J. Biol. Chem.* **2008**, *102*, 2036-2042.

(51) Perron, N. R.; Brumaghim, J. *Inorg. Chem.* **2008**, *47*, 6153-6161.

(52) Nowack, B.; Bucheli, T. D. *Environ. Pollut.* **2007**, *150*, 5-22.

(53) Carot, C.; Robert, P.; Idee, J.-M.; Port, M. *Adv. Drug Del. Rev.* **2006**, *58*, 1471-1504.

(54) Kumar, V.; Kalonia, D. S. *AAPS Pharm. Sci. Tech.* **2006**, *7*, E1-E7.

(55) Ha, E.; Wang, W.; Wang, Y. J. *J. Pharm. Sci.* **2002**, *91*, 2252-2264.

(56) Joo, H.; Yoo, Y. J.; Ryu, D. Y. *Enzyme Microb. Technol.* **1996**, *19*, 50-56.

(57) Mello-Filho, A. C.; Meneghini, R. *Mutat. Res.* **1991**, *251*, 109-113.

(58) Imlay, J. A.; Linn, S. *Science* **1988**, *240*, 1302-1309.

(59) Imlay, J. A.; Chin, S. M.; Linn, S. *Science* **1988**, *240*, 640-642.

(60) Henle, E. S.; Linn, S. *J. Biol. Chem.* **1997**, *272*, 19095-19098.

(61) Yamakoshi, Y.; Umezawa, N.; Ryu, A.; Arakane, K.; Miyata, N.; Goda, Y.; Masumizu, T.; Nagano, T. *J. Am. Chem. Soc.* **2003**, *125*, 12803-12809.

(62) Halliwell, B. *Drugs and Aging* **2001**, *18*, 685-716.

(63) Hoffmann, M. E.; Mello-Filho, A. C.; Meneghini, R. *Biochem. Biophys. Acta* **1984**, 234-238.

(64) Singal, P. K.; Khaper, N.; Palace, V.; Kumar, D., 40, 426-32. *Cardiovasc. Res.* **1998**, *40*, 426-432.

(65) Stewart, M. S.; Spallholz, J. E.; Neldner, K. H.; Pence, B. C. *Free Radic. Biol. Med.* **1999**, *26*, 42-48.

(66) Wu, C.; Szymanski, C.; Cain, Z.; McNeill, J. *J. Am. Chem. Soc.* **2007**, 12904-12905.

(67) Cho, Y. S.; Kim, H. S.; Kim, C. H.; Cheon, H. G. *Anal. Biochem.* **2006**, *351*, 62-68.

(68) Henle, E. S.; Zhengxu, H.; Tang, N.; Rai, P.; Luo, Y.; Linn, S. *J. Biol. Chem.* **1999**, *274*, 962-971.

(69) Dizdaroglu, M.; Laval, J.; Boiteux, S. *Biochemistry* **1993**, *32*, 12105-12111.

(70) Hatahet, Z.; Kow, Y. W.; Purmal, A. A.; Cunningham, R. P.; Wallace, S. S. *J. Biol. Chem.* **1994**, *269*, 18814-18820.

(71) Hazra, T. K.; Izumi, T.; Maidt, L.; Floyd, R. A.; Mitra, S. *Nucleic Acids Res.* **1998**, *26*, 5116-5122.

(72) DeLong, J. M.; Prange, R. K.; Hodges, D. M.; Forney, C. F.; Bishop, M. C.; Quilliam, M. *J. Agric. Food Chem.* **2002**, *50*, 248-254.

(73) Jansson, P. J.; Lindqvist, C.; Nordstrom, T. *Free Radic. Res.* **2005**, *39*, 1233-1239.

(74) Wasylaschuk, W.; Harmon, P. A.; Wagner, G.; Harman, A. B.; Templeton, A. C.; Xu, H.; Reed, R. A. *J. Pharma. Sci.* **2007**, *96*, 106-116.

(75) Donbrow, M.; Azaz, E.; Pillersdorf, A. *J. Pharm. Sci.* **1978**, *67*, 1676-1681.

(76) McGinity, J. W.; Patel, T. R.; Naqvi, A. H.; Hill, J. A. *Drug Dev. Commun.* **1976**, *2*, 505-519.

(77) Woodmansee, A. N.; Imlay, J. A. *Methods Enzymol.* **2002**, *349*, 3-9.

(78) Tchou, J.; Bodepudi, V.; Shibutani, S.; Antoshechkin, I.; Miller, J.; Grollman, A. P.; Johnson, F. *J. Biol. Chem.* **1994**, *269*, 15318-15324.

CHAPTER FIVE

INTERACTIONS OF CAFFEINE WITH POLYPHENOLS AND THE ABILITY OF PEACH ANTHOCYNANINS TO PREVENT OXIDATIVE DNA DAMAGE

Introduction

Reactive oxygen species (ROS) such as the hydroxyl radical ($^{\bullet}OH$) and hydrogen peroxide (H_2O_2) are the main cause of cellular oxidative stress, damaging DNA, lipids, and proteins.[1,2] Iron-generated hydroxyl radical is the main source of cell death in both prokaryotes and eukaryotes, including humans.[3-5] DNA-damaging $^{\bullet}OH$ is produced via the Fenton reaction when H_2O_2 generated from cellular respiration oxidizes Fe^{2+} to Fe^{3+} (Reaction 1).

$$Fe^{2+} + H_2O_2 \rightarrow Fe^{3+} + OH^- + {}^{\bullet}OH \qquad (1)$$

The production of $^{\bullet}OH$ becomes catalytic *in vivo* when Fe^{3+} is reduced back to Fe^{2+} by cellular reductants such as reduced nicotinamide adenine dinucleotide (NADH).[6] Oxidative DNA damage results in cellular mutations and death, causing several conditions including aging,[7] cancer,[8] Alzheimer's and Parkinson diseases,[9] and arteriosclerosis.[10,11] Therefore, prevention of DNA damage is important for both the treatment and prevention of these diseases, and antioxidants have been widely studied for such uses.

Polyphenols are compounds found in a variety of foods and beverages such as fruits, vegetables, tea, coffee, chocolates, and red wine.[12-15] These compounds have been widely studied for their antioxidant properties, and people have an average total dietary

intake of ~1 g/d, a value about 10 times higher than other commonly studied antioxidants such as vitamin C.[12-17] Due to their antioxidant properties, polyphenols have several other health benefits, such as the prevention of cardiovascular diseases, osteoporosis, cancer, and neurodegenerative diseases.[18]

Polyphenols constitute a diverse group of compounds categorized into several classes, including anthocyanins, catechins, flavonoids, flavones, and flavanones.[18,19] Of the many classes, flavonoids and catechins have been widely studied for their antioxidant properties. Catechins are an abundant group of polyphenols primarily found in green tea.[19] Green tea consumption is most popular in Asian diet and has been associated with many biological activities, including induction of cell cycle arrest and apoptosis, alteration of cell signaling, inhibition of proliferation and angiogenesis, and more recently, weight loss.[20-22]

Major green tea catechins include epicatechin (EC), epigallocatechin (EGC), and epigallocatechin gallate (EGCG). EGCG (Figure 6.1) is the major antioxidant polyphenol in green tea and constitutes 40% of the total catechin content.[20] The antioxidant ability of EGCG has been attributed to its radical scavenging and iron chelating abilities.[20,23] Because polyphenols are such an integral part of the human diet, it is important to understand their biological functions and antioxidant activity. Gel electrophoresis experiments used to investigate the ability of polyphenols to inhibit DNA damage from the Fenton reaction show that EGCG is a potent antioxidant with an IC_{50} (inhibitory concentration, the polyphenol concentration required to inhibit 50% DNA damage) of 1.1

± 0.01 μM, comparable to physiological plasma concentrations (~1 μM) after one cup of green tea.[18,24,25]

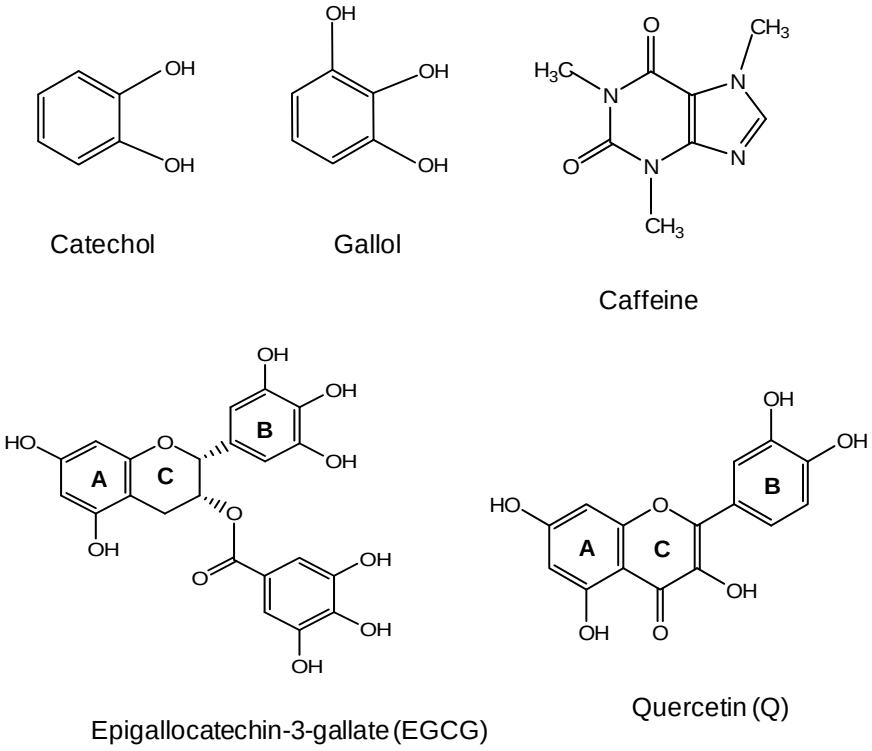

Figure 5.1. Structures of gallol, catechol, quercetin (Q), and compounds found in green tea: caffeine and epigallocatechin gallate (EGCG).

Flavonoids are ubiquitous to plants and are found in high quantities in fruits, vegetables, olive oil, red wine, and chocolate.[19,26] The main flavonoid found in the average Western diet is quercetin (Q, Figure 6.1), and humans have an average dietary intake of 16 mg/d.[26,27] Quercetin inhibits lipid peroxidation in the retina, oxidative stress in cutaneous tissue-associated cell types, and hydrogen peroxide-induced cell death.[28] Quercetin is also an effective antioxidant, inhibiting iron-mediated DNA damage with an IC_{50} of 10.4 ± 0.2 μM.[18,25] Experiments performed by Sestili *et al*. show that quercetin

prevents cell death from *t*-butyl hydroperoxide (*t*B-OOH) with an IC_{50} of 12.7 ± 0.9 μM, and reduces nuclear DNA single strand breaks with an IC_{50} of 2.7 ± 0.3 μM.[28]

In addition to polyphenols, caffeine (1,3,7-trimethylxanthine; Figure 6.1) is another major component of green tea, coffee, and chocolate.[29-31] The caffeine content in green tea is approximately 2-4%, whereas the polyphenol content is typically 10-30%.[32] Pharmacokinetic studies performed in adults indicate that caffeine is rapidly absorbed and eliminated from the body with a half life of 5-6 h.[29,33,34] Serum levels of caffeine are between 39-46 μM 1-2 h after consumption of 300 mg caffeine (5 mg/kg adult body weight).[29,35,36] In the US, the average daily caffeine intake from coffee by adults is estimated to be 2.4 mg/kg body weight and 5.3 mg/kg for heavier consumers, indicating that serum levels of caffeine rarely exceed 50 μM.[29,37]

Caffeine is widely studied for its physiological effects on human health, mainly focusing on behavior or mood. It is also a diuretic and weak bronchodilator, and more recently, high intakes of caffeine (> 300 mg/d) have been associated with low birth weight and miscarriage in pregnant women.[38] Caffeine also protects against mouse skin carcinogenesis induced by chemical agents in cigarette smoke, as well as glandular stomach carcinogenesis from lipid peroxidation.[29,39,40] While the mechanism of this anticarcinogenic effect of caffeine is uncertain, much interest lies in its role as a possible antioxidant.

Studies have shown that caffeine scavenges iron-generated hydroxyl radical, and also inhibits lipid peroxidation of rat liver microsomes in small doses.[29,41,42] The ability of caffeine to scavenge iron-generated hydroxyl radical was measured using electron

paramagnetic resonance (EPR) and found to be concentration dependent, with optimal scavenging at 0.16 M and no activity at concentrations less than 0.02 M.[29,41,42] These caffeine concentrations are much higher than physiological serum concentrations, and experiments performed on caffeine by the oxygen-radical absorbance capacity (ORAC) assay indicate that at physiologically relevant concentrations (40 μM), this compound has no antioxidant activity.[29] Experiments with low density lipoprotein (LDL) lipid oxidation also indicated that caffeine did not protect LDLs from peroxidation at physiological concentrations. However, caffeine metabolites, 1-methylxanthine and 1-methyluric acid, were found to have high antioxidant abilities and were able to prevent LDL oxidation at biologically relevant concentrations (40 μM).[29]

Interestingly, polyphenols found in black tea and coffee can form π–stacked complexes with caffeine.[43-47] The proposed B ring binding site (Figure 6.1) and the affinity of catechins for caffeine binding were based on the ^{1}H-NMR chemical shifts of the protons from gallol or catechol groups upon titrations with caffeine.[43,48] Based on these ^{1}H-NMR titrations, Hayashi *et al.* showed that EGCG, which contains two gallol substituents, forms more stable complexes with caffeine than catechins without gallol groups, and has a binding constant with caffeine of 90 ± 2% M^{-1}.[43] Complexation of polyphenols with caffeine is an interesting phenomenon, and very little has been done to investigate the biological activities of such π-stacking interactions. Both polyphenol compounds and caffeine are antioxidants individually, but it is not known how this π-stacking behavior would affect this antioxidant activity in combination.

In addition to the ability of catechin polyphenols to interact with caffeine, studies have shown that the complex formed between quercetin and transition metals such as Cu^{2+} can bind DNA via intercalation.[49] Several studies indicate that the catechol functionalization of the B ring of quercetin (Figure 6.1) is important for Cu^{2+} chelation.[49-53] A separate study showed a weak interaction between quercetin and DNA, and DNA damage occurring upon addition of Cu^{2+} to quercetin-DNA solutions.[54] Spectrophometric and electrochemical experiments indicate that this pro-oxidant effect of quercetin is caused by the intercalation of the quercetin-Cu^{2+} complex into DNA, resulting in DNA strand breakage.[49] This pro-oxidant behavior is consistent with additional investigations where flavonoids were found to damage DNA and induce mutagenesis in the presence of transition metals. In the latter case, reduction of transition metals by flavonoids resulted in the formation of the DNA-damaging hydroxyl radical.[49,55-58]

In this chapter, the effects of caffeine on the antioxidant activity of EGCG and quercetin are investigated using DNA gel electrophoresis. In addition, the ability of polyphenol compounds in various peach cultivars with different antioxidant contents is investigated for their ability to prevent iron-mediated DNA damage.

Results and Discussion

Iron-mediated DNA damage inhibition by caffeine, epigallocatechin-3-gallate (EGCG), and quercetin (Q)

The antioxidant activities of EGCG and quercetin have been previously studied via gel electrophoresis for their ability to prevent iron-mediated oxidative DNA damage.[18] EGCG was found to be a more potent antioxidant than quercetin with IC_{50} values of 1.1 ± 0.01 μM and 10.4 ± 0.2 μM, respectively.[18,25]

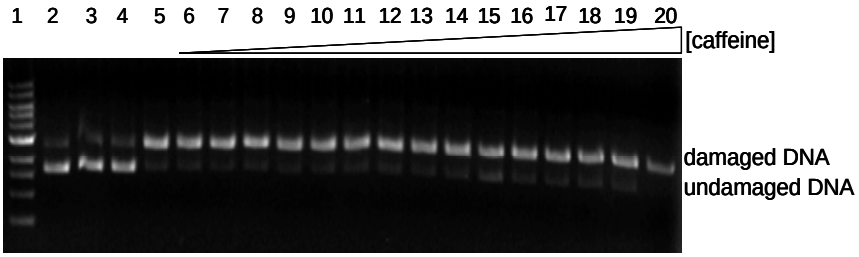

Figure 5.2. Gel electrophoresis image of caffeine under Fenton reaction conditions. Lane 1: 1 kb ladder, lane 2: plasmid only (p), lane 3: p + H_2O_2 (50 μM), lane 4: p + H_2O_2 (50 μM) + caffeine (500 μM), lane 5: p + H_2O_2 (50 μM) + Fe^{2+} (2 μM), lanes 6-20: lane 5 + increasing concentrations of caffeine (0.0005, 0.001, 0.01, 0.02, 0.05, 0.2, 2, 4, 10, 50, 100, 200, 300, 400 and 500 μM, respectively).

Similar DNA damage experiments were performed with caffeine alone. The gel in Figure 5.2 shows that Fe^{2+}/H_2O_2 (lane 5) damages a high percentage of DNA (~93%), and caffeine (lanes 6-20) has no significant antioxidant activity against iron-mediated oxidative DNA damage at concentrations up to 500 μM. Because studies have shown that polyphenols such as catechins form π-stacked complexes with caffeine, similar gel electrophoresis experiments were also performed with EGCG or Q and caffeine to determine the effects of caffeine on the antioxidant activity of EGCG and Q.

In the NMR study by Hayashi *et al.*, the stoichiometric ratio for polyphenol compounds π-stacking with caffeine was determined to be 1:1.[43] Therefore, in the gel experiments performed, the concentration of caffeine in each lane was equal to the concentration of EGCG. Also, since iron precipitates at pH > 6.5, MES buffer (10 mM) was added in each lane to maintain pH 6. Figure 6.3 is a gel showing both undamaged (circular) and damaged (nicked) DNA at various concentrations of EGCG/caffeine (0.0005-100 μM). Without iron, EGCG/caffeine and hydrogen peroxide have no effect on DNA damage (lane 4). Increasing concentrations of EGCG and caffeine in the presence of Fe^{2+}/H_2O_2 (lanes 6-16) showed an increase in undamaged DNA, with 64% DNA damage inhibition at 2 μM (Figure 6.3, lane 12). At the highest EGCG/caffeine concentration tested (100 μM), 100% DNA damage was inhibited (Figure 6.3, lane 16).

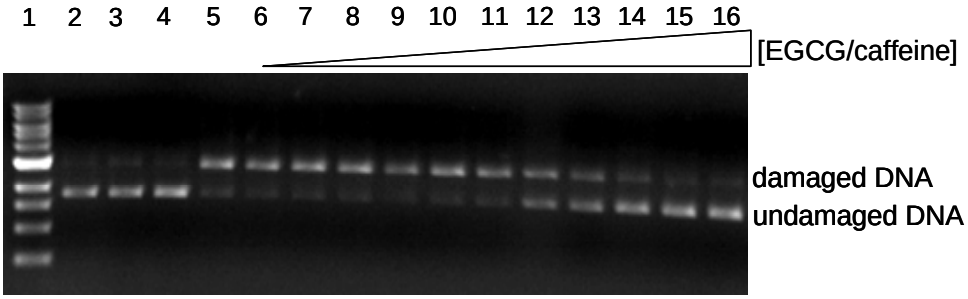

Figure 5.3. Gel electrophoresis image of (-)-epigallocatechin-3-gallate (EGCG) and caffeine under Fenton reaction conditions. Lane 1: 1 kb ladder, lane 2: plasmid only (p), lane 3: p + H_2O_2 (50 μM), lane 4: p + H_2O_2 (50 μM) + EGCG/caffeine (500 μM), lane 5: p + H_2O_2 (50 μM) + Fe^{2+} (2 μM), lanes 6-16: lane 5 + increasing concentrations of EGCG and caffeine (0.0005, 0.001, 0.01, 0.02, 0.05, 0.2, 2, 4, 10, 50, 100 μM, respectively).

A graph of the percent inhibition of DNA damage as a function of EGCG/caffeine concentration is shown in Figure 5.4. From the best-fit sigmoidal dose response curve,

the IC_{50} value (the concentration of polyphenol necessary for inhibition of 50% of the DNA damage produced by $^{\bullet}OH$) was obtained. The IC_{50} for EGCG/caffeine was 1.2 ± 0.2 μM (p = 0.01, Hillslope = 1.3), which is comparable to the IC_{50} for EGCG inhibition of DNA damage alone (1.1 ± 0.01 μM) and that of physiological plasma concentrations (~1 μM after one cup of green tea).[24] Thus, addition of one equivalent caffeine to EGCG has no significant effect (p = 0.48) on antioxidant activity compared to EGCG alone.

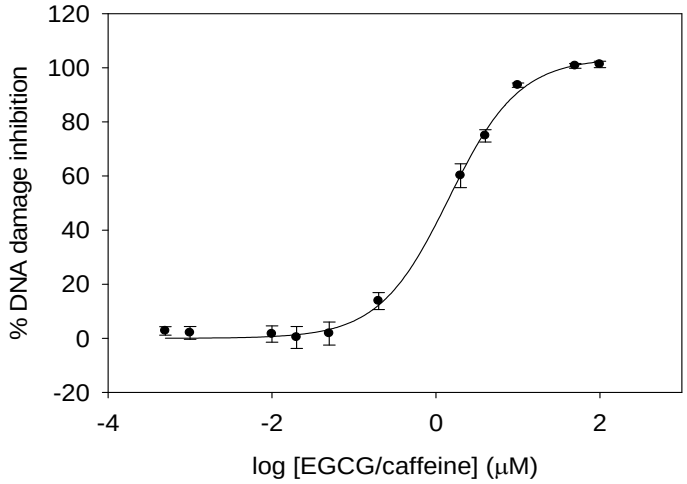

Figure 5.4. Percent DNA damage inhibition graph of a 1:1 ratio of (-)-epigallocatechin-3-gallate (EGCG) and caffeine under Fenton reaction conditions (2 μM Fe^{2+} + 50 μM H_2O_2). Standard deviations were calculated from three separate trials at the concentrations shown. The best-fit sigmoidal dose-response curve (black line) was used to determine the IC_{50} value.

Because quercetin also π stacks with caffeine, similar experiments were performed with a 1:1 ratio of quercetin and caffeine. Quantification of the gel band intensities shows that Q/caffeine does inhibit iron-mediated DNA damage (Figure 5.5). The highest concentration tested (500 μM) prevented 100% of damaged DNA. Figure 5.6 shows the best-fit sigmoidal dose-response curve, IC_{50} for Q/caffeine was determined to

be 72 ± 15 μM ($p < 0.02$, Hillslope = 1.39), a concentration much greater than that found for Q alone (IC_{50} = 10.4 ± 0.2 μM) under similar conditions ($p = 0.02$).[18,25] Thus, in contrast to caffeine combined with EGCG, caffeine in combination with quercetin significantly lowers the antioxidant activity of quercetin. Caffeine itself does not prevent iron-mediated DNA damage, and addition of this compound in a 1:1 ratio to EGCG has no effect on the antioxidant activity of this polyphenol. In contrast, the combination of Q and caffeine in a 1:1 ratio greatly lowers antioxidant activity compared to Q alone, indicating that π-stacking interactions have different effects on polyphenol antioxidant activity. ^{1}H NMR and Job's plot titration studies show that EGCG (2 mM and 5mM) binds caffeine (500 μM) in a 1:1 ratio, with similar binding constants (89 ± 10% M^{-1} and 90 ± 2% M^{-1}, respectively).[43]

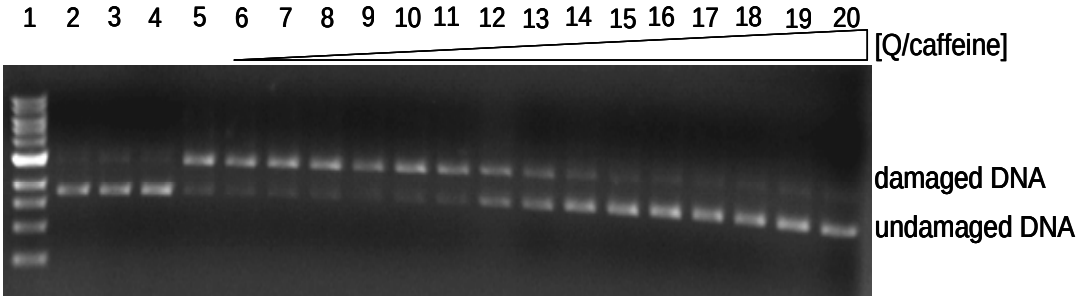

Figure 5.5. Gel electrophoresis image of quercetin (Q) and caffeine under Fenton reaction conditions. Lane 1: 1 kb ladder, lane 2: plasmid only (p), lane 3: p + H_2O_2 (50 μM), lane 4: p + H_2O_2 (50 μM) + Q/caffeine (500 μM), lane 5: p + H_2O_2 (50 μM) + Fe^{2+} (2 μM), lanes 6-20: lane 5 + increasing concentrations of Q and caffeine (0.0005, 0.001, 0.01, 0.02, 0.05, 0.2, 2, 4, 10, 50, 100, 200, 300, 400, and 500 μM, respectively).

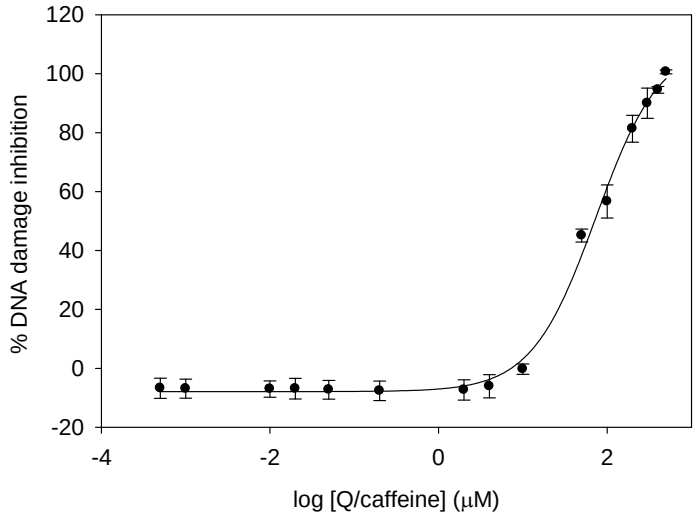

Figure 5.6. Percent DNA damage inhibition graph of a 1:1 ratio of quercetin and caffeine under Fenton reaction conditions (2 μM Fe^{2+} + 50 μM H_2O_2). Standard deviations were calculated from three separate trials at the concentrations shown. The best-fit sigmoidal dose-response curve (black line) was used to determine the IC_{50} value.

Similar results were also observed for other catechins including epicatechin and epigallocatechin; however, estimation of binding constants was difficult due to small changes in the proton chemical shifts resulting in large errors.[43] It should be noted that concentrations used in the NMR studies are significantly higher than those used for our gel electrophoresis experiments with EGCG and caffeine (0.005-100 μM), and there may be less interaction between the two compounds at such low concentrations. However, the decreased antioxidant activity of Q/caffeine (0.005-500 μM) compared to Q alone indicates that significant π-stacking may occur even at the low concentrations used for the DNA damage experiments.

Hayashi *et al*. showed that both the A and B rings of catechins are required for complexation with caffeine,[43] and ECGG contains two gallol substituents, both of which

are B-type rings, while quercetin contains only one catechol group as its B-ring (Figure 5.1). Therefore, one equivalent of caffeine may bind to one gallol ring of EGCG, and the presence of an additional gallol group to bind iron may still permit potent antioxidant activity. In the case of quercetin, once its catechol ring is involved in π-stacking interactions with caffeine, the catechol is unable to bind iron as efficiently and thus its antioxidant function is reduced. To fully understand the different effects of caffeine with EGCG and with Q, gel electrophoresis experiments using a higher caffeine to EGCG ratio (at least 2:1) would be enlightening. Higher ratios of caffeine to EGCG may promote π-stacking to both gallol substituents of EGCG and reduce antioxidant activity.

Since π-acidic polyphenols such as EGCG and Q π-stack with the π-basic caffeine[43,44,47] to yield different effects on antioxidant behavior, other polyphenol/caffeine interactions should be examined for their effects on antioxidant activity. UV-vis and NMR titrations of caffeine with various polyphenol compounds might also be performed to additionally investigate the potential π–stacking interactions and to determine the effects on antioxidant activity of one vs. two B ring gallol- and catechol-containing compounds. In addition, since compounds such as quercetin can intercalate into the DNA bases (also π bases), it is important to investigate the interactions of EGCG, Q, and other polyphenols with the electron-rich DNA bases adenine and guanine to determine the effects of DNA base binding on observed antioxidant activity. Lastly, because both polyphenol compounds and caffeine are found in regularly-consumed foods, it is crucial to fully understand how these combinations affect polyphenol antioxidant potency.

Investigating the antioxidant and phenolic content of peach cultivars

Regular consumption of fruits and vegetables has protective effects against cancer and cardiovascular diseases.[59-62] These health properties are due to the presence of antioxidant compounds in these foods, such as vitamins A, C, and E, and polyphenols.[59,63,64] Therefore, evaluating the phenolic content of fruit and the antioxidant properties of fruit polyphenols is an active area of research.[59,60,65-67] Several studies have reported the phenolic content of various stone fruits such as peaches, nectarines and plums.[59,60,65] Such quantification is difficult, since the phenolic content of fruits varies significantly among cultivars and is affected by several factors including sample size, polyphenol compounds present, and the amount of each cultivar analyzed.[59,60]

Commercial peaches (*Prunus persica* B.) belong to the *Rosaceae* family along with nectarines, plums, cherries, almonds and apricots.[68] The skin (peel) and juicy flesh (mesocarp) color are prominent features for peach cultivars.[68] Commercially, white- and yellow-fleshed peaches are the most popular varieties, and studies have shown that the peel tissue has a higher phenolic content than flesh tissues.[59,69] Polyphenol compounds found in stone fruits can prevent cardiovascular diseases and cancer due to their antioxidant properties.[59,60,67] Besides antioxidant effects, anthocyanins are responsible for the color of peaches, which range from blue to orange and red.[65,69,70] One of the main anthocyanins found in peach skin is cyanidin-3-rutinoside (Figure 5.7).[71] In one study, genotype variations in the composition and antioxidant properties of white and yellow peach cultivars showed a strong correlation between total phenolic content and antioxidant activity at the ripe or "ready-to-eat" stage as measured by scavenging of the

2,2'-diphenyl-1-picrylhydrazyl radical ($DPPH^{\bullet+}$) and the ferric reducing ability plasma (FRAP) methods.[59]

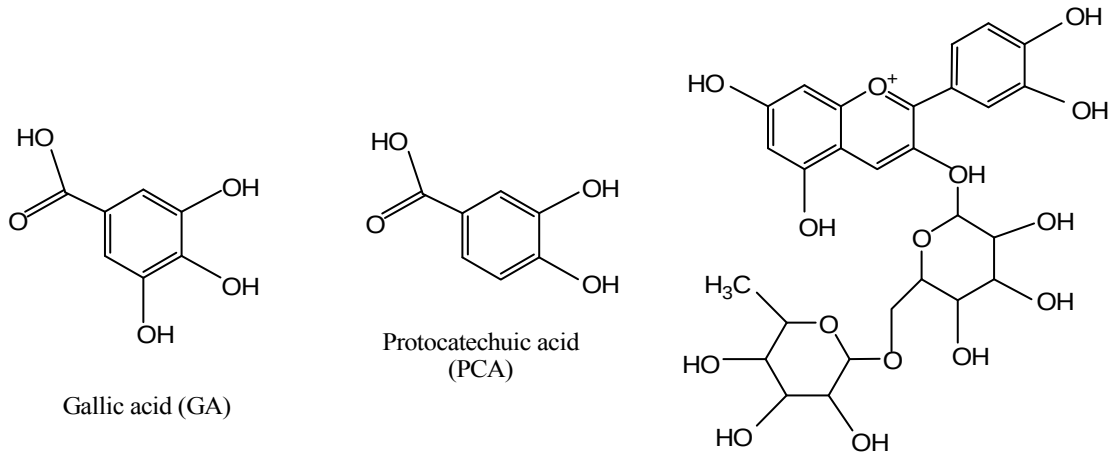

Figure 5.7. Structures of gallic acid (GA), protocatechuic acid (PCA), and the anthocyanin, cyanidin-3-rutinoside.

A study by Cevallos-Casals *et al*. showed that the total anthocyanin content in red-fleshed or blood peaches is approximately ten times higher than that of white or yellow fleshed cultivars.[72] Thus, peaches of the blood-red variety may have greater antioxidant-derived protective effects than the more popular white and yellow cultivars. The ability to genetically alter antioxidant content makes peaches, as well as other fruits, a target for breeding programs focusing on enhancement of phenolic composition and antioxidant activity.[65,72]

The Abbott laboratory at Clemson University has been successful in producing several natural and genetically-modified peach cultivars.[73] The four main varieties of peaches investigated by the Abbott group are Red Globe, Di-haploid Lovell, Sugar Giant

and the genetically-modified cultivar, BY99P4508 (BY). The characteristics of each peach cultivar with respect to the flesh and skin colors are shown in Table 5.1. In light of

Table 5.1. Flesh and skin color, and estimated anthocyanin concentrations of various peach cultivars discussed in this chapter.

Peach cultivar	Flesh color	Skin color	Total dissolved anthocyanin (mg/mL)	Estimated anthocyanin concentration (μM)[a]
Red Globe	Yellow	Red	0.2	~340
Lovell	Yellow	Yellow-green	0.2	~340
Sugar Giant	White	Red	0.2	~340
BY99P1508 (BY)	Blood-red	Blood-red	0.2	~340

[a]estimated anthocyanin concentration was calculated using the molecular mass of cyanidin-3-rutinoside (582 g/mol).

the health benefits and ongoing breeding programs with possible commercial value, it is of great interest to determine and compare the anthocyanin content of these cultivars with their ability to inhibit oxidative DNA damage.

The Brumaghim laboratory has used DNA gel electrophoresis assays to determine and compare the antioxidant activities of polyphenol compounds.[18] In these DNA damage experiments, the generation of the DNA-damaging hydroxyl radical ($^{\bullet}OH$) is produced upon oxidation of Fe^{2+} by hydrogen peroxide (H_2O_2).[6,74] Antioxidant activity of the polyphenol compounds was quantified by measuring the percentage of inhibited DNA damage.[18] In collaboration with the Abbott group, the antioxidant activities of aqueous extracts of the peach cultivars in Table 5.1 were determined via similar DNA damage assays.

Dried peach extracts from Red Globe, Lovell, Sugar Giant, and BY99P4508 (BY) cultivars were obtained from the Abbott lab by methanol extraction, and solid samples (0.75 mg) were prepared by lyophilization. Since the samples were only slightly soluble in distilled water, an estimated concentration of diluted peach extract was determined for each cultivar sample (340 μM) using the molecular weight of the anthocyanin, cyanidin-3-rutinoside (582 g/mol; Table 5.1). Increasing concentrations of each peach extract were used to determine the ability of each peach cultivar to inhibit iron-mediated DNA damage via gel electrophoresis.

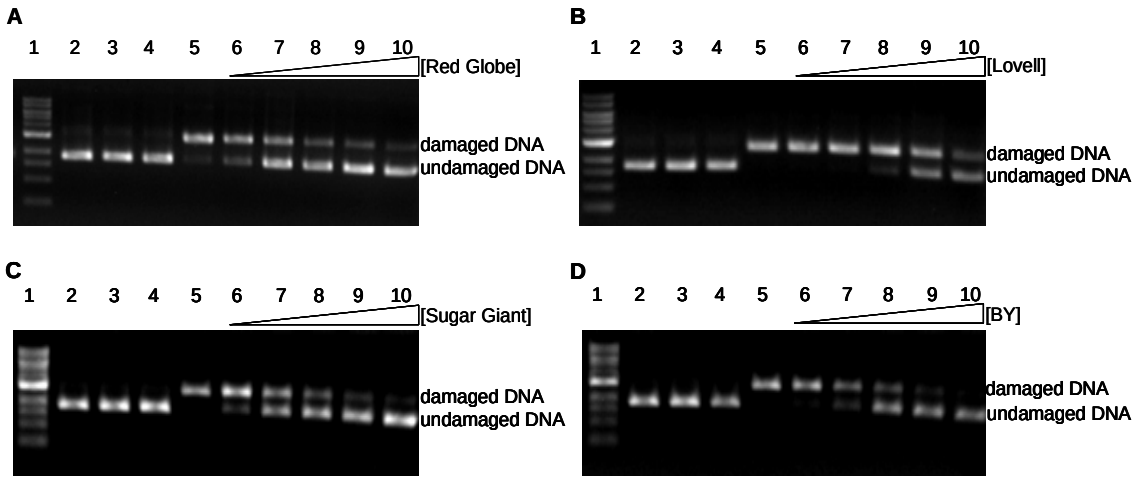

Figure 5.7. DNA gel electrophoresis experiments for peach extracts: (A) Red Globe, (B) Lovell, (C) Sugar Giant, and (D) BY under Fenton reaction conditions at pH 6. For each gel, lanes 1) 1 kb ladder; 2) plasmid (p); 3) p + H_2O_2 (50 μM); 4) p + H_2O_2 (50 μM) + Red Globe, Sugar Giant, BY, or Lovell; 5) p + H_2O_2 (50 μM) + Fe^{2+} (2 μM); and 6-10) 1.7, 3.4, 6.9, 17, and 34 μM of Red Globe, Sugar Giant, or BY extracts, respectively or 6.9, 17, 34, 68, and 170 μM of Lovell extract, respectively.

In these experiments a pH of 6 was maintained, since iron precipitates at pH > 6.5.[18] Figure 5.7 shows DNA gel electrophoresis images at various concentrations for

each peach cultivar tested. The control lanes (Figure 5.7, lanes 2 and 3) indicate that the plasmid is of good quality, and neither H_2O_2 nor the highest concentration of peach extract tested (lanes 4) damages DNA. Addition of Fe^{2+} (2μM) and H_2O_2 (50 μM) produced > 90 % DNA damage (Figure 5.7, lanes 5) as seen from the increase in the band intensities.

In the presence of Fe^{2+}/H_2O_2, Red Globe extract inhibited DNA damage in a concentration-dependent manner as seen by the gradual increase in undamaged DNA from Figure 5.7, lanes 6-10. Quantification of the gel band intensities showed that at the highest concentration tested (~34 μM), this peach extract inhibited 95% DNA damage ($p = < 0.0001$). Similarly, increasing concentrations of Lovell, Sugar Giant, and BY extracts also significantly inhibited DNA damage from Fe^{2+} and hydrogen peroxide. Lovell (~170 μM) extract at the highest concentration prevented 91% ($p = < 0.0001$, Figure 5.7B), Sugar Giant extract (~34 μM) prevented 80% ($p = < 0.0001$; Figure 5.7C), and BY extract (~34 μM) inhibited 99% ($p = < 0.0001$; Figure 5.7D) DNA damage. While all peach samples were found to be effective antioxidants, the genetically-modified extract, BY, prevented the most DNA damage (77%; $p = 0.001$), followed by Red Globe (64%; $p < 0.0001$), Lovell (22%; $p = 0.006$) and Sugar Giant (14%; $p = 0.02$) at ~6.9 μM (Figure 5.8A). These results correlate well with previous radical-scavenging and iron-reduction studies of peach antioxidant activity that found that blood-red peach cultivars had higher antioxidant activities than those with white or yellow mesocarps.[65,72]

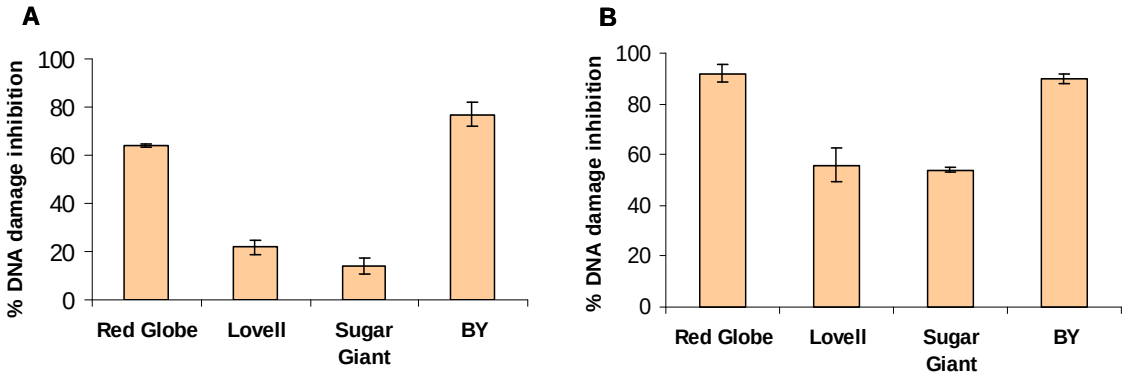

Figure 5.8. Percent DNA damage inhibition of Red Globe, Lovell, Sugar Giant, and BY peach extracts at A) ~6.9 μM and B) ~17 μM.

Interestingly, at higher concentrations of peach extracts (~17 μM), Red Globe (yellow flesh) and BY (red flesh) have similar antioxidant effects, inhibiting 92% ($p = <0.0001$) and 90% ($p = <0.0001$) oxidative DNA damage, respectively (Figure 5.8B). This data suggest that flesh color may not necessarily be a determining factor of peach extract antioxidant activity, especially since Lovell, with yellow flesh color has significantly low antioxidant activity when compared to Red Globe (Figure 5.8) at both ~6.9 μM ($p = 0.002$) and ~17 μM ($p = 0.01$). Although the high antioxidant activity of Red Globe and BY may be attributed to their red skin color, this factor seems unlikely since Sugar Giant, with red skin has significantly little antioxidant activity compared to Red Globe with similar skin color ($p = 0.002$ at ~6.9 μM and $p = <0.0001$ at ~17 μM).

Peach extracts have strong antioxidant activity and significantly prevent iron-mediated DNA damage. As expected, the genetically modified peach extract (BY) has the highest activity inhibiting 99% DNA damage at ~34 μM. This result correlates well with the reports that peach cultivars of the blood-red variety have the highest radical

scavenging ability and iron-reducing abilities when compared to peaches that are yellow or white in color.[72] Studies by Kader *et al*. demonstrate that the antioxidant activity of peaches is due to their phenolic content.[59]

Due to the strong correlation between antioxidant activity, peach flesh color, and anthocyanin content, attempts to determine total phenolic content in peach extracts using the Folin-Ciocalteu method were also undertaken for the four peach extracts. The Folin-Ciocalteu phenol reagent, consisting of a mixture of phosphotungstic and phosphomolybic acids, turns blue upon reduction by phenol compounds as tungsten blue and molybdenum blue are produced.[75] Thus, phenol content can be indirectly measured by UV-vis spectroscopy.[75] Calibration curves of either gallic acid (GA) or protocatechuic acid (PCA) are used as a standard to calculate total phenolic content from food extracts (Figure 5.9).[75,76] Suitable calibration curves may also be obtained by UV-vis measurements of the purple color obtained when Fe^{2+} is oxidized to Fe^{3+} by gallic acid or protocatechuic acid.

It is expected that the total polyphenolic content of the peach extracts (including anthocyanin compounds) could be determined using this method, since the estimated anthocyanin concentrations of the peach extracts are ~340 μM. Unfortunately, absorbances at lower polyphenol concentrations (1-10 μM) are extremely small using the Folin-Ciocalteu method, so this method is unsuitable for determining polyphenol content of solutions containing biologically-relevant phenolic concentrations.

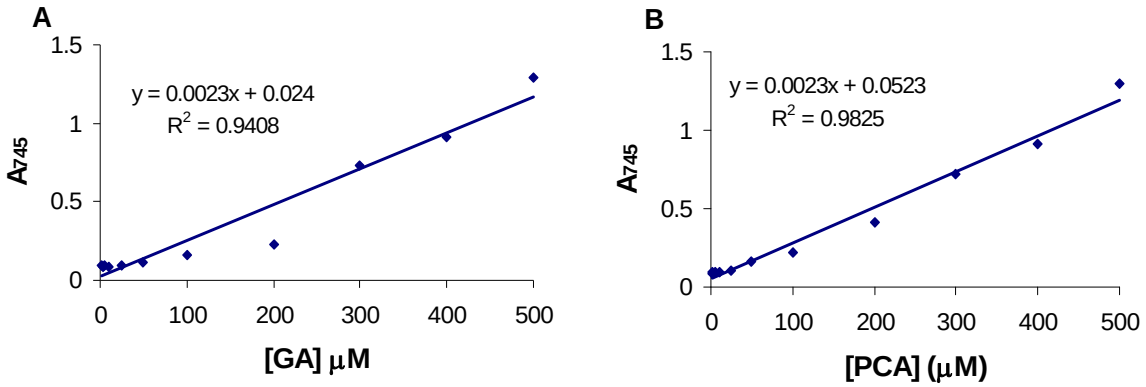

Figure 5.9. Calibration curves for A) gallic acid (GA) and B) protocatechuic acid (PCA) using the Folin-Ciocalteu method. Error bars for both graphs represent standard deviations calculated from the average of three trials. Error bars are smaller than the data points.

The peach extracts studied in this chapter came from the mesocarps (flesh) of these cultivars, and although they have significant antioxidant activity, it would be interesting to compare such activity with extracts obtained from the skin (peel), because the peel tissues of peaches have a higher phenolic content than the flesh tissues.[59] In addition, since peaches are often cooked using different methods, the effects of such cooking methods on the antioxidant content and activity of peach cultivars is also of particular interest .

Conclusions

Gel electrophoresis experiments to determine the ability of polyphenols combined with caffeine to inhibit iron-mediated DNA damage demonstrated that a 1:1 ratio of EGCG/caffeine had greater antioxidant activity (IC_{50} = 1.2 ± 0.2 μM) than a 1:1 ratio of Q/caffeine (IC_{50} = 72 ± 15 μM). Compared to similar experiments performed with

EGCG alone (IC_{50} = 1.1 ± 0.01 μM),[18,25] addition of caffeine has no significant effect on the antioxidant activity of EGCG (p = 0.48). However, the antioxidant activity of quercetin (IC_{50} = 10.4 ± 0.2 μM)[18,25] significantly decreased upon addition of one equivalent of caffeine (p = 0.02).

The addition of caffeine may play a significant role on polyphenol antioxidant activity depending on the specific polyphenol compound tested. Further studies are therefore warranted to determine the effects of caffeine on the antioxidant activity of other polyphenols such as epicatechin, myricetin, and epicatechin-3-gallate. To further examine the biological implications of such activity, the ability of polyphenols (π-acids) to interact with π-bases such as caffeine or the DNA bases adenine and guanine are necessary. These π-stacking interactions can be examined by UV-vis or NMR titrations of these compounds. Results from these experiments will determine the biological implications of polyphenol antioxidant combinations with caffeine, also a common dietary component, on human health.

Experiments performed to determine the antioxidant activity of Red Globe, Lovell, Sugar Giant, and genetically-modified BY peach extracts obtained from the Abbott lab at Clemson showed that all peach samples inhibited iron-mediated DNA damage in a concentration dependent manner. BY peach extract had the highest antioxidant activity followed by Red Globe, Lovell, and Sugar Giant extracts. To better evaluate the antioxidant activity of these peach extracts, their phenolic content must also be determined. Our experiments prove that peach polyphenols prevent oxidative DNA

damage at biological concentrations, and further validates the need for breeding programs that produce genetically-modified peach cultivars to increase their antioxidant activity.

Materials and Method

Materials

Quercetin (Q) and protocatechuic acid (PCA) were purchased from MP Biomedicals, Inc., and (-)-epigallocatechin-3-gallate (EGCG) was from Cayman Chemical Company. $FeSO•7H_2O$, NaCl (99.999%), hydrogen peroxide (30%), caffeine, guanosine, and bromophenol blue were from Alfa Aesar. Glucose, agarose, and ampicillin were from EMD Chemicals. TRIS hydrochloride and Na_2EDTA were from J. T. Baker; ethidium bromide was from Lancaster Synthesis Inc., and HCl was from VWR Scientific. Xylene cyanol, peptone, and yeast extract were purchased from EM Science; MES buffer (99.6%) was from Calbiochem, sodium carbonate and adenine were from Acros. Gallic acid (GA) was from TCI America and Folin-Ciocalteu's phenol reagent came from Fluka Analytical. Use of high purity MES buffer (99.6%) and NaCl (99.999%) were necessary to avoid metal contamination. Water was purified using the NANOpure Diamond water deionization system (Barnstead International. Dubuque, IA). Iron-free microcentrifuge tubes were prepared by washing the tubes in 1 M HCl and triple rinsing with ddH_2O. UV-vis absorption spectra were measured on a Shimadzu UV-3101PC spectrophotometer (Shimadzu Corp., Kyoto, Japan).

Purification of plasmid DNA

DH1 *E. coli* cells were transfected with pBSSK, plated on LB/amp plates, and incubated at 37 ^{o}C for 16 h. Cell cultures were grown in TB/amp medium inoculated with a single colony for 15 h at 37 ^{o}C. Plasmid DNA was purified from cell pellets using a QIAprep Spin Miniprep kit (Qiagen, Chatsworth, CA) with tris-EDTA (TE) buffer was used to elute the DNA. Dialysis of plasmid DNA was performed against 130 mM NaCl (99.999%) for 24 h at 4 ^{o}C. The resulting DNA concentration was found using UV-vis measurements at A_{260} (1 A_{260} = 50 ng/μL). Purity of plasmid DNA was determined via gel electrophoresis of a digested sample, and all absorbance ratios were within acceptable limits ($A_{250/260} < 0.95$, and $A_{260/280} > 1.8$).

Preparation of peach extracts

Red Globe, Di-haploid Lovell, Sugar Giant, and BY99P5508 (BY) peach cultivars were grown at Musser Farm, Clemson University in 2008. Samples (1 g) collected from 3-4 peaches at full maturation were frozen in liquid nitrogen and stored at -80°C. For antioxidant quantification via DNA damage assay, 1 g of each frozen peach flesh cultivar (mesocarp without skin, 1 g) was ground to a fine powder with liquid nitrogen and extracted twice with methanol and HCl (0.01%) at room temperature to a volume of 15 mL. Extract (1 mL) was lyophylized overnight to obtain a solid sample weighing ~0.75 mg. Solid peach samples were weighed and then dissolved in ddH_2O (1 mL). Since the samples were only somewhat soluble in water, the soluble fractions were transferred to another microcentrifuge tube and the remaining solid was weighed. The

two masses measured before and after dissolving the peach extract was subtracted, and an estimated concentration of dissolved polyphenols was determined using the molecular weight for an anthocyanin commonly found in large quantity in peaches, cyanidin-3-rutinoside (582 g/mol).

Inhibition of iron-mediated DNA damage by caffeine, epigallocatechin gallate (EGCG), quercetin (Q), and peach cultivars

The indicated concentrations of caffeine were combined with 0.1 pmol plasmid DNA, 130 mM NaCl, 10 mM ethanol, 2 μM $FeSO_4 \cdot H_2O$, 10 mM MES buffer at pH 6 and allowed to stand for 5 min at room temperature. H_2O_2 (50 μM) was then added and incubated for 30 min. EDTA solution (50 μM) was added after this time. All concentrations are reported as final concentrations, and a total volume of 10 μL was maintained with ddH_2O. DNA was separated on 1% agarose gel via electrophoresis, stained with ethidium bromide for 30 min, and imaged on an UVIproDBT-8000 gel imager (UVITec, Cambridge, UK). Quantification of closed-circular (undamaged) and nicked (damaged) DNA was performed using the UviPro software. Similar experiments were performed for the polyphenols EGCG and Q with caffeine (in a stoichiometric ratio of 1:1), Red Globe, Di-haploid Lovell, Sugar Giant, and BY99P4508 (BY) peach extracts, substituting either EGCG/caffeine, quercetin/caffeine, or the peach extracts for caffeine.

Gel analysis and IC_{50} determination

Percent DNA damage inhibition was determined using the formula 1-[% N / % B]*100, where % N = % nicked DNA in the polyphenol or peach extract containing lanes and % B = % of nicked DNA in the Fe^{2+}/H_2O_2 lane. Percentages are corrected for residual nicking prior to calculation. Results are the average of three trials, and standard deviations are indicated by error bars. Statistical significance was determined by calculation of p values at 95% confidence as described by Perkowski *et al*.[77] Sigma Plot (v.9.01, Sysat Software, Inc., San Jose, CA) was used to plot percent DNA damage inhibition as a function of log concentration of antioxidant compounds and fit to a variable-slope sigmoidal dose response curve using the equation: f = min + (max-min)/ (1 + $10^{(\log EC50 - x)*Hillslope}$). Results are the average of the fits of three trials, and errors are reported as standard deviations calculated by error propagation from gel results.

Calibration curves for GA and PCA via Folin-Ciocalteu method

Solutions of gallic acid and protocatechuic acid (0.001-0.5 mM, 100 μL) prepared in MES buffer (90 mM) to maintain a pH of 6 was combined with Folin-Ciocalteu phenol reagent (1 mL of phenol reagent was first diluted to 3 mL using ddH_2O), and allowed to stand for 5 min at room temperature. After this time, saturated Na_2CO_3 (2 mL, 3.5 M) was added and diluted to 6 mL with ddH_2O. The solution was allowed to stand at room temperature until it turned blue (~5-10 min) and the absorbance was measured via UV-vis at 745 nm. The absorbance of a blank solution, which remained yellow (the color of the phenol reagent) was also obtained using ddH_2O instead of GA or

PCA. The blank absorbance was subtracted from the experimental absorbances and the resulting absorbances at 745 nm were plotted as a function of concentration to obtain calibration curves.

Tabular data for gel electrophoresis experiments

Tabulated values for the percentages of undamaged (closed, circular) and damaged (nicked) DNA bands observed in the gel electrophoresis experiments for Fe^{2+}/H_2O_2 (pH = 6) with caffeine and polyphenols are given in Tables 5.2-5.8. All reported tabulated values are the average of three experimental trials with the indicated standard deviations.

Table 5.2. Tabulation for electrophoresis results for caffeine with Fe^{2+} (2 μM) and H_2O_2 (50 μM) at pH 6.

Lane	Concentration (μM)	% Supercoiled DNA	% Nicked DNA	% Damage Inhibition	p-value
5	0	5.6 ± 2.0	94.4	0	0
6	0.0005	6.6 ± 3.1	93.4	-6.8 ± 3.4	0.07
7	0.001	8.3 ± 0.56	91.7	-6.9 ± 3.2	0.06
8	0.01	5.7 ± 5.2	94.3	-7.0 ± 2.3	0.03
9	0.02	4.2 ± 3.8	95.8	-6.9 ± 3.5	0.08
10	0.05	5.9 ± 1.6	94.1	-7.3 ± 3.2	0.06
11	0.2	6.8 ± 1.6	93.2	-7.6 ± 33	0.06
12	2	6.9 ± 0.87	93.1	-7.3 ± 3.5	0.07
13	4	6.3 ± 1.8	93.7	0.82 ± 2.1	0.57
14	10	5.8 ± 2.9	94.2	0.25 ± 1.6	0.81
15	50	6.7 ± 3.6	93.3	1.2 ± 1.8	0.37
16	100	6.4 ± 1.3	93.6	0.97 ± 3.2	0.65
17	200	8.0 ± 1.7	92	2.9 ± 1.4	0.07
18	300	8.0 ± 3.2	92	2.8 ± 2.2	0.16
19	400	8.1 ± 3.4	91.9	2.9 ± 1.5	0.08
20	500	6.8 ± 6.1	93.2	1.5 ± 8.3	0.78

Table 5.3. Tabulation for electrophoresis results for EGCG and caffeine with Fe^{2+} (2 μM) and H_2O_2 (50 μM) at pH 6.

Lane	Concentration (μM)	% Supercoiled DNA	% Nicked DNA	% Damage Inhibition	p-value
5	0	6.7 ± 2.0	93.3	0	0
6	0.0005	7.9 ± 1.2	92.1	2.1 ± 0.79	0.04
7	0.001	7.4 ± 0.19	92.6	1.6 ± 1.9	0.28
8	0.01	6.7± 0.5	93.3	1.3 ± 2.8	0.51
9	0.02	6.3 ± 0.99	93.7	-0.45 ± 3.2	0.83
10	0.05	9.9 ± 1.9	90.2	1.7 ± 4.2	0.56
11	0.2	32 ± 4.9	68	14 ± 3.2	0.02
12	2	64 ± 5.2	36	57 ± 3.6	0.001
13	4	80 ± 4.2	20	74 ± 2.6	<0.0001
14	10	94 ± 2.6	6.0	93 ± 0.77	<0.0001
15	50	98 ± 1.9	2.0	100 ± 0.05	<0.0001
16	100	99 ± 1.5	1.0	101 ± 0.42	<0.0001

Table 5.4. Tabulation for electrophoresis results for Q and caffeine with Fe^{2+} (2 μM) and H_2O_2 (50 μM) at pH 6.

Lane	Concentration (μM)	% Supercoiled DNA	% Nicked DNA	% Damage Inhibition	p-value
5	0	7.2 ± 3.0	92.8	0	0
6	0.0005	1.0 ± 0.29	99.0	-6.8 ± 3.4	0.07
7	0.001	0.9 ± 0.99	99.1	-6.9 ± 3.2	0.06
8	0.01	0.8 ± 0.84	99.2	-7.0 ± 2.3	0.03
9	0.02	0.9 ± 0.69	99.1	-6.9 ± 3.5	0.08
10	0.05	0.6 ± 0.52	99.4	-7.3 ± 3.2	0.06
11	0.2	0.2 ± 0.12	99.8	-7.6 ± 3.3	0.06
12	2	0.5 ± 0.5	99.5	-7.3 ± 3.5	0.07
13	4	1.7 ± 0.63	98.3	-6.1 ± 3.9	0.11
14	10	6.9 ± 4.6	93.1	-0.31 ± 1.8	0.79
15	50	48 ± 2.4	52	45 ± 2.2	<0.0001
16	100	59 ± 6.7	41	57 ± 5.6	0.003
17	200	81 ± 4.9	19	81 ± 4.9	0.001
18	300	89 ± 2.7	11	90 ± 5.1	0.001
19	400	93 ± 1.1	7.0	95 ± 1.3	<0.0001
20	500	99 ± 1.6	1.0	100 ± 0.69	<0.0001

Table 5.5. Tabulation for electrophoresis results for Red Globe peach extract with Fe^{2+} (2 μM) and H_2O_2 (50 μM) at pH 6.

Lane	Concentration (μM)[a]	% Supercoiled DNA	% Nicked DNA	% Damage Inhibition	p-value
5	0	6.7 ± 9.7	93.3	0	0
6	~1.7	17 ± 2.4	83	11 ± 5.0	0.06
7	~3.4	36 ± 4.2	64	31 ± 7.4	0.02
8	~6.9	66 ± 2.1	34	64 ± 0.67	<0.0001
9	~17	92 ± 2.5	8.0	92 ± 3.4	<0.0001
10	~34	94 ± 2.2	6.0	95 ± 3.2	<0.0001

[a]Estimated anthocyanin concentration was calculated using the molecular mass of cyanidin-3-rutinoside (582 g/mol).

Table 5.6. Tabulation for electrophoresis results for Lovell peach extract with Fe^{2+} (2 μM) and H_2O_2 (50 μM) at pH 6.

Lane	Concentration (μM)[a]	% Supercoiled DNA	% Nicked DNA	% Damage Inhibition	p-value
5	0	4.0 ± 3.7	96	0	0
6	~6.9	25 ± 5.7	75	22 ± 3.0	0.006
7	~17	57 ± 8.3	43	56 ± 6.9	0.005
8	~34	78 ± 5.2	22	77 ± 4.7	0.001
9	~68	86 ± 3.5	14	86 ± 3.1	<0.0001
10	~170	91 ± 1.8	9.0	91 ± 1.2	<0.0001

[a]Estimated anthocyanin concentration was calculated using the molecular mass of cyanidin-3-rutinoside (582 g/mol).

Table 5.7. Tabulation for electrophoresis results for Sugar Giant peach extract with Fe^{2+} (2 μM) and H_2O_2 (50 μM) at pH 6.

Lane	Concentration (μM)[a]	% Supercoiled DNA	% Nicked DNA	% Damage Inhibition	p-value
5	0	0.8 ± 3.1	99.2	0	0
6	~1.7	3.7 ± 1.4	96.3	3.0 ± 1.3	0.06
7	~3.4	6.3 ± 0.93	93.7	5.7 ± 0.57	0.003
8	~6.9	15 ± 3.4	85	14 ± 3.5	0.02
9	~17	53 ± 1.9	47	54 ± 1.1	<0.0001
10	~34	79 ± 2.2	21	80 ± 0.89	<0.0001

[a]Estimated anthocyanin concentration was calculated using the molecular mass of cyanidin-3-rutinoside (582 g/mol).

Table 5.8. Tabulation for electrophoresis results for BY peach extract with Fe^{2+} (2 μM) and H_2O_2 (50 μM) at pH 6.

Lane	Concentration (μM)[a]	% Supercoiled DNA	% Nicked DNA	% Damage Inhibition	p-value
5	0	1.3 ± 1.1	98.7	0	0
6	~1.7	23 ± 3.5	77	22 ± 4.5	0.01
7	~3.4	46 ± 5.6	54	45 ± 6.3	0.006
8	~6.9	76 ± 4.8	24	77 ± 5.0	0.001
9	~17	89 ± 1.6	11	90 ± 1.8	<0.0001
10	~34	99 ± 1.1	1.0	99 ± 1.2	<0.0001

[a]Estimated anthocyanin concentration was calculated using the molecular mass of cyanidin-3-rutinoside (582 g/mol).

References

(1) Orrenius, S.; Gogvadze, V.; Zhivotovsky, B. *Annu. Rev. Pharmacol. Toxicol.* **2007**, *47*, 143-183.

(2) Park, S.; Imlay, J. A. *J. Bacteriol.* **2003**, *185*, 1942-1950.

(3) Macomber, L.; Rensing, C.; Imlay, J. A. *J. Bacteriol.* **2007**, *189*, 1616-1626.

(4) Mello-Filho, A. C.; Meneghini, R. *Mutat. Res.* **1991**, *251*, 109-113.

(5) Hoffmann, M. E.; Mello-Filho, A. C.; Mello-Filho, A. C. *Biochim. Biophys. Acta* **1984**, *781*, 234-238.

(6) Imlay, J. A.; Chin, S. M.; Linn, S. *Science* **1988**, *240*, 640-642.

(7) Henle, E. S.; Luo, Y.; Linn, S. *Biochemistry* **1996**, *35*, 12212-12219.

(8) Steinberg, D. J. *Biol. Chem.* **1997**, *272*, 20963-20966.

(9) Halliwell, B. *Drugs Aging* **2001**, *18*, 685-716.

(10) Huang, X. *Mutat. Res.* **2003**, *533*, 153-171.

(11) Singal, P. K.; Khaper, N.; Palace, V.; Kumar, D. *Cardiovas. Res.* **1998**, *40*, 426-432.

(12) Scalbert, A.; Johnson, I. T.; Salmarsh, M. *Am. J. Clin. Nutr.* **2005**, *81*, 215S-217S.

(13) Vinson, J. A.; Su, X.; Zubik, L.; Bose, P. *J. Agri. Food Chem.* **2001**, *49*, 5315-5321.

(14) Vinson, J. A.; Hao, Y.; Su, X.; Zubik, L. *J. Agri. Food Chem.* **1998**, *46*, 3630-3634.

(15) Vinson, J. A.; Proch, J.; Zubik, L. *J. Agri. Food Chem.* **1999**, *47*, 4821-4824.

(16) Manach, C.; Scalbert, A.; Morand, A.; Remesy, C.; Jimenez, L. *Am. J. Clin. Nutr.* **2004**, *79*, 727-747.

(17) Scalbert, A.; Williamson, G. *J. Nutr.* **2000**, *130*, 2073S-2085S.

(18) Perron, N. P.; Hodges, J. N.; Jenkins, M.; Brumaghim, J. L. *Inorg. Chem.* **2008**, *47*, 6153-6161.

(19) Manach, C.; Williamson, G.; Morand, C.; Scalbert, A.; Remesy, C. *Am. J. Clin. Nutr.* **2005**, *81*, 230S-242S.

(20) Seeram, N. P.; Henning, S. M.; Niu, Y.; Lee, R.; Scheuler, H. S.; Heber, D. *J. Agric. Food Chem.* **2006**, *54*, 1599-1603.

(21) Lambert, J. D.; Yang, C. S. *J. Nutr.* **2003**, *133*, 3262S-3267S.

(22) Saper, R. B.; Eisenberg, D. M.; Philips, R. S. *Am. Fam. Phys.* **2004**, *70*, 1731-1738.

(23) Cao, G.; Sofic, E.; Proior, L. R. *Free Radic. Biol. Med.* **1996**, *20*, 331-342.

(24) Yamamoto, T.; Hsu, S.; Lewis, J.; Wataha, J.; Dickinson, D.; Singh, B.; Bollag, W. B.; Lockwood, P.; Ueta, E.; Osaki, T.; Schuster, G. *J. Pharm. Exp. Ther.* **2003**, *307*, 230-236.

(25) Note: These IC_{50} and error values have been refined since publication.[18]

(26) Duthie, S. J.; Collins, A. R.; Duthie, G. G.; Dobson, V. L. *Mutat. Res.* **1997**, *393*, 223-231.

(27) Hertog, M. G. L.; Hollman, P. C. H.; Katan, M. B.; Krombout, D. *Nutr. Cancer* **1993**, *20*, 21-29.

(28) Sestili, P.; Guidarelli, A.; Dacha, M.; Cantoni, O. *Free Radic. Biol. Med.* **1998**, *25*, 196-200.

(29) Lee, C. *Clin. Chim. Acta* **2000**, *295*, 141-154.

(30) Curatolo, P. W.; Robertson, D. *Ann. Intern. Med.* **1983**, *98*, 641-653.

(31) Ashton, C. H. *Br. Med. J.* **1987**, *295*, 1293-1294.

(32) Pan, X.; Niu, G.; Liu, H. *Chem. Eng. Process.* **2003**, *42*, 129-133.

(33) Zylber-Katz, E.; Granit, L.; Levy, M. *Clin. Pharmacol. Ther.* **1984**, *36*, 133-137.

(34) Setchell, K. D. R.; Welsh, M. B.; Klooster, M. J.; Balistreri, W. F. *J. Chromatogr.* **1987**, *385*, 267-274.

(35) Newton, R.; Broughton, L. J.; Lind, M. J.; Morrison, P. J.; Rogers, H. J.; Bradbrook, I. D. *Eur. J. Clin. Pharmacol.* **1981**, *21*, 45-52.

(36) Campbell, M. E.; Spielberg, S. P.; Kalow, W. *Clin. Pharmacol. Ther.* **1987**, *42*, 157-165.

(37) Barone, J. J.; Roberts, H. R. *Food Chem. Toxicol.* **1996**, *34*, 119-129.

(38) Shishikura, Y.; Khokhar, S. *J. Sci. Food Agric.* **2005**, *85*, 2125-2133.

(39) Nishikawa, A.; Furukawa, F.; Imazawa, T.; Ikezaki, S.; Hasegawa, T.; Takahashi, M. *Food Chem. Toxicol.* **1995**, *33*, 21-26.

(40) Rothwell, K. *Nature* **1974**, *252*, 69-70.

(41) Shi, X.; Dalal, N. S.; Jain, A. C. *Food Chem. Toxicol.* **1991**, *29*, 1-6.

(42) Devasagayam, T. P.; Kamat, J. P.; Mohan, H.; Kesavan, P. C. *Biochim. Biophys. Acta* **1996**, *1282*, 63-70.

(43) Hayashi, N.; Ujihara, T.; Kohata, K. *Biosci. Biotechnol. Biochem.* **2004**, *68*, 2512-2518.

(44) Martin, R.; Lilley, T. H.; Falshaw, C. P.; Haslam, E.; Begley, M. J.; Magnolato, D. *Phytochem.* **1987**, *26*, 273-279.

(45) Martin, R.; Lilley, T. H.; Bailey, N. A.; Falshaw, C. P.; Haslam, E.; Magnolato, D.; Begley, M. J. *J. Chem. Soc., Chem. Commun.* **1986**, 105-106.

(46) Horman, I.; Viani, R. *J. Food. Sci.* **1972**, *37*, 925-927.

(47) Gaffney, S. H.; Martin, R.; Lilley, T. H.; Haslam, E.; Magnolato, D. *J. Chem. Soc., Chem. Commun.* **1986**, 107-108.

(48) Maruyama, N.; Suzuki, Y.; Sakata, K.; Yagi, A.; Ina, K. *Proc. Int. Sym. Tea Sci.* **1991**, 145-149.

(49) Oliveira-Brett, A. M.; Diculescu, V. C. *Bioelectrochemistry* **2004**, *64*, 133-141.

(50) Brown, J. E.; Khodr, H.; Hider, R. C.; Rice-Evans, C. A. *Biochem. J.* **1998**, *330*, 1173-1178.

(51) Yamamoto, N.; Moon, J. H.; Tsushida, T.; Nagao, A.; Terao, J. *Arch. Biochem. Biophys.* **1999**, *372*, 347-354.

(52) Plaper, A.; Golob, M.; Hafner, I.; Oblak, M.; Solmajer, T.; Jerala, R. *Biochem. Biophys. Res. Comm.* **2003**, *306*, 530-536.

(53) Hollstein, M.; Sidransky, D.; Vogelstein, B.; Harris, C. C. *Science* **1991**, *253*, 49-53.

(54) Perron, N. R.; Chaur, M. N.; Brumaghim., J. L. **2009**, submitted.

(55) Johnson, M. K.; Loo, G. *Mutat. Res.* **2000**, *459*, 211-218.

(56) Ohshima, H.; Yoshie, Y.; Auriol, S.; Gilibert, I. *Free Radic. Biol. Med.* **1998**, *25*, 1057-1065.

(57) Sahu, S. C.; Washington, M. C. *Cancer Lett.* **1991**, *60*, 259-264.

(58) Duthie, S. J.; Johnson, W.; Dobson, V. L. *Mutat. Res.* **1997**, *390*, 141-151.

(59) Gil, M. I.; Tomas-Barberan, F. A.; Hess-Pierce, B.; Kader, A. A. *J. Agric. Food Chem.* **2002**, *50*, 4976-4982.

(60) Tomas-Barberan, F. A.; Gil, M. I.; Cremin, P.; Waterhouse, A. L.; Hess-Pierce, B.; Kader, A. A. *J. Agric. Food. Chem.* **2001**, *49*, 4748-4760.

(61) Doll, R. *Proc. Nutr. Soc.* **1990**, *49*, 119-131.

(62) Knekt, P.; Jarvinen, R.; Reunanen, A.; Maatela, J. *Br. Med. J.* **1996**, *312*, 478-481.

(63) Bors, W.; Heller, W.; Michel, C.; Saran, M. *Methods Enzymol.* **1990**, *186*, 343-355.

(64) Rimm, E. B.; Katan, M. B.; Ascherio, A.; Stampfer, M. J.; Willett, W. C. *Ann. Intern. Med.* **1996**, *125*, 384-389.

(65) Cevallos-Casals, B. A.; Byrne, D.; Okie, W. R.; Cisneros-Zevallos, L. *Food Chem.* **2006**, *96*, 273.

(66) Duthie, G. G.; Duthie, S. J.; Kyle, J. A. *Nutr. Res. Rev.* **2000**, *13*, 79-106.

(67) Tsuda, T.; Horio, F.; Osawa, T. *Lipids* **1998**, *33*, 583-588.

(68) Shulaev, V.; Korban, S. S.; Sosinski, B.; Abbott, A. G.; Aldwinckle, H. S.; Folta, K. M.; Iezzoni, A.; Main, D.; Arus, P.; Dandekar, A. M.; Lewers, K.; Brown, S. K.; Davis, T. M.; Gardiner, S. E.; Potter, D.; Veilleux, R. E. *Plant Physiol.* **2008**, *147*, 985-1003.

(69) Bassi, D.; Monet, R. *Botany and Taxonomy* **2008**, pp 1-36.

(70) Cevallos-Casals, B. A.; Cisneros-Zevallos, L. *Food Chem.* **2004**, *86*, 69-77.

(71) Deineka, V.; Deineka, L.; Sirotin, A. *Chem. Natural Compounds* **2005**, *41*, 230-231.

(72) Cevallos-Casals, B. A.; Byrne, D.; Cisneros-Zevallos, L.; Okie, W. R. *Acta Hort.* **2002**, *592*, 589-592.

(73) Horn, R.; Lecouls, A. C.; Callahan, A.; Dandekar, A.; Garay, L.; McCord, P.; Howad, W.; Chan, H.; Verde, I.; Main, D.; Jung, S.; Georgi, L.; Forrest, S.; Mook, J.; Zhebentyayeva, T.; Yu, Y. S.; Kim, H. R.; Jesudurai, C.; Sosinski, B.; Arus, P.; Baird, V.; Parfitt, D.; Reighard, G.; Scorza, R.; Tomkins, J.; Wing, R.; Abbott, A. G. *Theor. Appl. Genet.* **2005**, *110*, 1419-1428.

(74) Imlay, J. A.; Linn, S. *Science* **1988**, *240*, 1302-1309.

(75) Ikawa, M.; Schapper, T. D.; Dollard, C. A.; Sasner, J. J. *J. Agri. Food Chem.* **2003**, *51*, 1811-1815.

(76) Obanda, M.; Owuor, P. O. *J. Sci. Food Agric.* **1997**, *74*, 209-215.

(77) Perkowski, D. A.; Perkowski, M.; Data and Probability Connections; Pearson Prentice Hall: New Jersey, 2007, pp 318-337.

CHAPTER SIX

CONCLUSIONS ABOUT THE ANTIOXIDANT ACTIVITIES OF INORGANIC SELENIUM, OXO-SULFUR, AND POLYPHENOL COMPOUNDS AND THE BIOLOGICAL IMPLICATIONS OF NANOPARTICLE FUNCTIONALIZATION

Generation of hydroxyl radical ($^{\bullet}OH$) from oxidation of redox-active metals such as iron and copper by hydrogen peroxide (H_2O_2) causes DNA damage, resulting in mutations cell death, and diseases such as cancer,[1] aging,[2] arteriosclerosis, Alzheimer's and Parkinson's diseases.[3-5] The ability of selenium, sulfur, and polyphenol compounds to exhibit antioxidant and/or pro-oxidant activities may be beneficial in the prevention or treatment of these diseases caused by oxidative stress.[6-11]

Since most studies have focused on the antioxidant activity of organosulfur and organoselenium compounds, our experiments investigated four inorganic selenium compounds for their ability to prevent DNA damage produced by either iron or copper and hydrogen peroxide.[12] The antioxidant efficacy of inorganic selenium compounds with iron-mediated DNA damage is complex, since these compounds exhibit both antioxidant and pro-oxidant properties depending on concentrations of the selenium compound or H_2O_2.[12] However, inorganic selenium compounds are antioxidants with copper-mediated DNA damage. Oxidation state of the selenium atom of inorganic selenium compounds is important for the activities of these compounds. Inorganic selenium compounds in the +4 oxidation state, such as selenite and selenium dioxide, are capable of both inhibiting and producing DNA damage, whereas those with oxidation

states of -2 and +6 have no effect on iron- or copper-mediated DNA damage. From our experiments, iron or copper coordination is proven to be a novel mechanism for the antioxidant activity of Na_2SeO_3 and SeO_2. This iron-binding mechanism is also responsible for the pro-oxidant ability of SeO_2 at low concentrations.[12] Previous studies have shown that both inorganic and organic selenium compounds have application for use in dietary supplements, food products, and in the treatment and prevention of diseases. However, little is understood about the antioxidant activity and antioxidant mechanisms of these compounds. Our results highlight the complexity of the antioxidant and pro-oxidant activities of inorganic selenium compounds and have elucidated a novel metal-binding mechanism for this activity. The results of this work will contribute to a better understanding of how inorganic selenium compounds exerts their effects, with great implications in determining proper nutritional quantities for fertilizers, food products, and supplements for disease prevention.

Similar experiments investigating the effects of five oxo-sulfur compounds indicate that these compounds are generally more effective at inhibiting copper-mediated DNA damage than that produced by iron. This result suggests that the metal ion affects antioxidant activity. Methionine sulfoxide (MetSO) and methyl cysteine sulfoxide (MeCysSO) both prevented copper-mediated DNA damage, with low IC_{50} values (8.1-18 μM), an effect not observed for iron-mediated DNA damage.[13] In addition, oxidation state of the thiolate sulfur atom may also be a determining factor for prevention of DNA damage by Cu^+/H_2O_2, but not against Fe^{2+}/H_2O_2 generated DNA damage. Interestingly, methyl methane thiosulfonate (MMTS) is a pro-oxidant in the presence of Cu^+/H_2O_2, but

exhibits a small amount of antioxidant activity with Fe^{2+}/H_2O_2 DNA damage. While our experiments indicate that iron binding to MMTS is responsible for the observed antioxidant activity, copper coordination plays no role in the observed pro-oxidant activity of MMTS, indicating that radical generation may be involved.[13]

The mechanisms for antioxidant and pro-oxidant activities of oxo-sulfur compounds are more complex than those for the inorganic selenium compounds. Copper coordination is a novel mechanism responsible for most, but not all, of the antioxidant properties of oxo-sulfur compounds. UV-vis spectroscopy of antioxidant sulfur compounds added to copper show Cu-S charge transfer bands at 240 nm, correlating to prevention of copper-mediated DNA damage.[13] However, gel electrophoresis experiments show that copper-binding is only partly responsible for the antioxidant activity observed for oxo-sulfur compounds, and indicate that a second mechanism, most likely radical scavenging, is also responsible for additional antioxidant activity observed.[13] Our results show the complex nature of the antioxidant effects and mechanisms for oxo-sulfur compounds, and give insight for disparities in disease prevention and treatment trials. Further investigations are therefore required to fully understand the mechanistic action of oxo-sulfur compounds advance treatment or prevention of disease with these or similar compounds. Additionally, since most oxo-sulfur compounds are consumed in foods, it is essential to establish accurate nutritional requirements for these compounds to maintain proper health.

Electrospray ionization mass spectroscopy (ESI-MS) experiments further support copper coordination as the mechanism for the antioxidant activity of both selenium and

sulfur compounds. Copper binds to selenium or sulfur compounds in a 1:1 ratio for most antioxidant sulfur compounds tested. Because several sulfur and selenium compounds that do not prevent copper-mediated DNA damage also show copper coordination in the mass spectrometry experiments, copper binding is required but not sufficient for the observed antioxidant activity. These studies suggest that the specific chemical properties of sulfur and selenium compounds, rather than the presence of sulfur or selenium alone, play an important role in determining antioxidant activity.

Polyphenols such as epigallocatechin-3-gallate (EGCG) and quercetin (Q) have been shown to prevent DNA damage produced by Fe^{2+}/H_2O_2. However, combination of these polyphenols with caffeine can affect their antioxidant ability. Comparatively, EGCG/caffeine (1:1 ratio) and EGCG alone have the same ability to prevent DNA damage. However, addition of caffeine to Q (1:1 ratio), significantly lowers the activity compared to Q alone. Our results show the importance of understanding the synergistic or antagonistic antioxidant activity of combining compounds commonly found in food. π-stacking interactions have been shown to occur between polyphenols and caffeine,[14] and these interactions may be responsible for the antioxidant activity changes when caffeine is combined with polyphenols. In addition to the gel electrophoresis experiments performed with one equivalent of caffeine, polyphenol compounds containing two gallol or catechol groups should be tested using two or more equivalents of caffeine to investigate whether π stacking of caffeine to both gallol or catechol groups affects antioxidant activity. Such studies will promote understanding of how these compounds interact with each other and how dietary combinations may modify antioxidant activity.

Additionally, since caffeine is structurally similar to DNA bases such as adenine and guanine, investigations to determine π-stacking interactions between polyphenol compounds and DNA bases will be beneficial in elucidating the effects of DNA interactions on polyphenol antioxidant activity.

Since inorganic selenium compounds are consumed in dietary supplements that may contain other antioxidant compounds, combinations of these components also can be tested via gel electrophoresis experiments to determine whether such combinations alter the antioxidant efficacy inorganic selenium compounds. Similar experiments can be performed with the oxo-sulfur compounds in combination with allicin, alliin, and methyl cysteine sulfoxide since these are commonly found in garlic and synthesized garlic extracts. Such experiments will elucidate the varying effects observed for inorganic selenium and oxo-sulfur compounds in the treatment or prevention of diseases.

The ability of peach extracts obtained from the Abbott group at Clemson University to inhibit iron-mediated DNA damage was examined using four samples. Extract from the genetically modified peach (BY) is showed the most potent antioxidant activity at ~6.9 μM, followed by Red Globe, Lovell, and Sugar Giant peach extracts at the same concentration. The ability of peach extracts to inhibit iron-mediated DNA damage is a new area of research, and these preliminary experiments indicate that peach polyphenols do prevent iron-mediated oxidative DNA damage. Further experiments to determine the antioxidant ability of anthocyanins on copper-mediated DNA damage should also be performed, as well as to determine the anthocyanin compounds responsible for the observed DNA damage activity. It is expected that antioxidant activity

of anthocyanin to prevent Cu^{+}/H_2O_2-mediated DNA damage will be different than that observed with Fe^{2+}/H_2O_2 since such differences have been previously observed for polyphenol compounds.[15] Because peaches are a widely consumed fruit, our results show that genetically modified peaches may be more beneficial for disease prevention due to their high antioxidant activity compared to unmodified, lower antioxidant peaches. Our preliminary results also support the need for breeding programs focused on producing genetically-modified peach cultivars with increased antioxidant properties and increased ability to prevent ROS-mediated DNA damage.

The ability of ROS to induce DNA damage and cell death has been applied to photodynamic therapy (PDT) for the treatment of cancer. Tetraphenyl porphyrin (TPP)-doped CP dot nanoparticles synthesized by the McNeill group at Clemson University have great potential for use as photosensitizers for PDT because of their high molar absorptivity (10^7-10^9 M^{-1} cm^{-1}) and generation of singlet oxygen upon irradiation.[16] Irradiation of TPP-doped nanoparticles produces both DNA backbone and base damage, which increases with increasing irradiation time, thus supporting the use of these nanoparticles as effective and efficient photosensitizers for PDT. To further develop this work, experiments using the Fpg, Nth, and OGG enzymes to determine specific types of DNA base damage produced upon irradiation. Our results also provide proof-of-principle experiments to indicate that similar nanoparticle photosensitizer carriers may be effective for PDT.

Apart from PDT, use of nanomaterials for medical applications is a quickly evolving field of research, making toxicity of such materials a serious concern. Our

preliminary experiments show that polyethylene glycol (PEG) can generate H_2O_2 and associate to iron in biologically relevant concentrations. These results suggest that PEG-functionalized nanoparticles used for medical purposes may result in cytotoxicity due to hydroxyl radical formation upon reaction of iron and peroxide. However, to fully understand the toxic effects of functionalized nanoparticles, studies to further evaluate peroxide formation and metal association of these nanoparticles are necessary. In addition, the effects of functionalized nanoparticles can be performed to quantify the amount of DNA damage produced upon reaction of iron with H_2O_2. Investigating the toxicity of nanomaterials will provide direction for the design of less toxic nanoparticles for medicinal applications.

These *in vitro* DNA damage studies are reliable for determining the antioxidant and pro-oxidant effects of inorganic selenium, oxo-sulfur, and polyphenol compounds. However, these experiments should be extended to cellular systems to further validate our *in vitro* results. Similar cellular studies can also be applied for determining the effectiveness and toxicity of doped or functionalized nanoparticles under more biological conditions. Ultimately, animal and clinical studies may be performed with inorganic selenium, oxo-sulfur, polyphenol compounds, and/or combinations of compounds with high antioxidant activity to better elucidate their ability and mechanisms of action in the prevention or treatment of disease. In addition, these studies will help in determining the most effective and efficient compounds or foods for supplementation to maintain good health, and prevent diseases produced by oxidative stress.

References

(1) Steinberg, D. J. *Biol. Chem.* **1997**, *272*, 20963-20966.

(2) Henle, E. S.; Luo, Y.; Linn, S. *Biochemistry* **1996**, *35*, 12212-12219.

(3) Halliwell, B. *Drugs Aging* **2001**, *18*, 685-716.

(4) Huang, X. *Mutat. Res.* **2003**, *533*, 153-171.

(5) Singal, P. K.; Khaper, N.; Palace, V.; Kumar, D. *Cardiovas. Res.* **1998**, *40*, 426-432.

(6) Valko, M.; Rhodes, C. J.; Moncol, J.; Izakovic, M.; Mazur, M. *Chemico-Biological Interactions* **2006**, *160*, 1-40.

(7) Huang, X. *Mutat. Res.* **2003**, *533*, 153-171.

(8) Gil, M. I.; Tomas-Barberan, F. A.; Hess-Pierce, B.; Kader, A. A. *J. Agric. Food Chem.* **2002**, *50*, 4976-4982.

(9) Sutherland, B. A.; Rahman, R. M. A.; Appleton, I. *J. Nutr. Biochem.* **2006**, *17*, 291-306.

(10) Holmgren, A. *Free Rad. Biol. Med.* **2006**, *41*, 862-865.

(11) Takahashi, M.; Sato, T.; Shinohara, F.; Echigo, S.; Rikiishi, H. *Int. J. Oncol.* **2005**, *27*, 489-495.

(12) Ramoutar, R. R.; Brumaghim, J. L. *J. Inorg. Biochem.* **2007**, *101*, 1028-1035.

(13) Ramoutar, R. R.; Brumaghim, J. L. *Main Group Chem.* **2007**, *6*, 143-153.

(14) Hayashi, N.; Ujihara, T.; Kohata, K. *Biosci. Biotechnol. Biochem.* **2004**, *68*, 2512-2518.

(15) Perron, N. R.; Chaur, M. N.; Brumaghim., J. L. **2009**, submitted.

(16) Grimland, J. L.; Wu, C.; Ramoutar, R. R.; Aristizabal, K.; Brumaghim, J.; McNeill, J. **2009**, in preparation.